KINETICS, TEMPERATURE DEPENDENCE, AND CATION INHIBITION OF BARLEY ROOT PLASMA MEMBRANE-BOUND ATPase IN RELATION TO BIOPHYSICAL PROPERTIES OF MEMBRANE LIPIDS

By

Charles Raymond Caldwell

A DISSERTATION

Submitted to

Michigan State University

In partial fulfillment of the requirements

for the degree of

DOCTOR OF PHILOSOPHY

Department of Botany and Plant Pathology

1981

ABSTRACT

KINETICS, TEMPERATURE DEPENDENCE, AND CATION INHIBITION OF BARLEY ROOT PLASMA MEMBRANE-BOUND ATPase IN RELATION TO BIOPHYSICAL PROPERTIES OF MEMBRANE LIPIDS

By

Charles Raymond Caldwell

A plasma membrane-rich microsome fraction isolated from the roots of barley (*Hordeum vulgare* L. cv. Conquest) contained considerable divalent cation-dependent ATPase activity. Double reciprocal plots of the Ca^{2+}- and Mg^{2+}-dependent ATPase activities as a function of substrate concentration were nonlinear, suggesting the presence of multiple catalytic sites or negative cooperativity. Both $CaATP^{2-}$ and $MgATP^{2-}$ served as the true enzyme substrates and bound to the same catalytic sites. Free ATP and Ca^{2+} inhibit the Ca^{2+}- and Mg^{2+}-dependent ATPase. Increasing free Mg^{2+} levels enhanced the affinity of the Mg^{2+}-dependent ATPase for $MgATP^{2-}$. The highest enzyme-substrate affinities (K_m) were obtained with divalent cation-ATP complexes, while other nucleoside triphosphates produced higher maximal velocities (V_{max}) than ATP. The high and low affinity catalytic components of the ATPase exhibited optimal V_{max} values at pH 5 and 6, respectively. Analysis of the pH-dependence of the enzyme K_m values indicated enzyme-substrate binding with charge neutralization at neutral and alkaline pH's. These results are discussed in terms of the kinetics of both plant and animal ATPases.

Arrhenius plots of the V_{max} values for the Ca^{2+}- and Mg^{2+}-dependent ATPase activities were curvilinear and could be accurately described by a thermodynamic model based on the reaction having a finite heat capacity of activation. The temperature dependence of the computed K_m values for the ATPase activities was also complex, with the highest enzyme-substrate affinities being obtained near the barley seedling growth temperature (16 °C). Using electron paramagnetic resonance spectroscopy on spin-labelled barley membranes, it was possible to demonstrate that temperature changes and Ca^{2+} ions could alter the mobility of the membrane lipid polar head groups, which, in turn, modulated ATPase activity. The possible role of lipid polar head group-protein interactions in the complex temperature dependence of the barley root ATPase kinetic constants is discussed.

The inhibitory action of divalent cations on the Ca^{2+}-dependent ATPase activity was investigated in detail. Applying electron paramagnetic resonance spectroscopy to measure cation-induced changes in membrane lipid properties, it was demonstrated that certain divalent cations (Ca^{2+}, UO_2^{2+}, Cd^{2+}) inhibit the ATPase by restriction of lipid polar head group mobility and not by alteration of membrane surface charge. Monovalent cations which stimulate the barley Ca^{2+}-dependent ATPase (Na^+, K^+, ethanolamine·HCl) also reverse the Ca^{2+}-ATPase inhibition by Cd^{2+}. The degree of Na^+ reversal of Cd^{2+}-induced Ca^{2+}-dependent ATPase inhibition was influenced by the nature of the anion. The ability of cations to inhibit or stimulate the ATPase was dependent upon their binding to or changing the binding properties of membrane lipids.

Charles Raymond Caldwell

The barley root membrane-bound ATPase was solubilized and purified by CrATP-Sepharose affinity chromatography. Experiments with the solubilized and purified ATPase indicated that certain functional characteristics of the ATPase were dependent upon the type of phospholipids present during the ATPase assay. The purified ATPase fraction contained primarily a single phosphorylatable protein, molecular weight 75,000 daltons.

The results obtained strongly suggest interactions between specific membrane lipids and the membrane-bound ATPase. Several properties previously thought to be characteristics of the ATPase protein *per se* may actually result from lipid-protein interactions between the membrane lipids and the ATPase protein. The results are discussed in terms of boundary lipids which represent the lipids immediately surrounding the membrane-bound ATPase.

ACKNOWLEDGMENTS

I am very grateful to Dr. Alfred Haug for his advice and support throughout this research project. I also appreciate the efforts of the members of my guidance committee; Dr. Ken Poff, Dr. Andrew Hanson, and Dr. Peter Carlson.

Finally, I would like to thank my wife Yang Li for accepting my idiosyncrasies.

TABLE OF CONTENTS

PAGE

LIST OF TABLES

LIST OF FIGURES

FIGURE PAGE

SCHEME

LIST OF ABBREVIATIONS

cAMP	3'-5' cyclic AMP
BB	Bovine Brain
BBAP	Bovine Brain Acetone Powder
$\Delta C_p^{\ddagger}$	Heat Capacity of Activation
CaM	Calmodulin
CAPP	2-Chloro-10-(3-aminopropyl)phenothiazine
CAT_{12}	N,N-Dimethyl-N-dodecyl-N-tempoylammonium Bromide
CCEP	2-Chloro-10-(3-cyanoethyl)phenothiazine
CDI	1,1'-Carbonyldiimidazole
CP	2-Chlorophenothiazine
CPZ	Chlorpromazine
DTT	Dithiothrietol
EDTA	Ethylenediaminetetraacetic Acid
EGTA	Ethyleneglycol-bis-(β-amino ether)-N,N'-teraacetic Acid
EPR	Electron Paramagnetic Resonance
ETC	Equivalent Temperature Change
F	Faraday's Constant
$\Delta H^{\ddagger}$	Activation Enthalpy
K_i	Apparent Inhibitor Association Constant
K_i'	Apparent Inhibitor Dissociation Constant
K_m	Michaelis-Menten Constant
$MeNTP^{2-}$	Metal-Nucleoside Triphosphate Complex
MES	Morpholinoethanesulfonic Acid

n	Nonlinearity Parameter
NMR	Nuclear Magnetic Resonance
NPP	Nitrophenylphosphate
5NS	5-Nitroxystearate
12NS	12-Nitroxystearate
NTP	Nucleosidetriphosphate
P	Partition Coefficient
PDE	Cyclic Nucleotide Phosphodiesterase
PEG-6000	Poly(ethylene glycol) [6000 daltons]
P_i	Inorganic Phosphate
PMSF	Phenylmethylsulfonylfluoride
R	Gas Constant
R^2	Nonlinear Correlation Coefficient
S	Order Parameter
SA	Specific Activity
SDS	Sodium Dodecyl Sulfate
T	Temperature (°K)
$2T_{//}$, $2T_{\perp}$	Hyperfine Splitting Parameters
THF	Tetrahydrofuran
Tris	Tris(hydroxymethyl)aminomethane
V_{max}	Maximal Velocity
Z	Charge
$\Delta\psi_s$	Change in Apparent Membrane Surface Charge

CHAPTER 1

GENERAL INTRODUCTION

Although methods have been available for the isolation of enriched plasma membrane fractions from plant cells for a number of years, very little is known about the biophysical and biochemical properties of plant plasma membranes. In contrast to the plasma membranes of animal and microbial cells, the functional characteristics of plant plasma membranes have not been investigated in detail. Most of the information concerning plant plasma membrane functions is based on circumstantial evidence obtained with intact plants. For example, a variety of agents can inhibit the activity of plasma membrane-bound ATPase. These agents have been used *in vivo* to determine the roles of the ATPase in various physiological processes. Since it must be assumed that the agents that inhibit the ATPase *in vitro* have the same activity *in vivo*, experiments of this type are often subject to artifact. Therefore, few of the properties attributed to plant plasma membranes have been conclusively demonstrated.

Investigations of the properties associated with plant plasma membranes require knowledge of both the physico-biochemical characteristics of the membrane lipids and those of the constituent membrane-bound enzymes and transport processes. Many studies of plant plasma membrane-bound ATPases have ignored the properties of the membrane lipids, even though it is well-known that the ATPases of both animal and microbial cells are sensitive to changes in the composition and physical state of the membrane lipids. Therefore, changes in the activities of membrane-bound ATPases of plant cells which have been

attributed to properties of the ATPase protein may actually result from the modulation of the ATPase activity by the properties of the enzyme-associated membrane lipids.

Therefore, a detailed investigation of the kinetic characteristics of the barley root plasma membrane-bound ATPase and the biophysical properties of the barley root plasma membranes was initiated. This approach allowed the comparison of temperature- and ion-dependent changes in the membrane physical properties with alterations in the observed ATPase activities.

Barley was chosen as the source of the experimental material because of its agricultural importance, its uniformity, ease of growth under defined conditions, relatively simple genetics (2n=14), and the considerable amount of research already performed on the growth and transport properties of barley *in vivo*. During the initial stages of this work, a method for the isolation of relatively pure (80%) barley root plasma membranes was published (Nagahashi *et al.* 1978). This procedure was modified (Caldwell and Haug 1980) to improve the purity of the isolated plasma membranes. However, since the lack of reliable markers for plant membranes made the determination of plasma membrane purity ambiguous, the membrane preparation used in this study is considered to be a plasma membrane-rich microsome fraction.

CHAPTER 2

KINETIC CHARACTERIZATION OF BARLEY ROOT PLASMA MEMBRANE-BOUND Ca^{2+}- AND Mg^{2+}-DEPENDENT ADENOSINE TRIPHOSPHATASE ACTIVITIES

The following manuscript was published in Physiologia Plantarum [50: 183-193 (1980)].

INTRODUCTION

There is considerable evidence which suggests that plasma membrane-bound, ion-stimulated ATPases are involved in ion transport of higher plants (Nissen 1977, Gomez-Lepe and Hodges 1978, Balke and Hodges 1979, Marmé and Gross 1979). Using isolated plasma membrane-rich microsome fractions, some kinetic properties of membrane-bound ATPases have been investigated in a number of plants (Hodges 1976). In general, such ATPase are characterized by simple Michaelis-Menten kinetics at 38 °C, a requirement for Mg^{2+} or certain other divalent cations, a pH optimum for enzymatic activity of pH 6.5, and a stimulation of the Mg^{2+}-dependent ATPase activity by K^{+}. Conversely, transport ATPases in membranes from animal cells often display more complex kinetics, characterized by nonlinear double reciprocal plots of the initial rate of ATP hydrolysis as a function of substrate concentration (Vianna 1975, DuPont 1977, Neet and Green 1977). Such complex kinetic properties have been attributed to negative cooperativity (Neet and Green 1977), although the presence of multiple, noninteracting substrate binding sites (Froelich and Taylor 1975, DuPont 1977) or certain random and branched processes (Frieden 1970, Taylor and Hattan 1979) could not be clearly excluded.

In this chapter, data are presented which strongly suggest that the membrane-bound ATPase activities found in a plasma membrane-rich microsome frcation isolated from barley roots possess kinetic properties similar to those of animal ATPases. Double reciprocal plots of the Ca^{2+}- or Mg^{2+}-dependent ATPase activities as a function of $MgATP^{2-}$ or $CaATP^{2-}$ concentration are decidedly nonlinear.

MATERIALS AND METHODS

Chemicals. Vanadium-free ATP, NPP, and all other NTP's were purchased from Sigma Chemical Company (St. Louis, MO, USA) as their sodium salts and converted to their Tris salts before use (Hodges and Leonard 1974). Tris, MES, DTT, PMSF, and oligomycin were also obtained from Sigma Chemical Co. Dextran T-500 was purchased from Pharmacia (Piscataway, NJ, USA). All other chemicals were purchased from various commercial sources and were of the highest purity available.

Plant material and membrane preparation. Barley seeds [*Hordeum vulgare* L. cv. Conquest (Early Seed Co., Saskatoon, Sask., Canada)] were germinated and grown over an aerated solution of 0.25 mM $CaSO_4$ (pH 6.5) in the dark at 16 ± 1 °C. The culture medium was changed daily. After 5 days, the primary roots were excised and washed in chilled distilled water. A plasma membrane-rich microsome fraction was isolated from the washed roots by a modification of the methods of Nagahashi *et al.* (1978). All procedures were performed at 4 °C. The roots were finely chopped with a razor blade and homogenized with a mortar and pestle without abrasives in a solution consisting of 250 mM sucrose, 3 mM EDTA, 1 mM DDT, 0.5 mM PMSF, and 1 mM Tris-ATP in 25 mM Tris-MES buffer (pH 7.2). The crude homogenate was filtered through Miracloth and centrifuged at 13,000 *g* for 15 min. The supernatant was collected and centrifuged at 80,000 *g* for 30 min. The pellet (crude microsomes) was resuspended in 1 mM Tris-MES buffer (pH 7.2), containing 250 mM sucrose. The membrane suspension was layered over a two-stage discontinuous sucrose gradient composed of 34% and 40 % sucrose (w/w) in 1 mM Tris-MES buffer (pH 7.2). After

centifugation at 80,000 *g* for 2 hr, a plasma membrane-rich microsome fraction was collected from the 34%/40% sucrose interface. The plasma membrane-rich microsome fraction was further fractionated by partition in an aqueous, two-phase polymer partition system composed of 5% dextran T-500, 4% PEG-6000, and 250 mM sucrose in 10 mM potassium phosphate buffer (pH 6.8)(Brunette and Till 1971). The membranes collected from the partition interface were washed 3 times with 250 mM sucrose in 1 mM Tris-MES buffer (pH 7.2). The washed membranes were resuspended in wash buffer at a final concentration of about 1 mg membrane protein/ml, frozen, and stored in liquid nitrogen for a maximum of 1 week prior to use. This storage method resulted in a minimal loss of enzymatic activities (<2.5%/week). Membrane protein was measured as described by Wang and Smith (1975).

ATPase assay procedures. ATPase activity was measured in a 1 ml reaction volume, containing 20 mM Tris-MES buffer at the desired pH and various concentrations of divalent cationa and Tris-ATP. Unless otherwise noted, all assays were performed at 16 °C. The enzyme reaction was started by the addition of membrane to give a final concentration of 2 μg membrane protein/ml. After incubation for the appropriate time, determined as described below, the reaction was stopped and the amount of released P_i determined (Rathbun and Betlach 1969). All experimental velocities presented are the means of at least two determinations and all experimental assay series have been repeated with different batches of membrane preparations. The divalent cation-dependent ATPase activity represents the enzymatic activity determined in the presence of cation, subtracting the activity determined in the absence of added cation and with 1 mM

EDTA (Tris salt). The apparent basal activity represents the ATPase activity determined without added cations or EDTA.

Since fixed-time assays require a constant rate of substrate hydrolysis during the entire assay period, the proper incubation times for each series of experiments were predetermined, using a continuous flow assay procedure. A 5 ml reaction volume of the same composition as that to be used in the fixed-time assays was incubated at the desired temperature and the reaction solution was continuously removed with a peristaltic pump. The reaction was stopped and the amount of released P_i determined by mixing the reaction solution with the one-step reagent of Lin and Morales (1978), using an oscillating coil mixer. After passage through a 2 min delay coil, the levels of released P_i were measured with a Gilford spectrophotometer equipped with a flow cell. Only incubation times during which the rate of substrate hydrolysis was linear for a variety of substrate concentrations were used in the subsequent fixed-time assays. Furthermore, the incubation times employed in the fixed-time assays resulted in less than 10% hydrolysis of the total available substrate.

Calculation of $CaATP^{2-}$ and $MgATP^{2-}$ concentrations. The approximate concentrations of the various ionic forms of the divalent cation-ATP complexes ($MeATP^{2-}$, $MeHATP^{1-}$, MeH_2ATP, and Me_2ATP), free Me^{2+}, $MeCl^{1+}$, Tris-ATP complexes, and the ionized forms of ATP (ATP^{4-}, $HATP^{3-}$, and H_2ATP^{2-}) were obtained with a computer program, written in BASIC, using a method of successive approximation (Storer and Cornish-Bowden 1974, Appendix 1). The program included corrections of the ionization and association constants associated with changes

in pH, ionic strength, and temperature. The same program was used to calculate the approximate concentrations of the various metal complexes and free forms of the other NTP's.

Kinetic constant determination. The apparent kinetic constants for the enzyme activities were calculated with a computer program based on the nonparametric, single-hyperbola-fitting method of Cornish-Bowden and Eisenthal (1978). For the data which generated nonlinear double reciprocal plots, the program utilized an iterative procedure, following the partition of the data into subsets (Burns and Tucker 1977). Details of this computer program can be found in Appendix 1. Other kinetic models were fitted to the experimental velocities by applying the nonlinear least squares method of Marquardt (1963), as modified by Nash (1979), having first refined the initial parameter estimates by the method of Nelder and Mead (1965). The sum of the squares of the residuals and a nonlinear correlation coefficient (R^2) were computed and used as goodness-of-fit criteria (Dammkoehler 1966). Numerical values for the degree of double reciprocal plot nonlinearity (n) were derived from linearized double reciprocal plots (Ting-Beall *et al.* 1973). Using a search program (Appendix 1), the value of n which provided the highest linear correlation coefficient (r) in double plots of 1/velocity against $1/substrate^n$ was computed. Only those values of n are presented for which $r > 0.975$. It should be noted that n is equivalent to the Hill coefficient used in the study of allosteric enzymes (Ting-Beall *et al.* 1973). All numerical constants given in the text were determined with the various computer methods. The various inhibitor plots presented were used only for the determination of the types of inhibitions.

All computer programs were pretested with simulated data given a known error distribution.

RESULTS

Membrane vesicles. A plasma membrane-rich microsome fraction was isolated from the roots of barley, as described in the Materials and Methods. The addition of ATP, DTT, and PMSF to the root homogenization solution resulted in a 4 to 6-fold increase in the specific activity of the Mg^{2+}-dependent ATPase found in the final membrane isolate, relative to that of membrane preparations isolated with homogenization solution which did not contain these additives. The aqueous, two-phase partition step in the membrane isolation procedure reduced by 65% the residual cytochrome c oxidase activity of the membrane fraction isolated from the partition interface (Table 1). A particulate fraction was found in the lower phase of the partition system which contained cytochrome c oxidase with relatively high specific activity. Thus, the partition system physically separated the membranes of mitochondrial origin from the plasma membrane-rich microsomes. The specific activities of other enzymes believed to be associated with cytoplasmic membranes also decreased during the plasma membrane isolation procedure. In a preliminary study, freeze-fracture electron microscopy indicated a rather homogeneous membrane material from the partition interface, composed of sealed vesicles with no observable background material. The membrane isolated from the sucrose gradient without subsequent two-phase partitioning consisted primarily of sealed vesicles, but also contained smaller particulate material of unknown origin.

Table 1. *Specific activities of membrane marker enzymes in the various fractions obtained during plasma membrane isolation.* All enzyme activities were determined in 30 mM Tris-MES buffer at 16 °C and, unless otherwise noted, pH 6.5. ATPase was determined with 3 mM ATP and 3 mM $MgCl_2$. All other enzyme activities were determined as described by Nagahashi (1975).

Enzyme	Specific Activity (μmol/mg-hr)		
	Crude Microsomes	Sucrose Interface	Partition Interface
ATPase (pH 6.0)	21.4	44.3	65.7
ATPase (pH 9.0)	11.3	6.5	5.8
Cytochrome c oxidase	11.5	5.1	1.8
Latent IDPase	1.7	1.8	1.9
NADH Cytochrome c red.	10.6	11.8	5.0
NADPH Cytochrome c red.	1.3	0.9	1.6
Malic dehydrogenase	0.04	0.0	0.0

Divalent cation requirements. The plasma membrane-rich microsome preparations from barley roots contained considerable divalent cation-dependent ATPase activity. The maximal stimulation of the apparent basal ATPase activity was $Ca^{2+} > Mg^{2+} > Mn^{2+} = Zn^{2+} > Co^{2+} > Ni^{2+}$ (Figure 1), but the relationship between the stimulation by different divalent cations varied with cation concentration. All other divalent cations tested were inhibitory according to $Hg^{2+} > Fe^{2+} > Cu^{2+} > Ba^{2+} = Sr^{2+}$. The apparent basal ATPase activity was significantly reduced by EDTA and EGTA (Figure 1), suggesting the presence of Ca^{2+} or other divalent cations in the membrane preparation or substrate solution. The reduction in relative velocity by chelator concentrations greater than 2.5 mM (Figure 1) resulted from chelator interference with the color reaction of the P_i assay. Since the concentration of unknown divalent cation was estimated to be 20 μM with a divalent cation-sensitive electrode (Orion model 93-32) and the added divalent cation levels were generally in the millimolar range, the concentration of unknown divalent cation was not included in the calculation of substrate concentrations. In the presence of chelators, the relatively low enzymatic activity indicated an essential requirement for divalent cations in the hydrolysis of ATP by the ATPase.

Ca^{2+}- and Mg^{2+}-dependent ATPase activities. Assuming that the $MeATP^{2-}$ complex serves as the true substrate for the ATPase (Lindberg *et al.* 1974, Balke and Hodges 1975, Leonard and Hotchkiss 1978, Hendrix and Kennedy 1977), both the Ca^{2+}- and Mg^{2+}-dependent ATPase activities did not follow simple Michaelis-Menten kinetics. Double reciprocal plots of the divalent cation-dependent ATPase activities as a function of $MeATP^{2-}$ concentration were nonlinear (Figure 2).

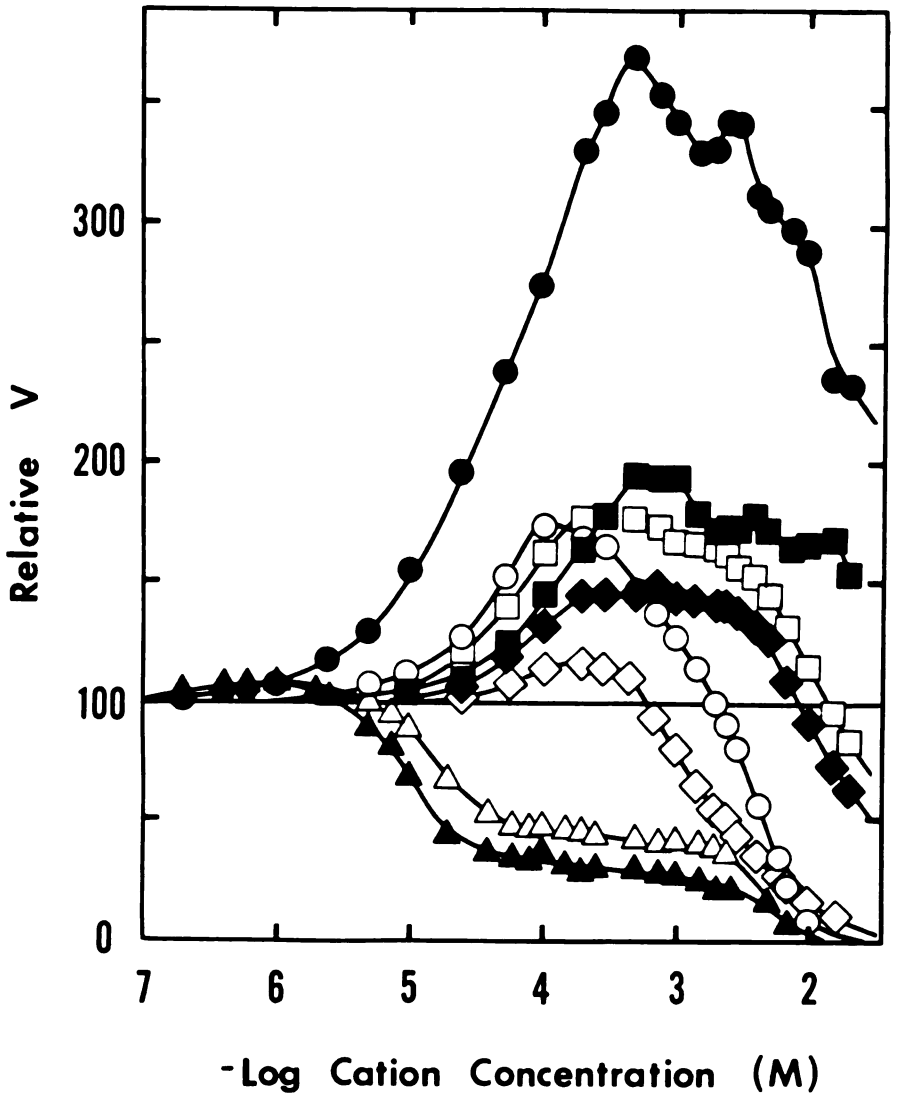

Figure 1. *Stimulation by divalent cations and inhibition by chelators of the apparent basal ATPase activity of barley root plasma membranes.* **The ATPase activities were determined as described in the Materials and Methods. The ATPase velocities [μmol P_i released x (mg protein)$^{-1}$ x h^{-1}] are given as the means of triplicate determinations relative to the enzyme activity determined without added cations or chelators [43.2 ± 1.83]. The standard error of the means was less than 5%. Activity was determined in the presence of Ca^{2+} (●), Mg^{2+} (■), Zn^{2+} (○), Mn^{2+} (□), Co^{2+} (◆), Ni^{2+} (◇), EDTA (▲), and EGTA (△).**

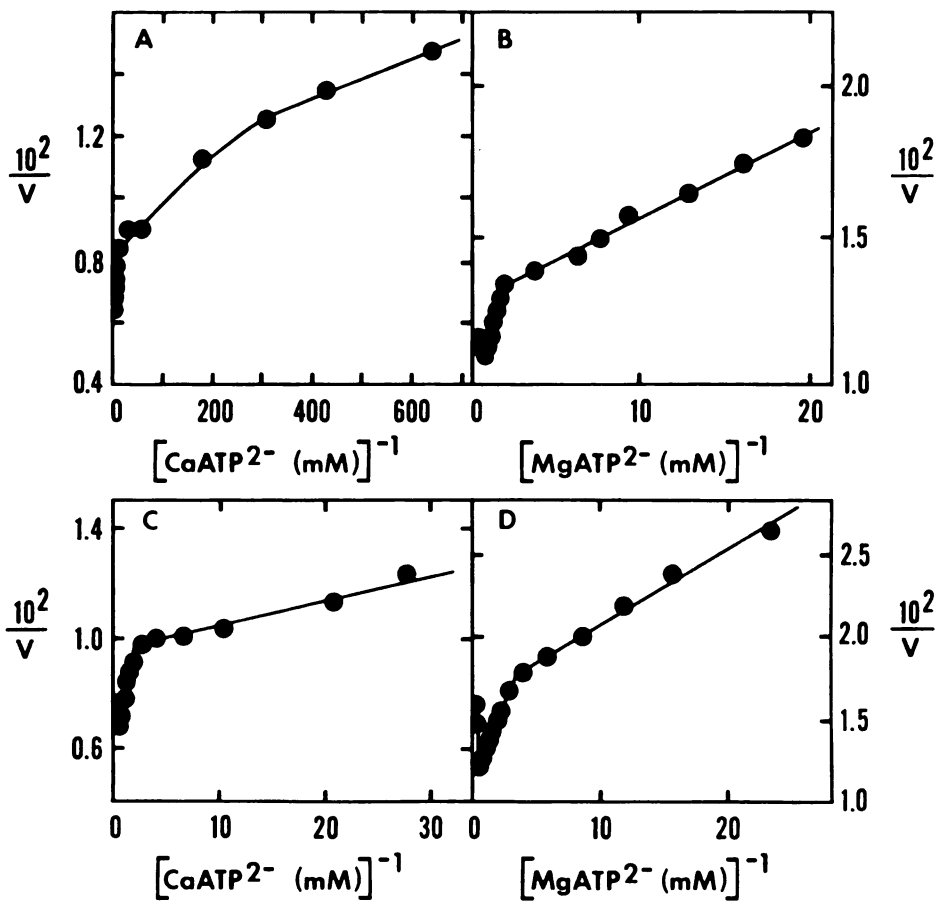

Figure 2. *Double reciprocal plots of the Ca^{2+}- and Mg^{2+}-dependent ATPase activities according to two methods of substrate activation.* Substrate activation was performed by adding divalent cation and ATP at a constant molar ratio of 1 (Parts A and B) or a constant molar excess of divalent cation over ATP concentration of 10 mM (Parts C and D). The assay conditions are described in the Materials and Methods. Parts A and C are the double reciprocal plots produced using $CaCl_2$ for substrate activation. Parts B and D are the double reciprocal plots produced using $MgCl_2$ for substrate activation. All velocities are presented as the means of duplicate determinations at 16 °C and have the unit μmol P_i released x $(mg\ protein)^{-1}$ x h^{-1}. The standard error of the means never exceeded 4% of the given values. $MgATP^{2-}$ and $CaATP^{2-}$ concentrations were calculated as described in the Materials and Methods and Appendix 1.

Furthermore, both the Ca^{2+}- and Mg^{2+}-dependent ATPase activities displayed substrate inhibition at high $MeATP^{2-}$ concentrations (Figure 2) and were insensitive to 5 μg/ml oligomycin (data not shown). As mentioned in the Introduction, kinetics of this type have been primarily explained in terms of negative cooperativity or the presence of multiple, noninteracting catalytic sites. Since confirmation of negative cooperativity requires either a highly purified enzyme preparation or the knowledge that a given preparation contains only one enzyme capable of acting upon the substrate in question, the relative impurity of the membrane material used in this study did not allow data analysis based on negative cooperativity. Therefore, the results have been presented and discussed in terms of multiple, noninteracting catalytic sites. Consequently, the experimental velocities were fitted to the sum of two Michaelis-Menten functions, representing the observed high and low affinity ATPase components (Figure 2). Since the experimental velocities used in the calculation of the apparent enzyme affinity constants (K_m) and maximal velocities (V_{max}) were generated by substrate concentrations well below those which produced substrate inhibition, substrate inhibition was not included in the model for data fitting. For clarity, the symbols K_H, V_H, K_L, and V_L designate the apparent K_m and V_{max} values for the high and low affinity ATPase activities, respectively.

Computer analysis of the data (Figure 2) demonstrated that both components of the Ca^{2+}- and Mg^{2+}-dependent ATPase activities had a considerably higher affinity for $CaATP^{2-}$ than for $MgATP^{2-}$ (Table 2). Furthermore, both V_H and V_L were higher for $CaATP^{2-}$ as the substrate than for $MgATP^{2-}$.

Table 2. *Calculated kinetic constants of the Ca^{2+}- and Mg^{2+}-dependent ATPase activities determined at different mM excesses for substrate activation and other nucleoside triphosphates as substrates.* Experimental velocities were determined as described in Figure 2, using the given mM excess of divalent cations over total ATP concentration. A 0 mM excess is equivalent to a constant molar ratio of 1. The values of K_H, V_H, K_L, V_L, R^2, and n were computed as described in the Materials and Methods. All K_H and K_L are presented in mM and all V_H and V_L values have the unit µmol P_i released x (mg protein)$^{-1}$ x h^{-1}. Each kinetic constant is immediately followed by the standard error of the computed value.

SUBSTRATE	mM EXCESS	K_H	V_H	K_L	V_L	R^2	n
$MgATP^{2-}$	0	0.025±0.0001	59.7±0.93	2.22±0.083	50.8±1.13	0.99	0.41
$MgATP^{2-}$	2.5	0.024±0.0005	57.7±0.88	2.05±0.092	48.3±1.42	0.98	0.37
$MgATP^{2-}$	5.0	0.021±0.0002	50.4±1.32	1.58±0.053	47.9±0.99	0.99	0.31
$MgATP^{2-}$	7.5	0.016±0.0003	50.3±1.00	1.48±0.055	49.3±0.99	0.99	0.31
$MgATP^{2-}$	10.0	0.014±0.0002	51.0±0.99	1.43±0.076	51.0±1.54	0.98	0.30
$MgUTP^{2-}$	10.0	0.025±0.0003	63.2±1.41	2.15±0.101	52.8±0.83	0.99	0.68
$MgCTP^{2-}$	10.0	0.019±0.0004	56.1±0.96	2.33±0.093	49.0±1.22	0.99	0.66
$MgITP^{2-}$	10.0	0.027±0.0004	39.0±0.61	1.92±0.084	63.5±1.07	0.99	0.50
$MgGTP^{2-}$	10.0	0.023±0.0003	51.2±1.20	1.97±0.088	46.7±0.91	0.99	0.58
$CaATP^{2-}$	0	0.0046±0.0001	113.4±1.42	0.32±0.011	73.5±1.16	0.98	0.33
$CaATP^{2-}$	5.0	0.0066±0.0001	98.5±1.38	0.68±0.023	74.2±1.38	0.98	0.42
$CaATP^{2-}$	7.5	0.0078±0.0001	85.9±0.97	1.03±0.057	71.4±1.22	0.98	0.45
$CaATP^{2-}$	10.0	0.0140±0.0001	73.9±1.21	1.30±0.073	66.5±1.18	0.97	0.56
$CaATP^{2-}$	15.0	0.0151±0.0002	75.7±0.87	2.33±0.101	65.5±1.63	0.98	0.66
$CaUTP^{2-}$	7.5	0.0185±0.0002	91.4±1.57	2.32±0.093	42.8±0.99	0.99	0.67
$CaCTP^{2-}$	7.5	0.0161±0.0002	83.7±1.35	2.63±0.087	97.1±1.41	0.99	0.71
$CaITP^{2-}$	7.5	0.0194±0.0004	84.2±1.29	2.48±0.131	91.4±1.38	0.98	0.73
$CaGTP^{2-}$	7.5	0.0205±0.0003	87.7±1.38	4.57±0.187	98.2±1.46	0.98	0.69

Effects of free ATP and divalent cations. The method of substrate activation by adding ATP and divalent cations to the ATPase reaction solutions at constant molar ratios (Figure 2, A and B) is only valid if the ATPase is insensitive to free ATP and divalent cations (Cleland 1970). Therefore, the effects of free ATP and divalent cations on the ATPase activities had to be determined. When the concentration of either total ATP or divalent cation was held constant and the amount of the other additive varied, it was apparent that both free ATP and divalent cation could inhibit the ATPase activity. Dixon plots of the inverse of the inhibited velocities as a function of inhibitor concentration (Dixon 1953a) indicated that free ATP competitively inhibited both the Ca^{2+}-dependent (K_i = 0.67 mM) and the Mg^{2+}-dependent (K_i = 0.056 mM) ATPase activities (Figure 3, C and D). However, Dixon plots cannot be used to distinguish between competitive and mixed-type inhibitions (Cornish-Bowden 1974). Plotting the same data as $MeATP^{2-}/v$ vs. I (Cornish-Bowden 1974) revealed that free ATP actually inhibited the Ca^{2+}-dependent (K_i' = 9.5 mM) and Mg^{2+}-dependent (K_i' = 2.5 mM) ATPase activities by a linear mixed-type mechanism (Figure 3, C and D, insets). A similar result was obtained for the inhibition of the Mg^{2+}-dependent ATPase by free Mg^{2+} (K_i = 4.4 mM, K_i' = 21.4 mM)(Figure 3, B and inset). Inhibition of the Ca^{2+}-dependent ATPase by free Ca^{2+} (K_i' = 3.7 mM) appeared to be uncompetitive according to both plotting methods (Figure 3, A and inset). It should be noted that the presence of high and low affinity catalytic sites (Figure 2) complicated the interpretation of these inhibitor plots. Two nonequivalent catalytic sites, each being competitively inhibited by the same inhibitor, could produce Cornish-Bowden plots suggestive of

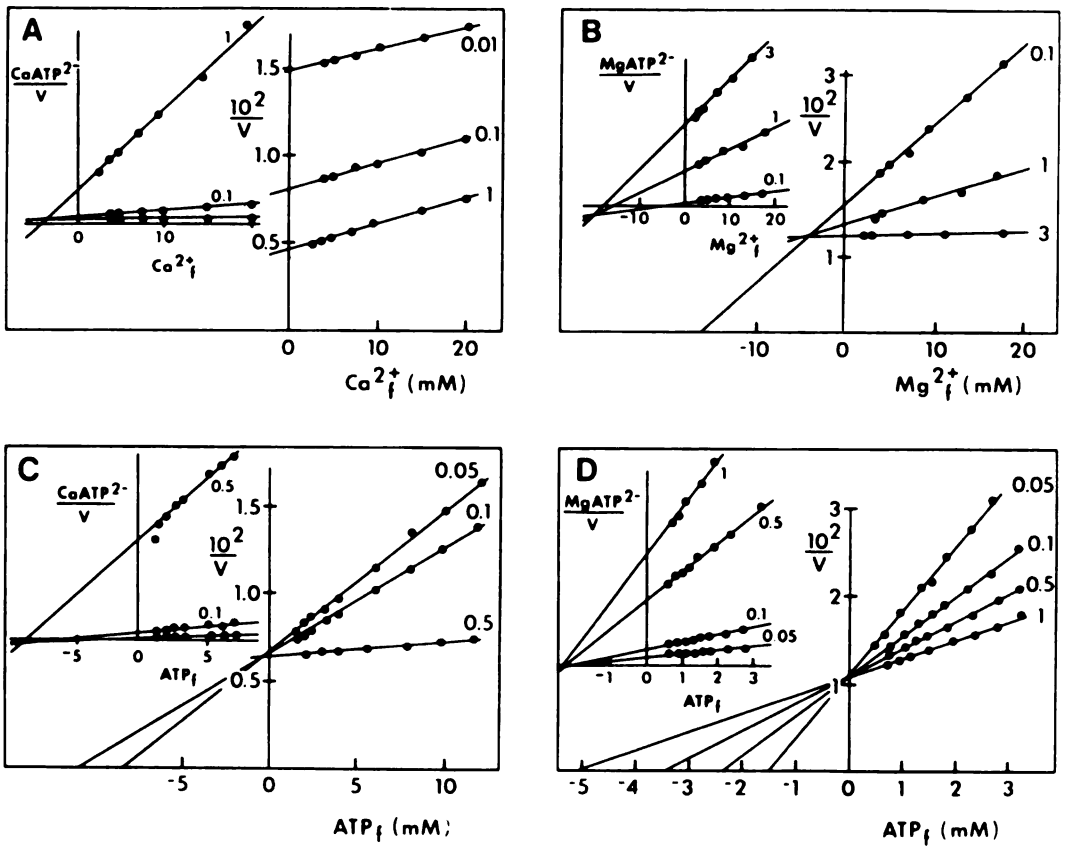

Figure 3. *Effect of free divalent cation and free ATP concentrations on the Ca^{2+}- and Mg^{2+}-dependent ATPase activities.* All velocities [μmol P_i released x (mg protein)$^{-1}$ x h^{-1}] are given as the means of duplicate dterminations at 16 °C and the standard error of the mean for any velocity never exceeded 6% of the given value. Each line is labelled with the total ATP or divalent cation concentration (mM) employed. Free Ca^{2+} (Ca^{2+}_f), free Mg^{2+} (Mg^{2+}_f), $CaATP^{2-}$, and $MgATP^{2-}$ levels (mM) were calculated as described in the Materials and Methods and Appendix 1. Total free ATP (ATP_f) is the sum of the concentrations of ATP^{4-}, $HATP^{3-}$, and H_2ATP^{2-}. Part A. Dixon and Cornish-Bowden (inset) plots of the measured, inhibited ATPase velocities at different fixed levels of total ATP and varying the amount of total $CaCl_2$. Part B. Same as Part A except that $MgCl_2$ was used instead of $CaCl_2$. Part C. Same as Part A except that the total $CaCl_2$ concentration was constant with varying total ATP. Part D. Same as Part C except that $MgCl_2$ was used instead of $CaCl_2$.

linear mixed-type inhibition.

Irrespective of the types of inhibitions present, it was apparent that free ATP was a more potent inhibitor of the ATPase activity than free divalent cation. Therefore, the constant molar excess method of substrate activation (Storer and Cornish-Bowden 1976) was used in all subsequent experiments. With a constant molar excess of 10 mM divalent cation over the total ATP concentration, complex kinetics of the type observed using the constant molar ratio method of substrate activation (Figure 2, A and B) were obtained (Figure 2, C and D). Furthermore, under these conditions, $CaATP^{2-}$ or $MgATP^{2-}$ were the predominant forms of ATP in the reaction mixture and the only significant variables. This demonstrated that these $MeATP^{2-}$ complexes serve as the primary enzyme substrates. Application of the constant molar excess method of substrate activation had one disadvantage. At pH 6.5, a constant molar excess of 10 mM was required to produce a linear increase in $MeATP^{2-}$ concentration with increasing total ATP, low free ATP levels, and a constant free Me^{2+} concentration. The resulting free Me^{2+} concentrations were high, 8.8 mM for Mg^{2+} and 9.6 mM for Ca^{2+}, and probably inhibitory (Figure 1). Nonetheless, this method was preferable, since application of the constant molar ratio method resulted in a nonlinear increase in $MeATP^{2-}$ with increasing total ATP, variable free Me^{2+}, and relatively high, variable concentrations of free ATP.

Employing various molar excesses of divalent cation over added ATP, an increase in free Mg^{2+} levels inhibited V_H (Table 2). More significantly, an increase in free Mg^{2+} concentration enhanced the affinity of both enzyme components for $MgATP^{2-}$ (Table 2). This

suggests that Mg^{2+} can modify substrate binding by interacting with a site other than the catalytic site (Segel 1975), as was previously suggested for the ATPases of wheat and oat (Kylin and Kähr 1973). It is also possible that free Mg^{2+} acts as a deinhibitor by reducing the concentration of free ATP. If free ATP inhibits the enzyme activities competitively, then the removal of free ATP by the formation of Mg^{2+}-ATP complexes at high free Mg^{2+} levels would decrease the K_H and K_L values. In contrast to the effects of free Mg^{2+}, free Ca^{2+} markedly reduced the affinities of both enzyme components for $CaATP^{2-}$ and lowered both V_H and V_L (Table 2).

At mM excesses of divalent cation over total ATP concentration above 5 mM for the Ca^{2+}-dependent ATPase activities, the maximal velocities were essentially constant, while the enzyme-substrate affinities continued to change with increasing free Ca^{2+} levels (Table 2). V_L for the Mg^{2+}-dependent ATPase activity did not significantly change above a 0 mM excess (Table 2). These results indicate that above certain divalent cation concentrations, any further increase in free cation levels primarily influenced enzyme-substrate affinity. For the Ca^{2+}-dependent ATPase activities, this suggests that free Ca^{2+} can inhibit both the low and high affinity components of the ATPase activity by a competitive mechanism, since increasing free Ca^{2+} increased the value of K_m without influencing V_{max}. However, the data presented in Figure 3A indicated that free Ca^{2+} inhibits the Ca^{2+}-dependent ATPase activity by an uncompetitive mechanism. As previously mentioned, the presence of multiple catalytic sites complicated the interpretation of the data presented in Figure 3. Furthermore, even though the concentration

of free ATP was low, both free ATP and Ca^{2+} were present under the experimental conditions used to obtain the data presented in Figure 3A. Since both of these free components can inhibit the Ca^{2+}-dependent ATPase activities, the Dixon plot indicating uncompetitive inhibition (Figure 3A) might have been generated by the presence of the two inhibitors, if they inhibit the enzyme competitively and compete with each other for sites on the enzyme (Semenza and von Balthazar 1974).

(Ca^{2+} + Mg^{2+})-dependent ATPase activity. To determine whether the Ca^{2+}-dependent ATPase activity and the Mg^{2+}-dependent ATPase activity represent two separate classes of enzymes or a single enzyme type which can utilize both $CaATP^{2-}$ and $MgATP^{2-}$, enzyme velocities were determined with various combinations of Mg^{2+} and Ca^{2+}. There was no additivity of the Ca^{2+}- and Mg^{2+}-dependent ATPase activities when a supraoptimal concentration of Ca^{2+} (1 mM) was used while simultaneously varying the level of Mg^{2+} (Figure 4B). However, there was a slight increase in the Ca^{2+}- and Mg^{2+}-dependent ATPase when a fixed supraoptimal Mg^{2+} concentration (1.5 mM) was employed and the Ca^{2+} concentration varied (Figure 4A). Essentially the same results were obtained at other total ATP concentrations (data not shown). At suboptimal concentrations of fixed divalent cation, the relative velocities were increased by the varied divalent cation (Figure 4). However, the maximal relative velocities produced never exceeded those generated by the varied divalent cation alone. Consequently, both $CaATP^{2-}$ and $MgATP^{2-}$ probably bind to the same catalytic sites. It also seems possible that the inhibitory action of free divalent cation is additive. These results may be interpreted as the conversion of $CaATP^{2-}$ to $MgATP^{2-}$ or $MgATP^{2-}$ to $CaATP^{2-}$. Since

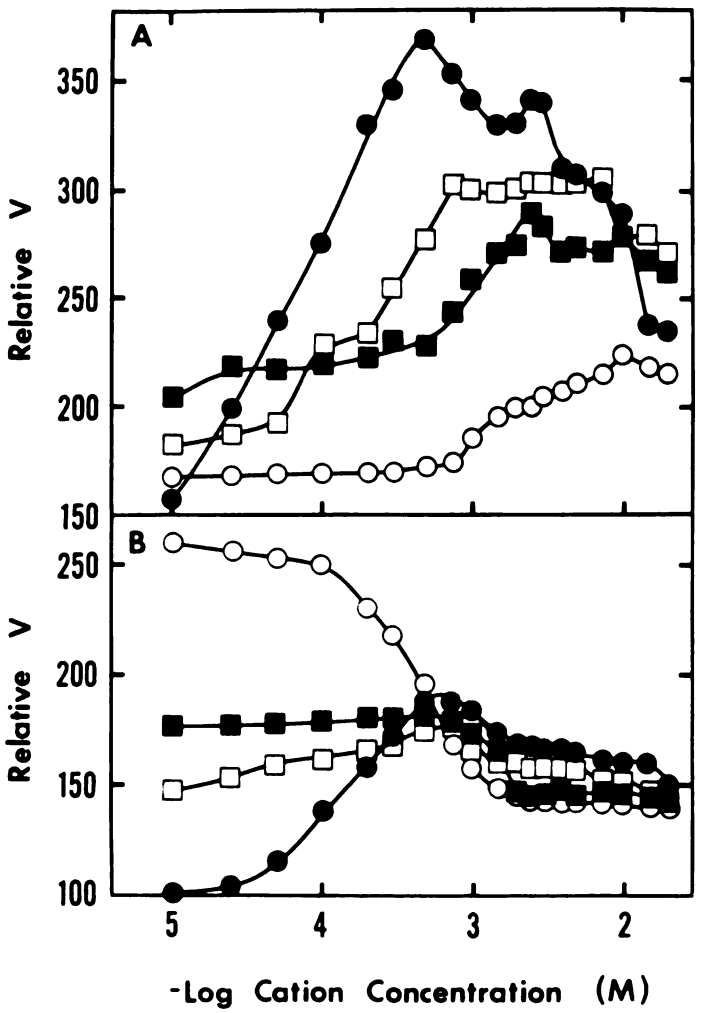

Figure 4. *Effect of combinations of Ca^{2+} and Mg^{2+} on the Ca^{2+}- and Mg^{2+}-dependent ATPase activities.* Assay conditions and data presentation are described in Figure 1. Standard error of the means of triplicate determinations was less than 5% of the given values. Part A. Effect of varying the total concentration of $CaCl_2$ on the ATPase activity produced by fixed concentrations of $MgCl_2$ [0 mM (●), 0.25 mM (□), 0.75 mM (■), 1.5 mM (○)]. Part B. Effect of varying the total concentration of $MgCl_2$ on the ATPase activity produced by fixed concentrations of $CaCl_2$ [0 mM (●), 0.01 mM (□), 0.025 mM (■), 1.0 mM (○)].

$CaATP^{2-}$ produced higher rates of hydrolysis than $MgATP^{2-}$ (Figure 2, Table 2), these conversions may account for the reduction of ATPase activity using $CaATP^{2-}$ by increasing levels of Mg^{2+} (Figure 4B) and the apparent additivity in relative velocity at supraoptimal Mg^{2+} concentration and varying total Ca^{2+} (Figure 4A).

Substrate specificity. Because it has been reported that the membrane-bound ATPase activity of barley roots exhibits poor substrate specificity (Tikhaya *et al.* 1976, Nagahashi *et al.* 1978), the kinetic constants for the divalent cation-dependent NTPase activities were determined. All NTP's produced the same type of kinetics as ATP, generating values of the nonlinearity parameter lying significantly below 1 (Table 2). The V_H and V_L values obtained with $CaNTP^{2-}$ and $MgNTP^{2-}$ as substrates were generally equal to or greater than those produced by $CaATP^{2-}$ and $MgATP^{2-}$ (Table 2). However, K_H and K_L were significantly lower for $CaATP^{2-}$ and $MgATP^{2-}$ when compared to those of the other NTP's. Even though the barley root ATPase must be considered to be relatively substrate nonspecific when compared to the substrate specificity of the ATPases from other cereals, these results indicate that $MeATP^{2-}$ is the preferred substrate for the barley ATPase.

Effect of pH on the Ca^{2+}- and Mg^{2+}-dependent ATPase activities. At high substrate concentrations, the Ca^{2+}- and Mg^{2+}-dependent ATPase activities had a pH maximum at 6.0. However, as the substrate concentrations were decreased, a second pH optimum for the enzyme activities became apparent at pH 5.0 (Figure 5). Considering the relative affinities of the two components of both the Ca^{2+}- and Mg^{2+}-dependent ATPase activities, these results are interpreted to indicate that the high affinity ATPase components functioned

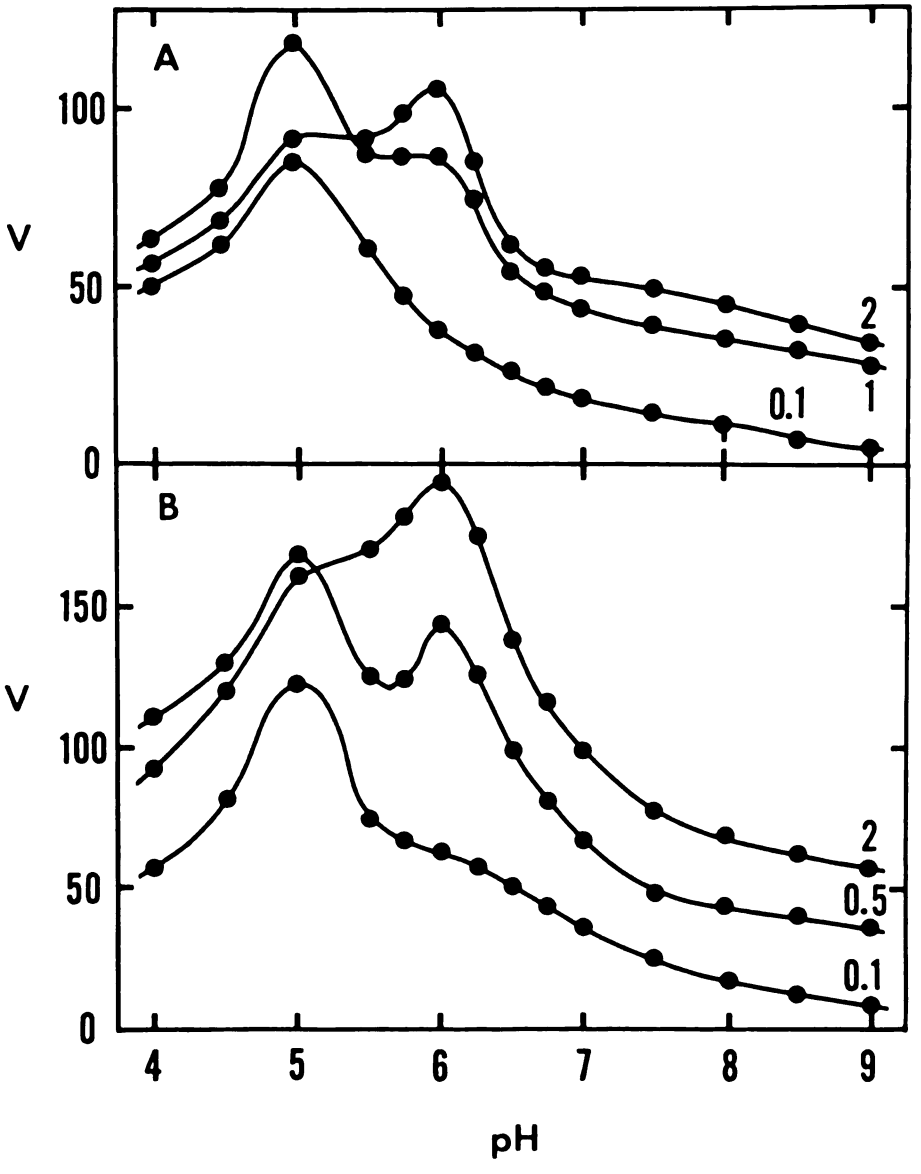

Figure 5. *pH Dependence of the Ca^{2+}- and Mg^{2+}-dependent ATPase activities.* Assay conditions were the same as those reported in Figure 4 except that the composition of the Tris-MES buffer was altered to give the desired pH and ionic strength. Each curve is labelled with the concentration of total ATP (mM) used. Part A. Mg^{2+}-dependent ATPase activity. Part B. Ca^{2+}-dependent ATPase activity.

optimally at pH 5, while the low affinity components had optimal activity at pH 6. This possibility was confirmed by calculating the kinetic constants for the Ca^{2+}- and Mg^{2+}-dependent ATPase activities at each pH, assuming $MeATP^{2-}$ to be the enzyme substrate at all pH's. The calculated maximal velocities of the high affinity ATPase component had a pH optimum at pH 5 (Figure 6), while the low affinity component had a pH optimum at pH 6 (Figure 6). However, kinetic analysis of the low affinity component was complicated by a pH-dependent increase in the magnitude of substrate inhibition. It was not clear whether the decline in the values of V_L, which occurred at pH values below 6, was related to the increase in substrate inhibition or to some other pH-dependent change in enzymatic activity.

It should be noted that both the Ca^{2+}- and Mg^{2+}-dependent NPPase activities were low until the pH was dropped below 5 and had no apparent pH activity optimum within the range of pH values studied (Figure 6). Therefore, it seemed unlikely that the results obtained using ATP could be attributed to the action of a nonspecific acid phosphatase.

Applying Dixon's rules for the analysis of the pH dependence of the ATPase affinity constants (Dixon 1953b), the low affinity Ca^{2+}- and Mg^{2+}-dependent ATPase components exhibited charge neutralization for enzyme-substrate binding at pH values above 6.4 (Figure 7). Similar apparent charge neutralization was observed for the high affinity components of the Ca^{2+}-dependent (pH 5.9) and Mg^{2+}-dependent (pH 5) ATPase activities (Figure 7). Below these pH values enzyme-substrate binding resulted in charged enzyme-substrate complexes, as indicated by the slopes of the lines in the pK_m vs. pH plot

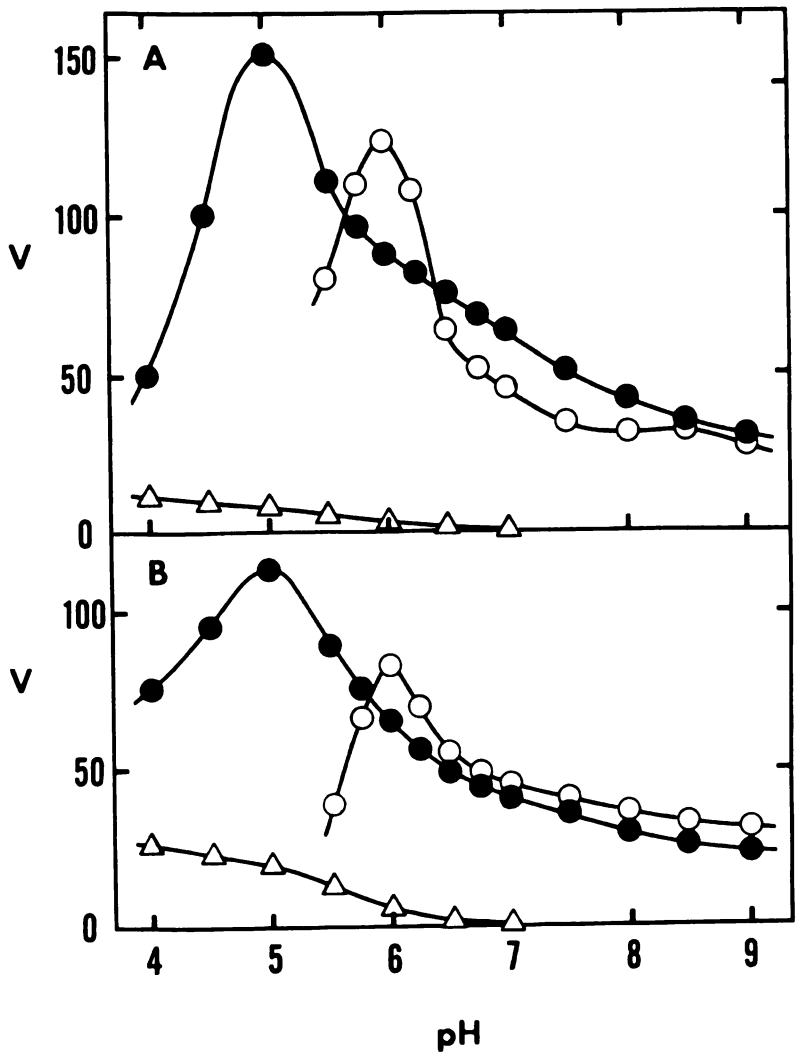

Figure 6. *pH-Dependence of the maximal velocities of the Ca^{2+}- and Mg^{2+}-dependent ATPase activities.* The values of V_H and V_L were calculated as described in the Materials and Methods and have the unit μmol P_i released x (mg protein)$^{-1}$ x h^{-1}. Enzyme velocities were determined under the conditions described in Figure 2, Parts C and D. The substrates were assumed to be the $MeATP^{2-}$ complexes. The standard error of each computed values never exceeded 5%. Part A. The pH dependence of V_H (●) and V_L (○) for the Ca^{2+}-dependent ATPase and the velocity produced using 1 mM NPP instead of ATP (△). Part B. The pH dependence of V_H (●) and V_L (○) for the Mg^{2+}-dependent ATPase and the velocity produced using 1 mM NPP instead of ATP (△).

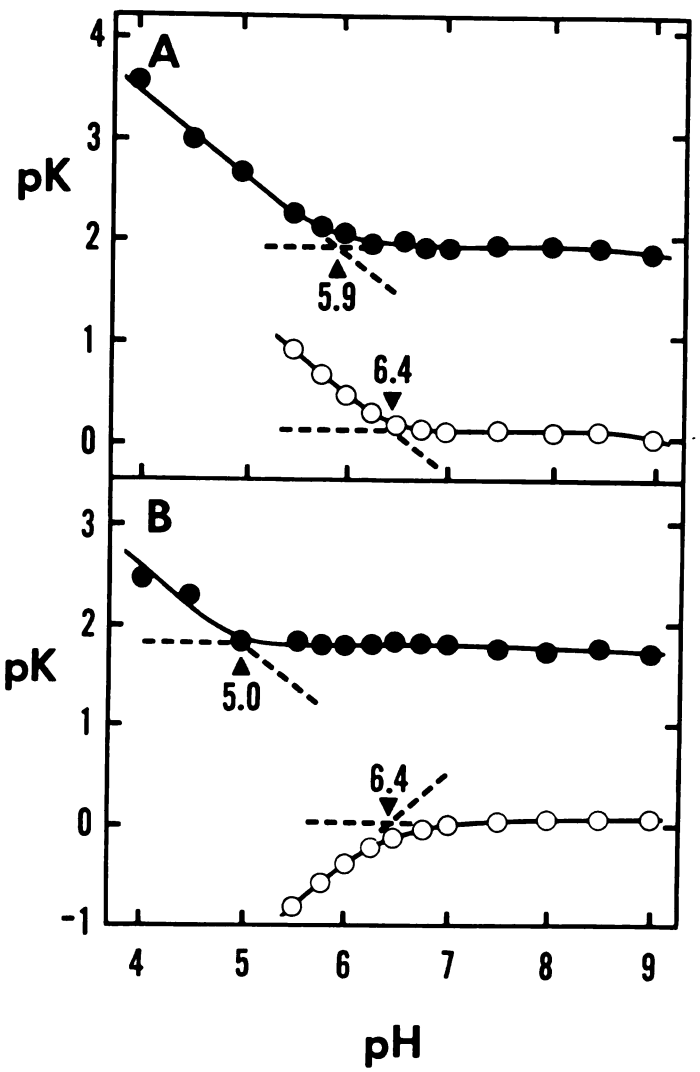

Figure 7. *Effect of pH on pK_H and pK_L of the Ca^{2+}- and Mg^{2+}-dependent ATPase activities.* The kinetic constants K_H and K_L were calculated from the ATPase velocities determined as described in Figure 5. The standard error never exceeded 3% of the computed values. The solid line was drawn as the best visual fit to the data presented as pK_m (-log K_m) in mM. The broken lines were drawn as the best visual fit to the calculated constants within the limitation that the lines must have integral slopes of +1, 0, or -1 (Dixon 1953b). The pK_{int} values are given at the intersections of the broken lines. Part A. pK_H (●) and pK_L (○) for $CaATP^{2-}$ as a function of pH. Part B. pK_H (●) and pK_L (○) for $MgATP^{2-}$ as a function of pH.

having integral values of either +1 or -1 (Figure 7). The deviation of signs cannot be easily explained. Perhaps, this discrepancy resulted from the assumption that $MeATP^{2-}$ was the only substrate for the enzymatic activity measured below pH 6. Nonetheless, at pH values above the inflexion pH (Figure 7), enzyme-substrate binding with charge neutralization was apparent. This type of enzyme-substrate binding has been previously suggested for ATPases in general (Laidler and Bunting 1973).

Effect of temperature on the Mg^{2+}-dependent ATPase activity.

Although a more detailed analysis of the temperature dependence of the ATPase activities will be found in the following chapter, for the purpose of comparison of the results presented in this chapter with those of the ATPases of other plants, some of the preliminary results of the study of the temperature dependence of the Mg^{2+}-dependent ATPase will be presented here. Nonlinear double reciprocal plots of the Mg^{2+}-dependent ATPase activity were observed at assay temperatures ranging from 2 to 36 °C (Figure 8). However, as the assay temperature was increased, the degree of nonlinearity decreased, as indicated by an increase in the value of n (Figure 8). At 36 °C, the double reciprocal plot was sufficiently linear so that the slight deviation from linearity might not be readily apparent.

DISCUSSION

The results of the present experiments reveal complex kinetics of the Ca^{2+}- and Mg^{2+}-dependent ATPase activities of a plasma membrane-rich microsome fraction isolated from the roots of barley by an improved procedure. The data are inconsistent with simple kinetics

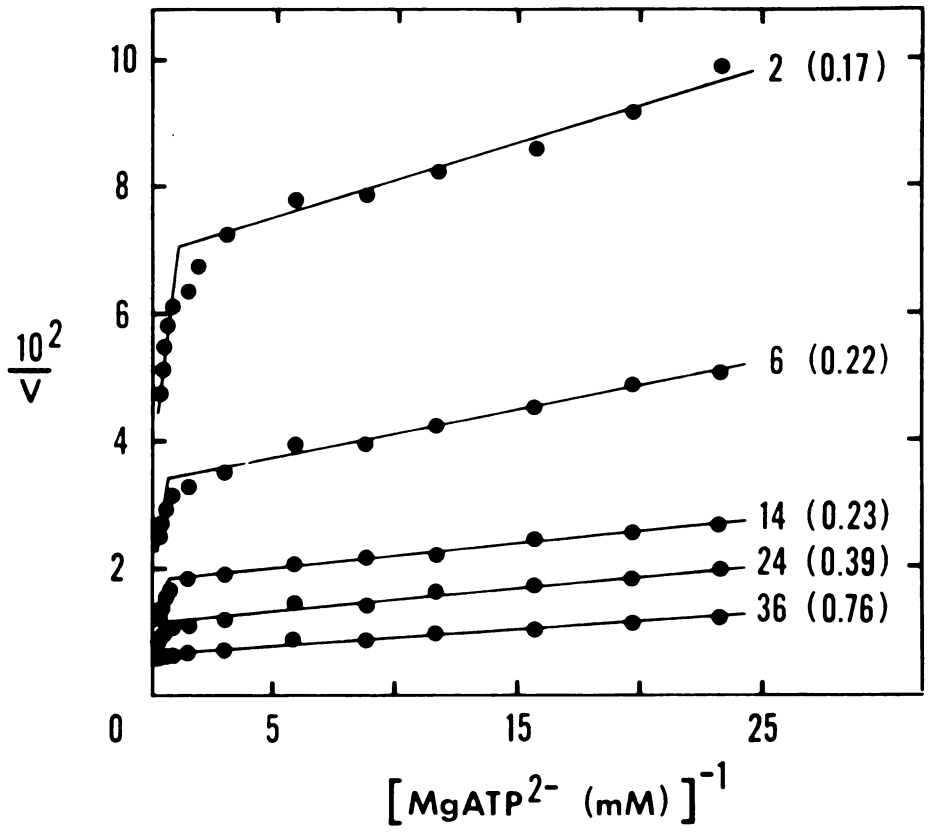

Figure 8. *Effect of assay temperature on the Mg^{2+}-dependent ATPase activity.* **The assay conditions were the same as those described in Figure 2D except that the assay temperature was varied. The data are presented as double reciprocal plots of the ATPase velocities [μmol P_i released x (mg protein)$^{-1}$ x h^{-1}] as a function of $MgATP^{2-}$ concentration. Each plot is labelled with the assay temperature in °C and the calculated value of the nonlinearity parameter in parentheses.**

for one catalytic site. However, they may be conveniently interpreted in terms of multiple, noninteracting catalytic sites. The presence of multiple catalytic sites is by no means the only possible mechanism which would produce kinetics of the type observed. Considering the kinetics of animal plasma membrane-bound ATPases, negative cooperativity is also a likely mechanism for the complex barley root ATPase kinetics. Since both the high and low affinity ATPase catalytic components are enriched with increasing plasma membrane purity (data not shown), it is likely that the multiple catalytic sites for the ATPase are localized in the plasma membranes of barley root cells and do not represent different ATPases from different cytoplasmic membranes.

At the growth temperature of the barley seedlings (16 °C), nonlinear double recuprocal plots for ATPase activity vs. substrate concentration are obtained. This type of kinetic behavior appears to be the first of its kind for plant ATPases. Previously, similar plots for ATPase activity have been obtained as a function of cation concentration (Nissen 1977). The kinetics described in the experiments presented here are possibly unique features of divalent cation-dependent ATPase activities in barley roots. However, frequently assays for plant ATPases have been carried out at 38 °C (Balke and Hodges 1975, Hendrix and Kennedy 1977, Nagahashi *et al.* 1978), whereas the assay temperature used in this study coincides with the barley seedling growth temperature. As shown in Figure 8, at elevated temperatures the barley root ATPase activity may be described by rather simple kinetics, similar to those previously reported for the ATPases of other plants (Leonard *et al.* 1973, Leonard and Hotchkiss 1978, Travis and Booz 1979). Furthermore, the most common procedure for substrate activation in the study of

plant ATPases is the addition of ATP and divalent cation at a constant molar ratio of 1 (Balke and Hodges 1975, Hendrix and Kennedy 1977). However, at pH values below 8, application of this method produced variable concentrations of free ATP and Me^{2+}, and a nonlinear increase in $MeATP^{2-}$ when the total ATP and divalent cation concentrations were raised. Considering the inhibitory action of free ATP and divalent cations on many plant divalent cation-dependent ATPases (Balke and Hodges 1975, Christiansen and Lindberg 1976), the results thus derived have to be interpreted with caution.

At high substrate concentrations, the Ca^{2+}- and Mg^{2+}-dependent ATPase from barley roots had optimal activity at pH 6 (Figure 5). This is consistent with the results of Nagahashi (1975) for barley Mg^{2+}-dependent ATPase measured at 38 °C with 3 mM concentrations of both Mg^{2+} and ATP. Under these conditions, Nagahashi (1975) would not have observed the second pH optimum for ATPase activity at pH 5 (Figure 5). Furthermore, Nagahashi's use of a single substrate concentration did not allow any further analysis of the pH dependence of the ATPase activity. Since the substrates for the barley ATPase are the $MeATP^{2-}$ complexes, it is essential that substrate ionization be considered in the analysis of the pH dependence of the ATPase activity (Segel 1975), assuming one wishes to determine the pH optimum of the ATPase itself. Since the level of $MeATP^{2-}$ declines as the pH is reduced from pH 7 to pH 5, it is possible that the pH optima for many plant ATPases around pH 6.5 (Hodges 1976, Leonard and Hotchkiss 1978, Kawasaki *et al.* 1979) may, in part, result from the pH-dependent decline in substrate concentration.

The Ca^{2+}-dependent and Mg^{2+}-dependent ATPase activities had the same pH optimum for the maximal velocities of both the high and low affinity catalytic components (Figure 6). This result is consistent with the data presented in Figure 4, which were interpreted to indicate that both $CaATP^{2-}$ and $MgATP^{2-}$ bind to the same catalytic sites. Furthermore, the oligomycin insensitivity of the Ca^{2+}-dependent ATPase, the relative purity of the membrane material used in this study (Table 1), and the acidic pH optima of the Ca^{2+}-dependent ATPase activities (Figure 6) strongly suggest that this enzymatic activity is not of mitochondrial origin, as has been suggested for some of the Ca^{2+}-dependent ATPases from other plants (Hodges 1976).

Despite the methodological differences in the amalysis of plant ATPases, certain characteristics of the barley root ATPase activities are quite similar to the ATPase activities of other plants and barley cultivars. For the divalent cation-dependent ATPases from plant membranes, the $MeATP^{2-}$ complex is the primary enzyme substrate (Lindberg *et al.* 1974, Balke and Hodges 1975, Hendrix and Kennedy 1977, Leonard and Hotchkiss 1978). Barley divalent cation-dependent ATPase activity was higher in the presence of Ca^{2+} than in the presence of Mg^{2+} (Nagahashi *et al.* 1978). A similar result has been reported for the divalent cation-dependent ATPase from wheat roots (Kylin and Kähr 1973). Many plant ATPases are inhibited by high free ATP levels (Lindberg *et al.* 1974, Balke and Hodges 1975, Christiansen and Lindberg 1976) and high substrate levels (Balke and Hodges 1975, Travis and Booz 1979).

From a general biological perspective, the barley root ATPase activities possess characteristics in common with animal transport

ATPases. The Ca^{2+} transport ATPase of sarcoplasmic reticulum (Neet and Green 1977, DuPont 1977), Ca^{2+}-ATPase of human red blood cell membranes (Richards *et al.* 1978), and Na^{+}, K^{+}-ATPase (Cantley and Josephson 1976, Glynn and Karlish 1976) all possess kinetics indicating high and low affinity catalytic sites. Using methods essentially identical to those used in this study, Barron and Disalvo (1979) concluded that the Ca^{2+}- and Mg^{2+}-dependent ATPase activities from bovine, aortic microsomes are ascribable to a single enzyme. The value of the Hill coefficient for the sarcoplasmic reticulum (Ca^{2+} + Mg^{2+})-ATPase increases with increasing assay temperature (Neet and Green 1977). This result is similar to the temperature-dependent increase in the nonlinearity parameter for the barley ATPase (Figure 8).

In conclusion, the results of this study demonstrate that barley root, plasma membrane-bound ATPase kinetics determined at physiological temperatures differ appreciably from those reported for other plants. These differences can be partially explained in terms of methodological considerations and do not necessarily result from inherent differences between barley ATPase activities and those of other plants. The similarity between the kinetics of the barley divalent cation-dependent ATPase activities and those of various ion-stimulated animal ATPases, conclusively implicated in ion transport, suggests the possibility that the barley ATPase might perform similar functions.

CHAPTER 3

TEMPERATURE DEPENDENCE OF THE BARLEY ROOT PLASMA MEMBRANE-BOUND Ca^{2+}- AND Mg^{2+}-DEPENDENT ATPase

The following manuscript has been accepted for publication in Physiologia Plantarum.

INTRODUCTION

The kinetic parameters of membrane-bound enzymes often display a complex temperature dependence, generally characterized by nonlinear Arrhenius and van't Hoff plots (Thilo *et al.* 1977, Silvius *et al.* 1978, McMurchie 1979, Silvius and McElhaney 1980, Wolfe and Bagnall 1980, Silvius and McElhaney 1981). Until recently, Arrhenius plot nonlinearities for plant membrane-bound enzymes have usually been attributed to temperature-dependent changes in the physical state of the membrane bulk lipids in the form of lipid phase transitions or lateral phase separations (Raison 1973, Raison and Chapman 1976). However, there is an increasing body of evidence which suggests that the bulk lipid phase transitions and separations of most plant membranes may occur at temperatures significantly below the physiological temperature range (Quinn and Williams 1978, Bishop *et al.* 1979, Pike *et al.* 1979). Nonetheless, a large number of enzymatic and transport processes known to be localized in plant membranes have been found to display Arrhenius plot discontinuities in the temperature range of 10 to 20 °C (Quinn and Williams 1978, Lyons *et al.* 1979).

In the literature (Quinn and Williams 1978, Lyons *et al.* 1979), numerous examples are described which seem to indicate strong correlations between abrupt temperature-dependent changes in the motion of membrane-associated stearate spin labels, monitored by electron spin resonance spectroscopy (EPR), and Arrhenius plot discontinuities recognized in measurements of the temperature dependence of membrane-bound enzymes. On the other hand, with nuclear magnetic resonance spectroscopy (NMR), it has been demonstrated

that there exist no abrupt changes in the bulk lipid acyl chain mobility in the sarcoplasmic reticulum membrane from 5 to 40 °C (Davis *et al.* 1976). Conversely, the Arrhenius plot derived from sarcoplasmic reticulum Ca^{2+}-ATPase experiments indicates a change in activation energy between 15 and 20 °C which coincides with an altered mobility of a stearate spin probe measured with EPR (Inesi *et al.* 1973, Davis *et al.* 1976). Rice *et al.* (1979) have suggested that variations in lipid polar head group mobility may be transmitted to the lipid acyl chains. In turn, the rate of catalysis by the membrane-bound enzyme may be determined by the lipid acyl chain ordering within the membrane (Sinensky 1979). Therefore, the enzymatic reaction site may be modulated by temperature- or ion-dependent changes in lipid polar head group mobility and their respective spatial arrangements.

As briefly discussed in the previous chapter, the kinetic properties of the Ca^{2+}- and Mg^{2+}-dependent ATPase activity from a plasma membrane-rich microsome fraction isolated from the roots of barley are modified by changes in the assay temperature. Therefore, a detailed analysis of the temperature dependence of the ATPase kinetic constants was performed and the results compared to EPR measurements of temperature-dependent changes in the properties of the membrane lipids.

MATERIALS AND METHODS

Chemicals and syntheses. 5NS and 12NS were purchased from Syva Corp. (Palo ALto, CA, USA). CAT_{12} was synthesized according to the methods of Mehlhorn and Packer (1976), using precursors obtained from Aldrich

Chemical Co. (Milwaukee, WI, USA). All other chemicals were obtained from the sources given in Chapter 2.

Plant material and membrane isolation. Barley seeds (*Hordeum vulgare* L. cv. Conquest) were germinated and grown over an aerated solution of 0.25 mM $CaSO_4$ (pH 6.5) in the dark at 16 ± 1 °C. A plasma membrane-rich microsome fraction was isolated from the roots of 5-day-old seedlings as previously decribed (Caldwell and Haug 1980, Chapter 2) and used immediately for ATPase and EPR experiments. Membrane protein was measured by the method of Wang and Smith (1975).

ATPase assay procedures. ATPase activity was measured in a 1 ml reaction volume, containing 20 mM Tris-MES buffer (pH 6.5), Tris-ATP, and divalent cation as its dichloride salt or EDTA as its Tris salt. The pH of the reaction buffer was adjusted to pH 6.5 at the temperature for the ATPase assay. Unless otherwise noted, divalent cation was added at a constant molar excess of 10 mM over the concentration of added ATP and the concentration of enzyme substrate, $CaATP^{2-}$ or $MgATP^{2-}$, calculated (Caldwell and Haug 1980, Chapter 2, Appendix 1). The ATPase reaction solutions and the membrane suspension were preincubated at the desired temperature for 15 min before the initiation of the reaction by the addition of membrane preparation to the reaction solution to give a final concentration of 2 µg membrane protein/ml. The proper incubation times were predetermined at each temperature, using a continuous flow assay procedure (Caldwell and Haug 1980, Chapter 2). After incubation for the appropriate time, the reaction was stopped and the amount of released P_i determined (Rathbun and Betlach 1969). All experimental velocities are the means of at least two determinations and have the unit µmol P_i released x $(\text{mg protein})^{-1}$ x h. The divalent cation-dependent

ATPase activity represents the enzymatic activity found in the presence of added cations, subtracting the activity determined in the absence of added cations and with 1 mM EDTA (Caldwell and Haug 1980, Chapter 2). All experiments were repeated with different batches of membrane preparations.

Kinetic constant calculation and Arrhenius plot analysis. The kinetic constants of the observed high and low affinity catalytic components of the Ca^{2+}- and Mg^{2+}-dependent ATPase were calculated as previously described (Caldwell and Haug 1980, Chapter 2). Nonlinear Arrhenius plots were analyzed either by fitting a series of straight line segments to the computed V_{max} values, using standard linear regression procedures, or by fitting the V_{max} values directly to equation 1 (Sprague *et al.* 1980), using nonlinear least squares (Caldwell and Haug 1980, Chapter 2).

$$\log(V)=\left[\ln K_{T_{ref}} - \frac{\Delta H^{\ddagger}_{T_{ref}} - T_{ref}\Delta C^{\ddagger}_{p}}{R}\left(\frac{1}{T}-\frac{1}{T_{ref}}\right) + \frac{\Delta C^{\ddagger}_{p}+R}{R}\ln\left(\frac{T}{T_{ref}}\right)\right]2.3^{-1} \quad (1)$$

The parameters determined in equation 1 were $\ln K_{T_{ref}}$, $\Delta H^{\ddagger}_{T_{ref}}$ in kcal mol^{-1}, and $\Delta C^{\ddagger}_{p}$ in cal mol^{-1} $°K^{-1}$. T represents the absolute temperature where V_{max} had been determined and T_{ref} was an arbitrary reference temperature (303 °K). The nonlinear correlation coefficient (R^2) was computed and used as a goodness-of-fit criterion (Dammkoehler 1966).

Electron paramagnetic resonance spectroscopy. Total membrane lipids were isolated from the barley root plasma membrane-rich microsomes by the methods of Williams and Merrilees (1970) with 0.05% butylated hydroxytoluene being included during the chloroform-methanol extraction. All manipulations were performed under N_2 and the isolated lipids

stored under N_2 at -40 °C until needed. Aqueous lipid dispersions were prepared from the isolated lipids and 20 mM Tris-MES buffer (pH 6.5) as described by Leonards and Haug (1980). There was no detectable protein in the isolated lipids.

CAT_{12} was added to the membrane suspensions at a concentration of 10 nmol/mg membrane protein and to the aqueous lipid dispersions at a concentration of about 15 nmol/mg lipid. The stearate spin probes (5NS, 12NS) were added to the microsomes and lipid dispersions so that the probe concentration was about 0.1% of the lipid weight of the sample. Insertion of the stearate spin probes into the microsomes or lipid dispersions was facilitated by a 15 min sonication in an ultrasonic cleaner (Cole-Parmer 8845-4).

EPR spectra were obtained with a Varian X-band EPR spectrometer, model E-112, equipped with variable temperature controller. Sample temperatures were monitored with an Omega Eng., model 250, copper/constantan thermocouple. All spectra were obtained at a microwave power of 15 mW. The hyperfine splitting parameters, $2T_{//}$ and $2T_{\perp}$ (gauss), were measured directly from the first derivative EPR spectra (Figure 9).

RESULTS

Temperature dependence of the ATPase kinetic constants. The Ca^{2+}- and Mg^{2+}-dependent ATPase activities of the barley root plasma membrane-rich microsomes displayed complex kinetics characterized by nonlinear double reciprocal plots, suggesting the presence of multiple catalytic sites (Caldwell and Haug 1980, Chapter 2). Therefore, it was necessary to use a computer program

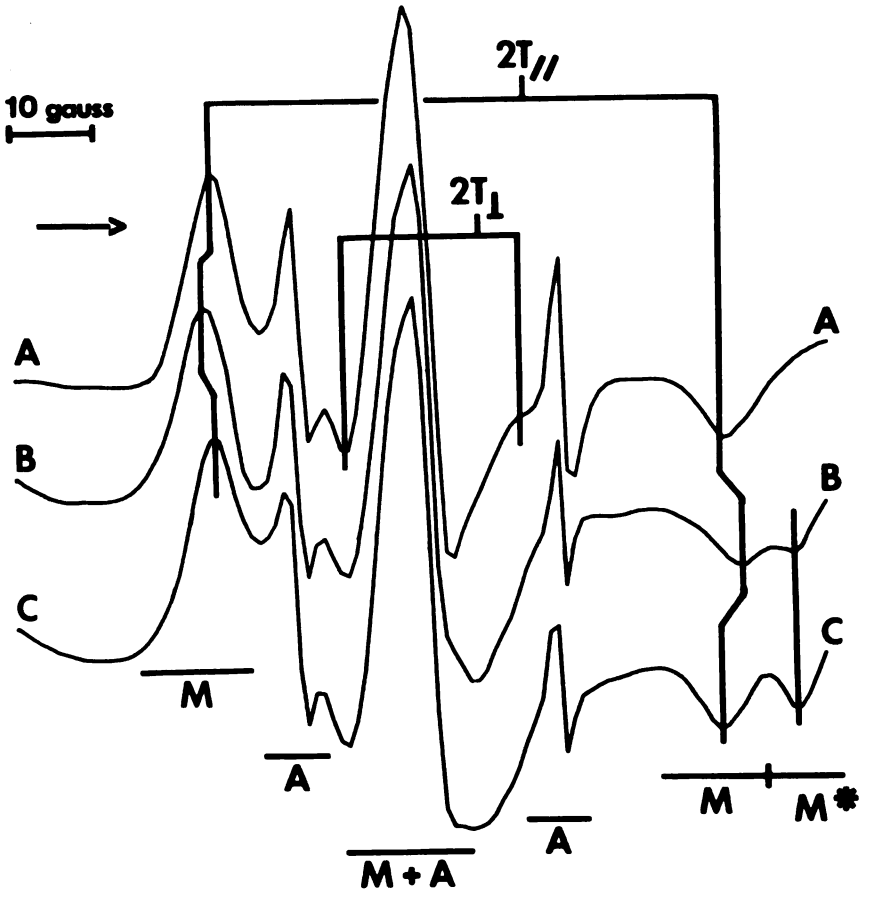

Figure 9. *First derivative EPR spectra of the barley root plasma membranes and aqueous lipid dispersions spin labelled with* CAT_{12}. Barley root plasma membrane-rich microsomes and aqueous lipid dispersions prepared from the total lipids isolated from the microsomes were spin labelled with CAT_{12} and EPR spectra obtained as described in the Materials and Methods. The particular spectra shown were drawn using a computer program after the original spectra were digitized. The method for the measurement of $2T_{//}$ and $2T_{\perp}$ in gauss is demonstrated. $2T_{\perp}$ could not be accurately determined for spectra B and C. The arrow indicates the direction of increasing magnetic field strength. Spectral components resulting from the signal of membrane-associated spin probe are denoted with a M. A highly immobilized spin probe signal in spectra B and C is labelled with a M*. CAT_{12} spectral components resulting from free probe are denoted with an A. Spectrum A was obtained with an aqueous lipid dispersion at 15 °C. Spectra B and C were obtained with microsomes at 5 and 15 °C, respectively.

to calculate the apparent K_m and V_{max} values for the observed high and low affinity catalytic components (Appendix 1). The symbols K_H, V_H, K_L, and V_L have been used to designate the apparent K_m and V_{max} values for the high and low affinity catalytic components, respectively.

Arrhenius plots of the computed V_H and V_L for both the Ca^{2+}- and Mg^{2+}-dependent ATPase activities are clearly triphasic (Figure 10). Excluding the low temperature region (Silvius *et al.* 1978, Silvius and McElhaney 1980), a series of straight line segments did not accurately fit the Arrhenius plots (Figure 10). However, curves drawn according to equation 1, using the computed values of $\ln K_{T_{ref}}$, $\Delta H^{\ddagger}_{T_{ref}}$, and $\Delta C^{\ddagger}_{p}$ given in Table 3, accurately fit the V_{max} values (Table 3, Figure 10).

Plots of K_m as a function of temperature were also complex (Figure 11). Both the high and low affinity ATPase catalytic components markedly increased in enzyme-substrate affinity as the temperature was raised from 4 to 14 °C. This temperature range with increasing affinities was followed by a temperature region in which the K_m values were relatively temperature independent (Figure 11). At even higher temperatures, an increase in K_m was observed. With the exception of the low affinity Ca^{2+}-dependent ATPase component (Figure 11B), the highest enzyme-substrate affinities were obtained at temperatures near the barley seedling growth temperature (16 °C).

Lipid acyl chain and polar head group mobility in the intact membrane. Analysis of the EPR spectra of spin probes incorporated into biological membranes often involves the calculation of an order parameter (S) to assess the motional order or fluidity of the membrane lipids

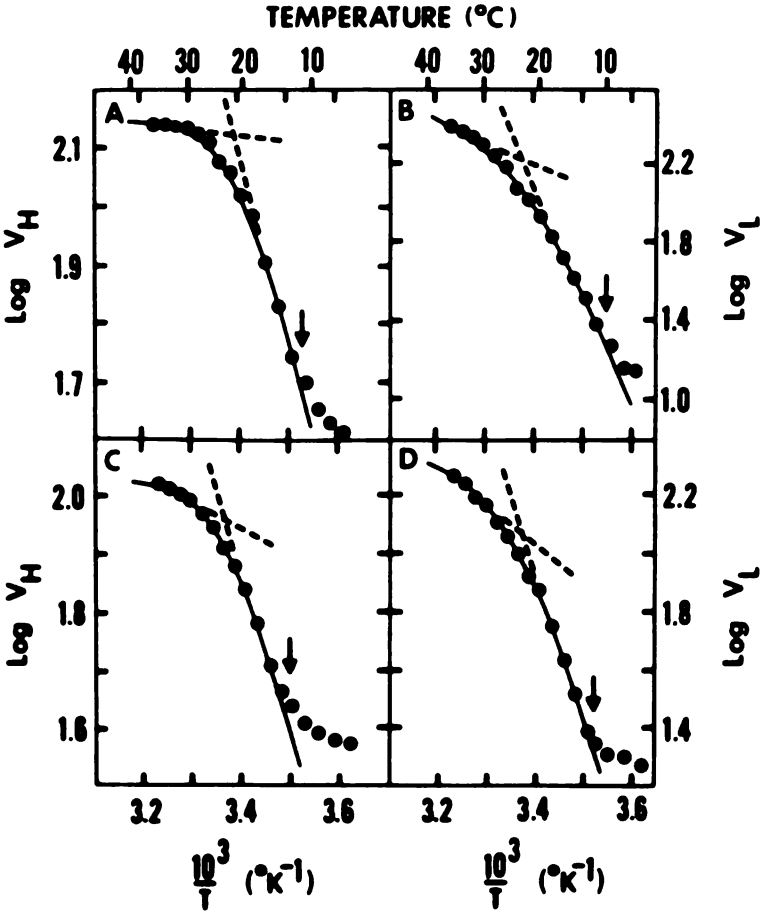

Figure 10. *Arrhenius plots of the computed V_{max} values for the Ca^{2+}- and Mg^{2+}-dependent ATPase activities.* The assay mixture contained 20 mM Tris-MES buffer (pH 6.5), Tris-ATP, and divalent cation added at a constant molar excess of 10 mM over the Tris-ATP concentration. V_H and V_L represent the computed V_{max} values for the high and low affinity catalytic components, respectively, and have the unit μmol P_i released x (mg protein)$^{-1}$ x h^{-1}. All V_{max} values presented have standard errors of less than 5% of the computed values. The dashed line represents an attempt to analyze the Arrhenius plots using linear segments. The solid curve was drawn with equation 1 and the computed parameters given in Table 3. Only V_{max} values for enzyme velocities determined at temperatures above those denoted by the arrows were used in the calculation of the parameters of equation 1. Parts A and B are the Arrhenius plots of the Ca^{2+}-dependent ATPase activities. Parts C and D are the Arrhenius plots of the Mg^{2+}-dependent ATPase activities.

Table 3. *Calculated parameters from the fitting of equation 1 to Arrhenius plots of the barley root plasma membrane-bound* Ca^{2+}- *and* Mg^{2+}-*dependent ATPase activities.* **The unknown parameters of equation 1 were calculated by fitting the Arrhenius plots of the high affinity (HA) and low affinity (LA) catalytic components of the ATPase activities to equation 1 by nonlinear least squares. The values of these parameters are given with their standard errors. The nonlinear correlation coefficient (R^2) was also computed.**

Substrate	Component	(Figure)	$\ln(K)_{T_{ref}}$	$\Delta H^{\ddagger}_{T_{ref}}$ (kcal mol^{-1})	$\Delta C^{\ddagger}_{p}$ (cal $mol^{-1} {}^{\circ}K^{-1}$)	R^2
$CaATP^{2-}$	HA	(10A)	4.9 ± 0.15	2.1 ± 0.12	-785 ± 67	0.99
$CaATP^{2-}$	LA	(10B)	4.8 ± 0.18	10.9 ± 0.43	-770 ± 49	0.99
$MgATP^{2-}$	HA	(10C)	4.6 ± 0.11	4.2 ± 0.29	-716 ± 57	0.99
$MgATP^{2-}$	LA	(10D)	5.0 ± 0.22	9.2 ± 0.37	-738 ± 82	0.99

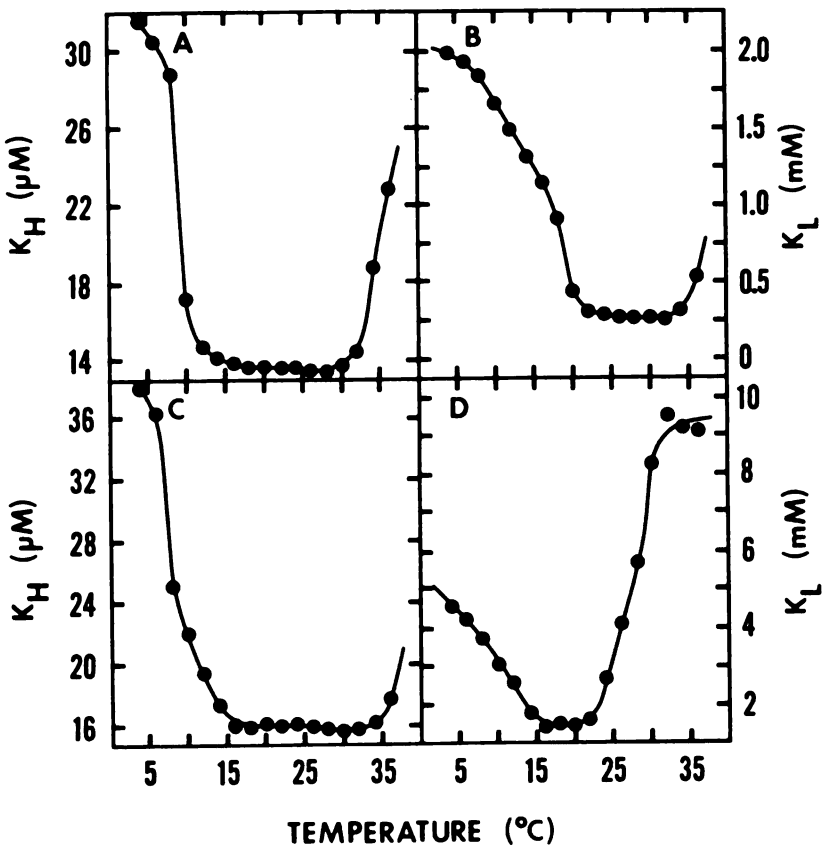

Figure 11. *Temperature dependence of the computed K_m values for the Ca^{2+}- and Mg^{2+}-dependent ATPase activities.* The ATPase assay conditions are described in Figure 10. K_H (μM) and K_L (mM) represent the computed K_m values of the high and low affinity ATPase catalytic components, respectively. All K_m values presented have standard errors of less than 2.5% of the computed values. The solid curve was drawn as the best visual fit to the data. Parts A and B give the temperature dependence of the K_m of the Ca^{2+}-dependent ATPase activities. Parts C and D give the temperature dependence of the K_m values of the Mg^{2+}-dependent ATPase activities.

(Griffith and Jost 1976, Gordon *et al.* 1978). However, calculation of S requires the accurate determination of both $2T_{//}$ and $2T_{\perp}$ from the EPR spectra (Figure 9). As shown in Figure 9, $2T_{\perp}$ could not be measured from the EPR spectra of CAT_{12} incorporated into the microsomes. Similarily, an accurate determination of $2T_{\perp}$ was not possible for 5NS-labelled membranes at temperatures below 14 °C (data not shown). Since calculation of S was not possible for all the spin probes employed in this study and, if polarity effects are ignored, $2T_{//}$ is linearly related to S (Griffith and Jost 1976), the values of $2T_{//}$ have been used as approximate measures of membrane lipid fluidity (Griffith and Jost 1976, Herring and Weeks 1979). Therefore, an increase in the value of $2T_{//}$ by a reduction of sample temperature is indicative of spin probe immobilization as a result of a temperature-dependent restriction of lipid mobility. Since $2T_{\perp}$ has often been difficult to measure for spin labels in biological membranes, the use of $2T_{//}$ alone as an index of membrane lipid fluidity has been considered useful in studies of membranes where interpretations are based on relative changes in the EPR spectra (Griffith and Jost 1976).

Discontinuities in the plot of $2T_{//}$ versus temperature for 5NS in the barley root plasma membrane-rich microsomes were observed at 7 and 32 °C in the absence of Ca^{2+} and at 11 and 33 °C in the presence of 10 mM Ca^{2+} (Figure 12). The restriction of 5NS mobility by Ca^{2+} suggests that Ca^{2+} binding to the lipid polar head groups (McLaughlin *et al.* 1971) can reduce the mobility of the lipid acyl chains near the membrane surface.

Although designed to measure changes in membrane surface charge (Mehlhorn and Packer 1976), the positively charged spin probe CAT_{12}

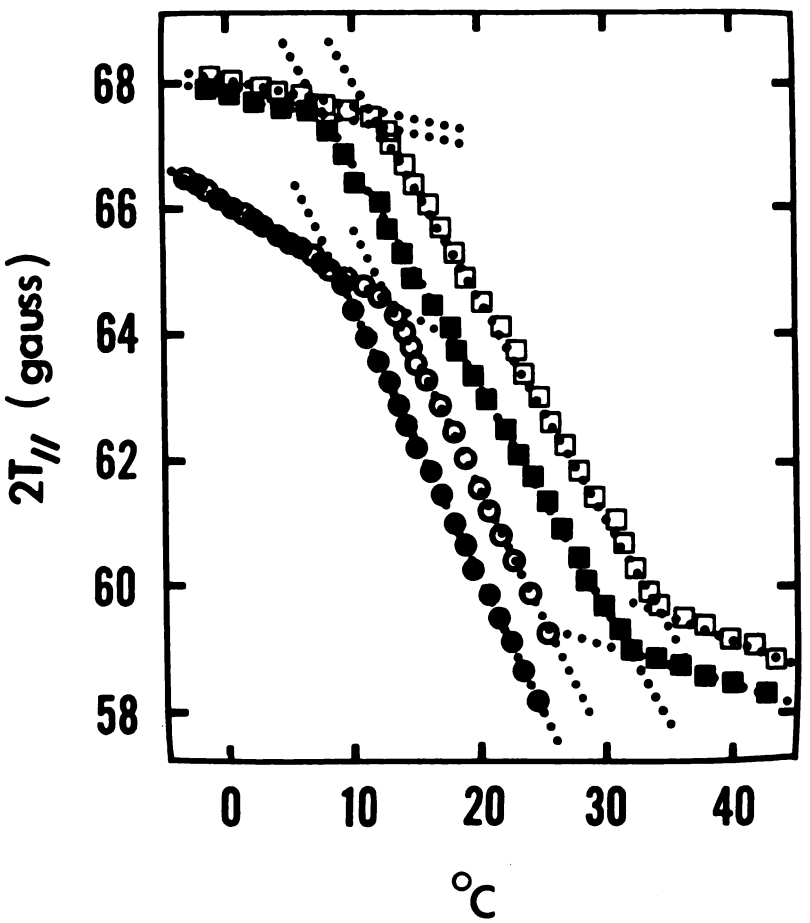

Figure 12. *$2T_{//}$ as a function of temperature in barley root plasma membranes spin labelled with CAT_{12} and 5NS.* The hyperfine splitting parameter, $2T_{//}$ (gauss), was measured from EPR spectra (Figure 9) of barley root plasma membrane-rich microsomes spin labelled with CAT_{12} and 5NS as described in the Materials and Methods. The dotted lines were drawn using standard linear regression procedures. The membranes were spin labelled with either CAT_{12} in the presence (○) and absence (●) of 10 mM $CaCl_2$ or 5NS in the presence (□) and absence (■) of 10 mM $CaCl_2$.

can also be used to measure the mobility of the lipid polar head groups, assuming that its amphiphilic characteristics results in the nitroxide being situated at the level of the charged lipid head groups. Plots of $2T_{//}$ for CAT_{12} in the microsomes as a function of temperature display discontinuities at 8.5 °C in the absence of added Ca^{2+} and at 13 °C in the presence of 10 mM Ca^{2+} (Figure 12). Unfortunately, the low field signal which results from the immobilization of CAT_{12} in the membrane was distorted by the signal of free probe at temperatures above 25 °C and, therefore, $2T_{//}$ could not be determined (Figure 9).

Increasing concentrations of $CaCl_2$ reduced the mobility of the lipid polar head groups at constant temperature (16 °C), as measured with CAT_{12} (Figure 13). Under the same conditions, increasing concentrations of Ca^{2+} also resulted in a decrease in the mobility of 5NS and 12NS in the membrane (Figure 13). Assuming that Ca^{2+} acts at the membrane surface (McLaughlin *et al.* 1971, Gordon *et al.* 1978), this indicates that the stearate spin probes are sensitive to Ca^{2+}-induced changes in the motion of the lipid polar head groups. Furthermore, the magnitude of the Ca^{2+}-induced reduction in spin probe motion diminished in terms of a gradient, as the position of the nitroxide was moved from the membrane surface (CAT_{12}) into the membrane (5NS, 12NS)(Figure 13). This suggests that the influence of lipid polar head group mobility decreases with increasing depth into the membrane. The inhibition of the Ca^{2+}-dependent ATPase activity by high levels of free Ca^{2+} appears to be correlated to the Ca^{2+}-induced decrease in lipid polar head group mobility (Figure 13). This result is consistent with the observations of Gordon *et al.* (1978), who suggested that

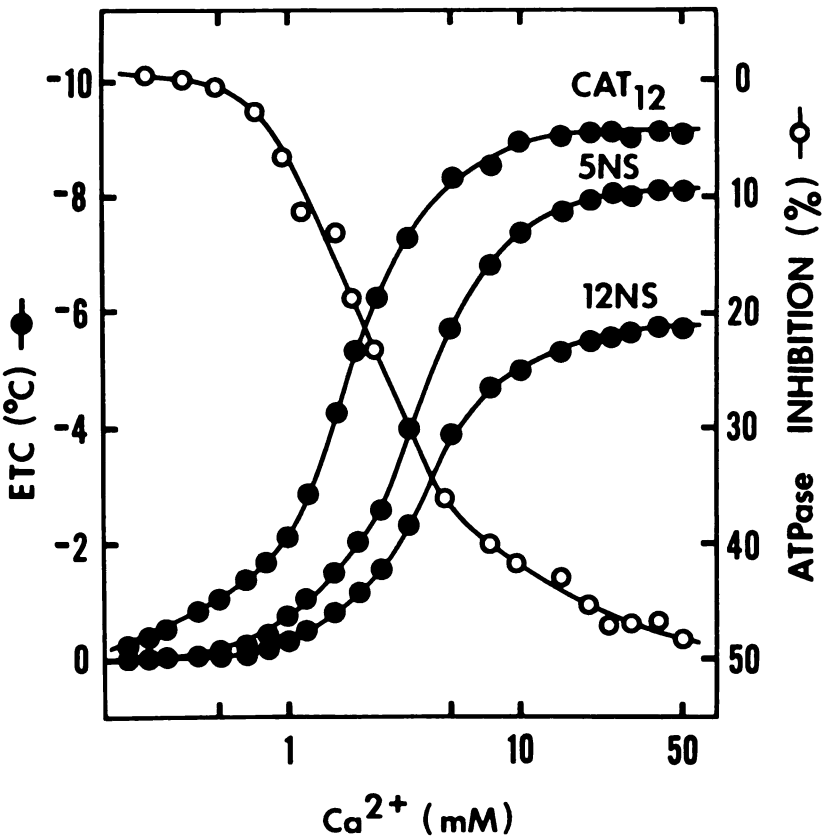

Figure 13. *The effects of Ca^{2+} on the rotational mobilities of CAT_{12}, 5NS, and 12NS in barley root plasma membranes and the Ca^{2+}-dependent ATPase activity.* The barley root plasma membrane-rich microsomes were spin labelled with either CAT_{12}, 5NS, or 12NS as described in the Materials and Methods. The effects of increasing concentrations of Ca^{2+} on the rotational mobilities of the spin probes in the membrane are presented as an equivalent temperature change (ETC) in °C determined at 16 °C. ETC represents, in this case, the decrease in temperature necessary to produce the same value of $2T_{//}$ as that caused by the given concentration of Ca^{2+}. The inhibition of the Ca^{2+}-dependent ATPase by increasing levels of Ca^{2+} was determined according to the assay conditions given in the Materials and Methods and given in the form of the % inhibition by Ca^{2+} of the optimal Ca^{2+}-dependent ATPase activity [114 ± 4.2 μmol P_i released x $(mg\ protein)^{-1}$ x h^{-1}]. The ATPase velocities were the means of triplicate determinations and had standard errors of less than 4% of the given values.

the inhibition of the membrane-bound Na^+, K^+-ATPase of rat liver by Ca^{2+} was related to a Ca^{2+}-mediated decrease in membrane fluidity. Temperature dependence of lipid polar head group mobility in aqueous dispersions of membrane lipids. To determine whether the observed discontinuities in the plots of $2T_{//}$ versus temperature for the spin probes incorporated into the intact membranes represent properties of the bulk membrane lipids or of the lipids directly associated with the membrane-bound proteins, the same experiments which produced the results presented in Figure 12 were repeated with aqueous dispersions of lipids isolated from the plasma membrane-rich microsomes. Discontinuities in the plots of $2T_{//}$ versus temperature for 5NS in the lipid dispersions were observed 7 °C in the absence of Ca^{2+} and at 12 °C in the presence of 10 mM $CaCl_2$ (Figure 14). As was the case for CAT_{12} in the membrane above 25 °C, the increased mobility of 5NS in the lipid dispersions did not allow the measurement of $2T_{//}$ for 5NS above 30 °C. Plots of $2T_{//}$ for CAT_{12} in the lipid dispersions as a function of temperature display discontinuities at 7 °C in the absence of Ca^{2+} and at 12 °C in the presence of 10 mM Ca^{2+} (Figure 14). Therefore, it seems likely that the discontinuities in the temperature dependence of 5NS and CAT_{12} mobility in the membrane at 7 °C and 8.5 °C, respectively, (Figure 12) represent properties of the bulk membrane lipids, since similar discontinuities were observed at essentially the same temperatures in the absence of membrane protein (Figure 14).

It is interesting to note that the EPR spectra of CAT_{12} incorporated into the aqueous lipid dispersions are composed of a signal resulting from free probe and a signal from a single relatively immobilized component (Figure 9). Conversely, the

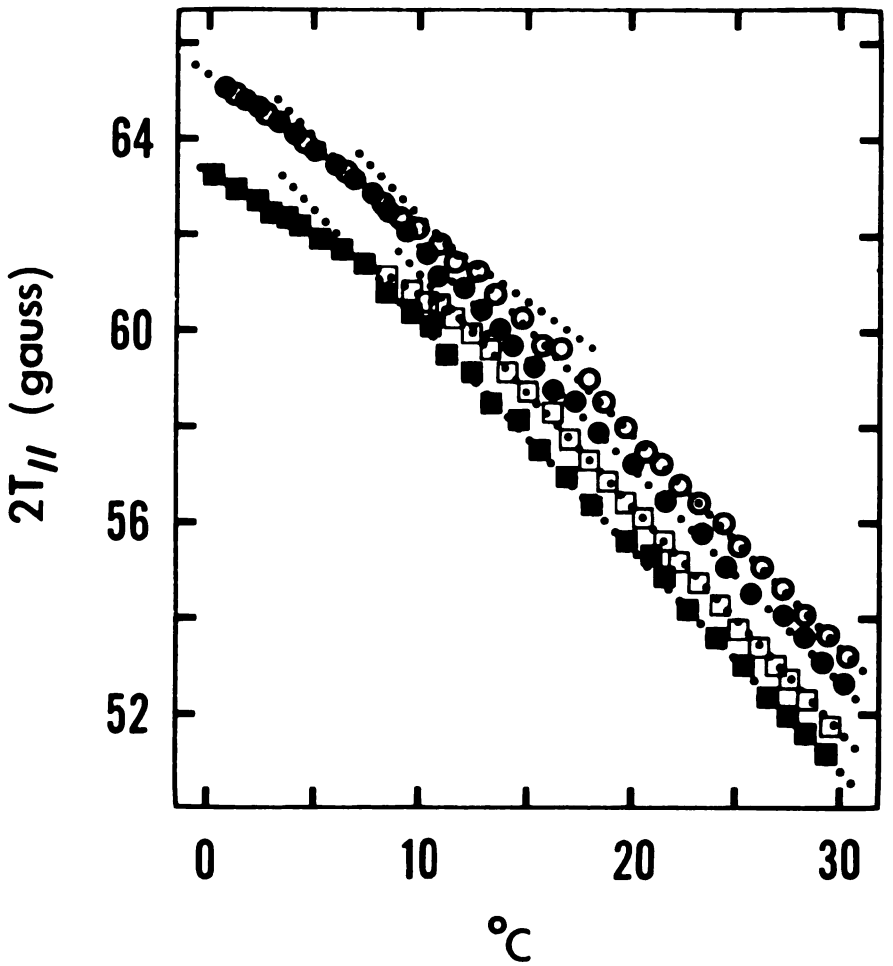

Figure 14. *$2T_{//}$ as a function of temperature in aqueous lipid dispersions spin labelled with CAT_{12} and 5NS.* With the exception that aqueous lipid dispersions prepared from the total lipids isolated from barley root plasma membrane-rich microsomes were used instead of intact membranes, the experimental conditions, method of data presentation, and symbol designation are the same as those presented in Figure 12.

spectra of CAT_{12} incorporated into the microsomes are the superimposition of the same free and immobilized spin probe signals, as well as signals of one or more highly immobilized components (Figure 9). The highly immobilized signal(s) may represent spin probes directly associated with membrane-bound proteins or lipids whose motion is restricted by their association with membrane-bound proteins.

DISCUSSION

Temperature dependence of the ATPase kinetic parameters. The changes in the activation energy for the Ca^{2+}- and Mg^{2+}-dependent ATPase activities over the temperature range 4 to 14 °C (Figure 10) apparently result from temperature-dependent alterations in K_m (Figure 11)(Silvius *et al.* 1978). However, with the possible exception of the low affinity Mg^{2+}-dependent ATPase component (Figures 10 and 11), the curvature of the Arrhenius plots above 14 °C could not be attributed to temperature-dependent K_m changes until the temperature exceeded approximately 34 °C (Figures 10 and 11). This situation allowed the analysis of the Arrhenius plots by the application of equation 1, which is conceptually similar to a relation recently described by Silvius and McElhaney (1980). Silvius and McElhaney (1980) based their equation on the assumption that the enzymatic reaction has a finite $\Delta C_p^{\ddagger}$. They obtained a $\Delta C_p^{\ddagger}$ of -515 cal mol^{-1} $°K^{-1}$ when they fitted Arrhenius plots of the Na^+, Mg^+-ATPase of *Acholeplasma laidlawii* to their equation. The values of $\Delta C_p^{\ddagger}$ for the barley root ATPase activities are of the same order of magnitude and, within computational error,

identical for all the Arrhenius plots presented in Figure 10 (Table 3).

Even though it is apparent that equation 1 accurately describes the temperature dpendences of the V_{max} values for the barley root ATPase activities, the significance of the computed parameters is not clear. Only the enthalpy values differ for the different ATPase components (Table 3). Recently, Silvius and McElhaney (1981) have presented a variety of models which allow the fitting of Arrhenius plots to models based on different aspects of lipid-protein and protein-protein interactions in membranes. However, all the models fit curvilinear Arrhenius plots equally well and substantiating experiments are required to prove the validity of the model employed. In regard to the significance of the computed values produced by fitting Arrhenius plots to the various models, Silvius and McElhaney (1981) stated that the current knowledge of the energetics of protein-lipid interactions was insufficient to allow detailed analysis of the values of the computed parameters.

With the possible exception of the low affinity Ca^{2+}-dependent ATPase component (Figure 11), the optimal enzyme-substrate affinities were obtained over a temperature range from near the growth temperature of the barley seedlings (16 °C) to about 34 °C (Figure 11). The increase in K_m at low and high temperatures observed for the barley root ATPase activities is similar to the influence of temperature on the enzyme affinities of poikilothermic marine animals, where the highest enzyme-substrate affinities were observed at the growth temperature of the organism (Somero and Hochachka 1976). It remains to be determined whether the temperatures for optimal K_m values for the barley root ATPase activities can be

modified by changing the growth temperature of the seedlings.

Effect of membrane fluidity on ATPase activity. The temperatures at which large changes in K_m are observed (Figure 11) roughly coincide with the temperatures for the discontinuities in the plots of $2T_{//}$ as a function of temperature (Figures 12 and 14). In the presence of Ca^{2+} at a concentration roughly equivalent to that used in the ATPase assay (10 mM), a significant change in the mobility of the lipid polar head groups occurred at 13 °C, as measured with CAT_{12} (Figure 12). If the alterations in lipid polar head group mobility represent a change in the molecular ordering of the head groups, then the decrease in polar head group ordering, as the temperature is raised above 13 °C, could allow a protein conformational change, which requires a change in protein volume or results in the formation of oligomeric structures (Hoffman *et al.* 1979). Conversely, even at assay temperatures above 13 °C, the addition of a sufficient quantity of Ca^{2+} could inhibit the ATPase activity by the binding of Ca^{2+} to the lipid polar head groups, increasing the head group ordering. This interpretation is consistent with the results presented in Figure 13. Increasing concentrations of Ca^{2+} decreased the mobility of the lipid polar head groups, as well as the fluidity of the lipid acyl chains and inhibited the barley root Ca^{2+}-dependent ATPase activity.

At temperatures above 34 °C, the affinity of the ATPase activities for substrate decreases (Figure 11) concomitant with a change in the temperature dependence of 5NS motion in the membrane (Figure 12). This situation is similar to that which occurs at 13 °C. However, the increase in K_m at higher temperatures is not reflected in a change in V_{max} (Figure 10). Since for technical reasons it was not

possible to measure the motion of the spin probes in the aqueous lipid dispersions at high temperatures, it is not clear what the change in the temperature dependence of spin probe motion observed near 34 °C may represent.

The possible involvement of boundary lipids in the temperature dependence of the ATPase activities. Even though it is possible to correlate the change in ATPase kinetic parameters at low and high temperatures to temperature-dependent alterations in the mobility of the membrane lipids, the possible involvement of temperature-dependent changes in lipid mobility at intermediate temperatures is less clear. Above 13 °C to about 34 °C, the K_m values for the catalytic components of the Ca^{2+}- and Mg^{2+}-dependent ATPase activities were relatively temperature independent (Figure 11), while the Arrhenius plots of the ATPase maximal velocities displayed curvilinear characteristics over the same temperature range (Figure 10). These results are quite similar to those of the temperature dependence of the Na^+, Mg^{2+}-ATPase of *Acholeplasma laidlawii* (Silvius and McElhaney 1980). Silvius and McElhaney (1980) interpreted their results as indicating the involvement of boundary lipids in the regulation of the membrane-bound ATPase activity. Similarily, McMurchie (1979) has recently obtained curvilinear Arrhenius plots for plant membrane-bound ATPase activities, although the use of a single substrate concentration did not allow a detailed analysis of the Arrhenius plots (Silvius *et al.* 1978). Since the Arrhenius plot curvature was the result of experiments performed at temperatures believed to be above the temperature for the completion of the bulk lipid phase transition, McMurchie (1979) interpreted these plots as possibly indicating the presence of boundary lipids

around the ATPases. The indication of boundary lipids in the barley root plasma membrane-rich microsomes (Figure 9) suggests that boundary lipids may play a significant role in the regulation of the barley root membrane-bound ATPase activities over the temperature range 13 to 34 °C.

From EPR studies, the acyl chains of lipids associated with membrane-bound proteins appear to be immobilized relative to the acyl chain mobility of the bulk lipids (Jost *et al.* 1973). Therefore, these boundary lipids may have different physical characteristics than the bulk lipids. However, on the time scale of NMR, little evidence was found for the immobilization of lipid acyl chains by the addition of purified sarcoplasmic reticulum ATPase to an artifical phospholipid bilayer (Rice *et al.* 1979). On the other hand, ^{31}P-NMR spectral changes strongly suggested the presence of interactions between the phospholipid polar head groups and charged groups on the ATPase. The interactions restricted the lipid polar head group mobility which, in turn, may be transmitted to the lipid acyl chains (Rice *et al.* 1979). This interpretation is similar to the interpretation of the results presented in Figure 13, which indicated that a reduction in lipid polar head group mobility by Ca^{2+} could induce a decrease in lipid acyl chain fluidity, as measured with the stearate spin probes. Boss and Mott (1980) recently observed a similar reduction in spin probe mobility by Ca^{2+} with carrot protoplasts.

As mentioned in the chapter Introduction, it is no longer appropriate to automatically interpret changes in spin probe mobilities in terms of cooperative bulk lipid phase transitions. Moreover, EPR data indicating lipid changes in the 10 to 20 °C temperature

range may reflect minor changes in lipid organization (Quinn and Williams 1978). However, considering the results presented here and the large number of plant membrane-bound enzymes which are characterized by Arrhenius plot discontinuities above 10 °C, then subtle changes in the physical state of the plant membrane lipids observed at temperatures above 10 °C may be of greater physiological significance than the bulk lipid phase transitions *per se*.

CHAPTER 4

DIVALENT CATION INHIBITION OF THE BARLEY ROOT PLASMA MEMBRANE-BOUND Ca^{2+}-DEPENDENT ATPase AND ITS REVERSAL BY MONOVALENT CATIONS

The following manuscript has been submitted for publication in Physiologia Plantarum.

INTRODUCTION

In general, the activities of membrane-bound enzymes are sensitive to changes induced by environmental factors in the physical state of the surrounding lipids. As shown in Chapter 3, the kinetic constants of the Ca^{2+}- and Mg^{2+}-dependent ATPase activities in a plasma membrane-rich microsome fraction isolated from the roots of barley displayed complex temperature dependencies. The change in ATPase kinetic constants were attributed to temperature-dependent alterations in the mobility of the membrane lipid polar head groups. It was also observed that increasing concentrations of Ca^{2+} reduced the mobility of the lipid polar head groups at constant temperature, concomitant with a decrease in ATPase activity (Caldwell and Haug 1981, Chapter 3). Such a cation-induced inhibition may be similar to the reduction in ATPase activity obtained by lowering the assay temperature, in that both processes result in a decrease in the mobility of the membrane lipid polar head groups.

Therefore, it was of interest to characterize in greater detail the effects of cations on the barley root plasma membrane structure and its constituent ATPase activity. The inhibition of plant ATPases by divalent cations (Hodges 1976) - which has previously been considered to be the result of ion-protein interactions - may actually result from ion-lipid interactions.

MATERIALS AND METHODS

Chemicals and syntheses. The sources of required chemicals and the methods for CAT_{12} synthesis can be found in the Materials and Methods of Chapter 3.

Plant material and membrane isolation. The growth conditions for the barley seedlings and the procedure for the isolation of a plasma membrane-rich microsome fraction from the barley roots can be found in the Materials and Methods of Chapter 2.

ATPase assay procedures. ATPase activity was measured in a 1 ml reaction volume, containing 20 mM Tris-MES buffer (pH 6.5), 1 mM Tris-ATP, 0.75 mM $CaCl_2$, and, depending upon the experimental protocol, various concentrations of other cations. Unless otherwise noted, all cations were added as their chloride salts. Prior to the addition of Tris-ATP, membrane preparation was added to the reaction solutions to give a final concentration of 2 µg membrane protein/ml and the solutions were preincubated at 16 °C for 15 min. The reactions were initiated by the addition of Tris-ATP. The proper incubation times were predetermined as previously described (Caldwell and Haug 1980, Chapter 2). After incubation for the appropriate time at 16 °C, the reactions were stopped and the amount of released P_i determined (Rathbun and Betlach 1969). All experimental velocities [µmol P_i released x $(mg\ protein)^{-1}$ x h^{-1}] are the means of at least two determinations and all experimental assay series have been repeated with different batches of membrane preparations. The Ca^{2+}-dependent ATPase activity represents the ATPase activity determined in the presence of 0.75 mM $CaCl_2$, subtracting the ATPase activity determined in the absence of added Ca^{2+} and with 1 mM EDTA (Caldwell and Haug 1980, Chapter 2). The Ca^{2+}-dependent ATPase inhibition by the addition of cations is expressed on a percent inhibition basis with the ATPase activity found with 0.75 mM $CaCl_2$ being considered to be 100 % or uninhibited. In experiments involving monovalent cation reversal of Cd^{2+}

inhibition of the ATPase activity, the % inhibition of the Ca^{2+}-dependent ATPase activity in the presence of monovalent cations was based on the ATPase activity in the presence of 0.75 mM $CaCl_2$ and the given concentration of monovalent cation being 100 %. In all experiments, the Ca^{2+}-dependent ATPase activities were corrected for the reduction in $CaATP^{2-}$ levels by increasing concentrations of cations (Caldwell and Haug 1980, Chapter 2, Appendix 1).

Electron paramagnetic resonance spectroscopy. EPR spectra were obtained with a Varian X-band spectrometer, model E-112, equipped with variable temperature controller. Sample temperature was monitored with an Omega Eng., model 250, copper/constantan thermocouple. All spectra were obtained at 16 ± 0.25 °C. CAT_{12} was added to the membrane suspensions at a ratio of 15 nmol/mg membrane protein. Various concentrations of cations were added to the spin labelled membranes such that the increase in sample volume never exceeded 5% of the original volume. After the addition of cations, the sample was incubated at 16 °C for 5 min before the EPR spectra were obtained. The hyperfine splitting parameter, $2T_{//}$ (gauss), was measured directly from the first derivative EPR spectra (Figure 15) and is an index of relative changes in the mobility of the spin probe in the membrane (Caldwell and Haug 1981, Chapter 3). As previously described (Caldwell and Haug 1981, Chapter 3), the values of $2T_{//}$ were converted to an equivalent temperature change (ETC), a quantity expressing the change in $2T_{//}$ caused by the addition of cations to the membrane. ETC represents the change in temperature necessary to match the observed change in membrane lipid polar head group mobility measured with CAT_{12} resulting from cation

application. Therefore, a negative value of ETC indicates a reduction in lipid mobility.

Application of CAT_{12} to the membrane suspensions resulted in EPR spectra (Figure 15) which allowed the simultaneous measurement of both ETC and $\Delta\psi_s$. Therefore, after the addition of cations, a $\Delta\psi_s$ value was calculated from the first derivative EPR spectra (Figure 15) as previously described (Quintanilha and Packer 1977).

RESULTS

Effect of divalent cation on $\Delta\psi_s$, ETC, and Ca^{2+}-dependent ATPase activity. As previously demonstrated (Caldwell and Haug 1981, Chapter 3), the addition of increasing concentrations of Ca^{2+} to barley root plasma membrane suspensions markedly reduced the lipid polar head group mobility and the Ca^{2+}-dependent ATPase activity (Figure 16A). However, the magnitude of the change in the membrane surface charge, $\Delta\psi_s$ also changed with increasing Ca^{2+} levels (Figure 16A). This represents the effect of increasing concentrations of Ca^{2+} in the electrical double layer at some distance above the membrane surface. These results are consistent with the ability of Ca^{2+} to both bind to acidic phospholipids and screen the surface charge (McLaughlin *et al.* 1971). Therefore, to distinguish between the inhibition of ATPase activity by the restriction of lipid polar head group mobility by Ca^{2+} binding and ATPase inhibition by the decrease in membrane surface charge by Ca^{2+} screening, it was necessary to employ divalent cations known to have distinct effects on phospholipids. Sr^{2+} mainly screen surface charge (McLaughlin *et al.* 1971). The addition of Sr^{2+} did not alter the values of ETC or inhibit the

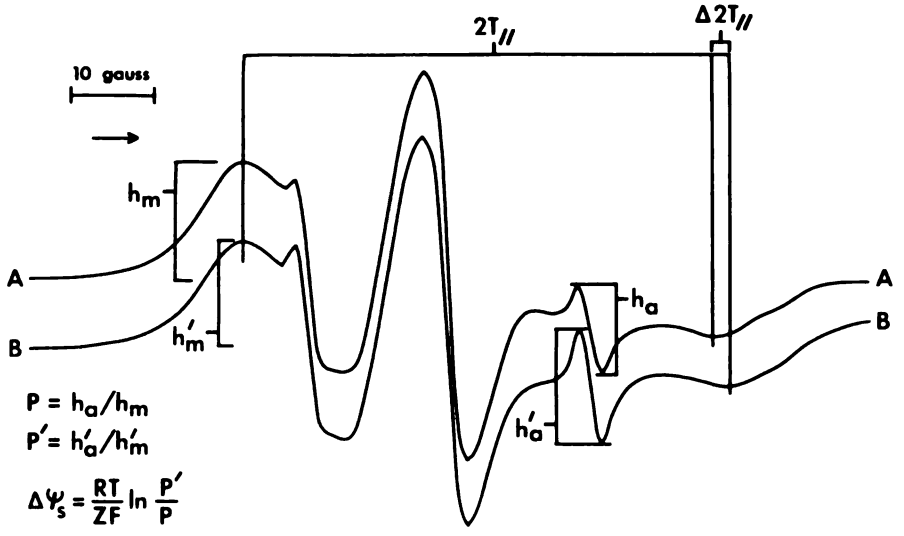

Figure 15. *Representative first derivative EPR spectra of barley root plasma membranes spin labelled with* CAT_{12}. Barley root plasma membrane-rich microsomes were spin labelled with CAT_{12} as described in the Materials and Methods. $2T_{//}$ was measured directly from the first derivative EPR spectra. The partition coefficient, P, for CAT_{12} partition between the membrane and aqueous environment was determined by measuring the heights of the low field membrane-bound signal (h_m) and the high field free probe signal (h_a). The change in the membrane surface potential, $\Delta\psi_s$ (mV), after the addition of ions could then be calculated as shown. The arrow indicates the direction of increasing magnetic field strength.

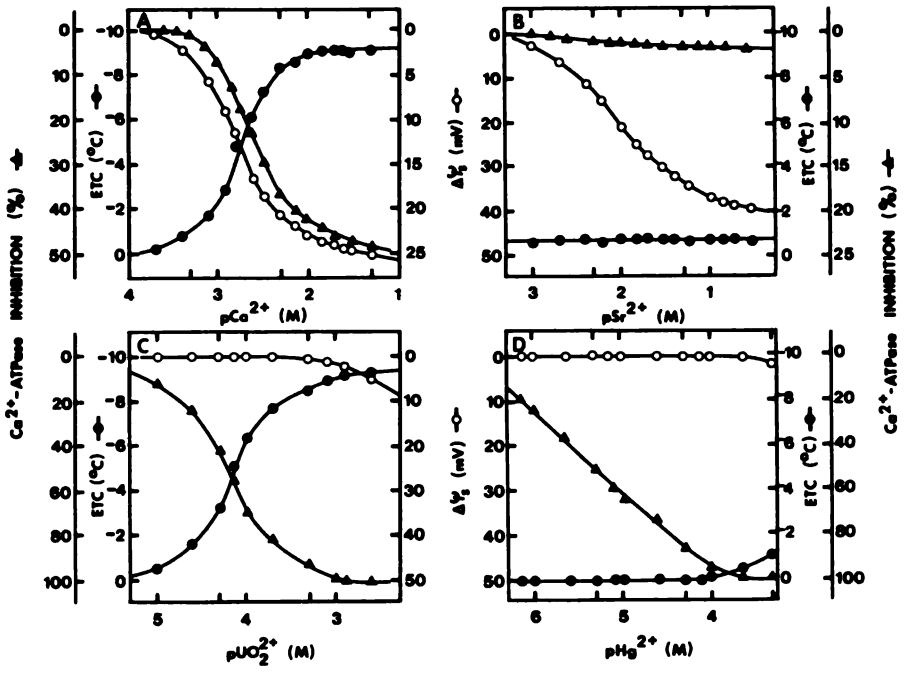

Figure 16. *Effect of divalent cations on the ETC, $\Delta\psi_s$, and Ca^{2+}-dependent ATPase activity of barley root plasma membranes.* The effects of varying concentrations of Ca^{2+} (A), Sr^{2+} (B), UO_2^{2+} (C), and Hg^{2+} (D) on the Ca^{2+}-ATPase activity, ETC, and $\Delta\psi_s$ were determined at 16 °C as described in the Materials and Methods. The effect of the cations on the ATPase activity is presented as the % inhibition of the enzyme activity determined in the presence of 0.75 mM $CaCl_2$ [122 ± 3.6 μmol P_i released x (mg protein)$^{-1}$ x h^{-1}]. The ATPase activities had standard errors of less than 5% of the given values.

Ca^{2+}-dependent ATPase (Figure 16B). Sr^{2+} did induce a decrease in membrane surface negativity (Figure 16B), as would be expected from its ability to screen membrane surface charge. Conversely, UO_2^{2+} strongly interacts with the phosphodiester groups of acidic phospholipids (McLaughlin *et al.* 1971). As shown in Figure 16C, the UO_2^{2+}-induced inhibition of Ca^{2+}-dependent ATPase activity closely follows the reduction in lipid polar head group mobility by UO_2^{2+}. UO_2^{2+} can also change $\Delta\psi_s$ (Figure 16C). However, the effect of UO_2^{2+} on membrane surface charge is observed at concentrations of cation at which the UO_2^{2+}-induced restriction of lipid polar head group mobility and ATPase inhibition are essentially complete. Even though Hg^{2+} changes both ETC and $\Delta\psi_s$ at higher concentrations, Hg^{2+} had already completely inhibited the Ca^{2+}-dependent ATPase activity before the effects of Hg^{2+} on the membrane were observed, suggesting that Hg^{2+} acts directly upon the ATPase protein.

Effect of Cd^{2+} on $\Delta\psi_s$, ETC, and Ca^{2+}-dependent ATPase activity and its reversal by monovalent cations. Increasing levels of Cd^{2+} inhibited the Ca^{2+}-dependent ATPase activity and changed both the lipid polar head group mobility and the membrane surface charge (Figure 17A). In the presence of 1 mM Cd^{2+}, the addition of increasing concentrations of NaCl could partially reverse the effects of Cd^{2+} on the ATPase activity with a concomitant increase in ETC and a decrease in membrane surface negativity (Figure 17B). Although less effective than NaCl, KCl had similar effects (data not shown). Ethanolamine·HCl was more effective than NaCl in reversing the Cd^{2+}-induced inhibition of the ATPase while not altering ETC or $\Delta\psi_s$ to the same extent at NaCl (Figure 17C). Choline chloride could change $\Delta\psi_s$, but had little effect on ETC and Cd^{2+} inhibition of the

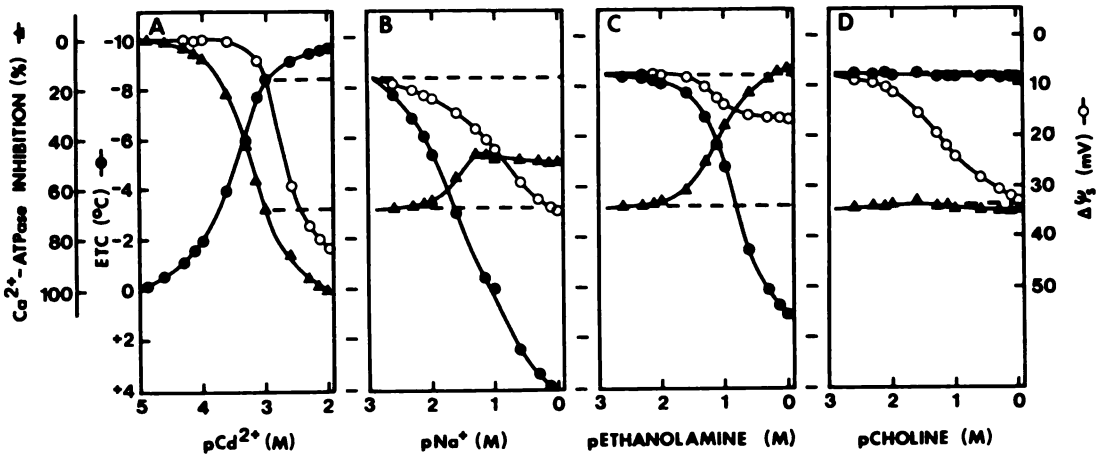

Figure 17. *Effect of Cd^{2+} on ETC, $\Delta\psi_s$, and Ca^{2+}-dependent ATPase activity and the modification of the Cd^{2+}-induced changes by monovalent cations.* The assay conditions and calculations are the same as those presented in Figure 16. Part A shows the effect of varying levels of Cd^{2+} on ETC, $\Delta\psi_s$, and ATPase activity. Parts B, C, and D show the effects of NaCl, ethanolamine·HCl, and choline chloride, respectively, on the ETC, $\Delta\psi_s$, and Ca^{2+}-ATPase activity found in the presence of 1 mM $CdCl_2$.

Ca^{2+}-dependent ATPase activity (Figure 17D).

Since the inhibition of the Ca^{2+}-dependent ATPase by Cd^{2+} was reversible (Figure 17), the reversibility of the observed inhibitions of the ATPase by Ca^{2+}, UO_2^{2+}, and Hg^{2+} (Figure 16) was determined by method of Ackermann and Potter (1949). As shown in Figure 18, the degree of inhibition of the ATPase by the various divalent cations was independent of membrane concentration, thus indicating that the inhibitions were indeed reversible. Even though the reversibility of the Ca^{2+}-dependent ATPase inhibition by Cd^{2+} had already been demonstrated (Figure 17), an Ackermann-Potter plot for the Cd^{2+}-induced inhibition of the ATPase was prepared (Figure 18C) to confirm the utility of this plotting method for the system under investigation.

Effect of anions on the Na^+ reversal of the Cd^{2+}-induced inhibition of the Ca^{2+}-dependent ATPase. Since anions also interact with membrane phospholipids by both screening and binding (Hauser *et al.* 1976), the effect of anions on the Na^+ reversal of Cd^{2+} inhibition of the Ca^{2+}-dependent ATPase was examined. The nature of the Na^+ counterion influenced the degree of Na^+ reversal of the Cd^{2+} inhibition of the ATPase (Figure 19). Cl^- was the least effective, while SCN^- anion produced the best reversal of the ATPase inhibition by Cd^{2+}. Overall, the various anions followed the sequence $SCN^- > I^- > NO_3^- \cong Br^- > Cl^-$ in their capacity to modulate the Na^+ reversal of Cd^{2+}-induced Ca^{2+}-dependent ATPase inhibition (Figure 19). For the purpose of calculating the percent inhibition of the ATPase by Cd^{2+}, the Ca^{2+}-dependent ATPase activity in the presence of the various Na^+ salts and in the absence of Cd^{2+} had to be determined. Therefore, the effects of the various anions on the Na^+ stimulation

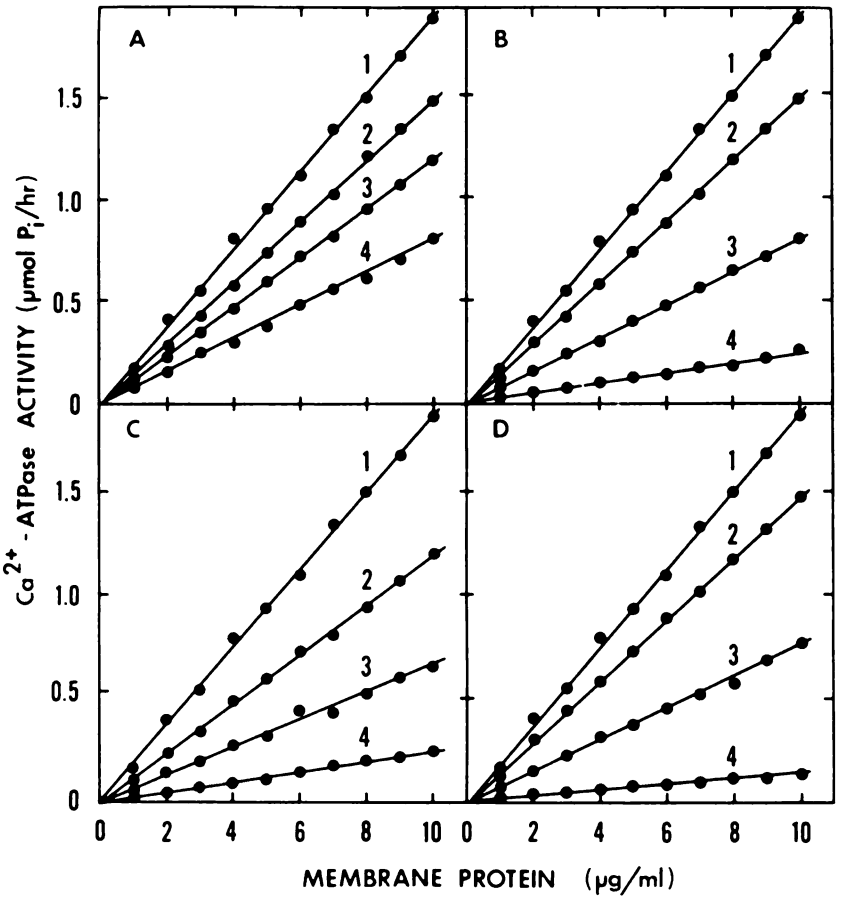

Figure 18. *Ackermann-Potter plots of the Ca^{2+}-dependent ATPase activities found in the presence of inhibitory divalent cations.* The % inhibition of the Ca^{2+}-ATPase activity by various divalent cations was calculated as described in the Materials and Methods and in Figure 16, and plotted as a function of membrane protein concentration in the reaction solution. Part A shows the % inhibition of the ATPase activity versus membrane concentration in the presence of 0 mM (1), 2.5 mM (2), 7.5 mM (3), and 50 mM (4) $CaCl_2$. Part B is the same as Part A except with 25 μM (2), 75 μM (3), and 200 μM (4) UO_2Cl_2. Part C is the same as Part A except with 0.5 mM (2), 1 mM (3), and 2.5 mM (4) $CdCl_2$. Part D is the same as Part A except with 0.75 μM (2), 7.5 μM (3), and 100 μM (4) $HgCl_2$.

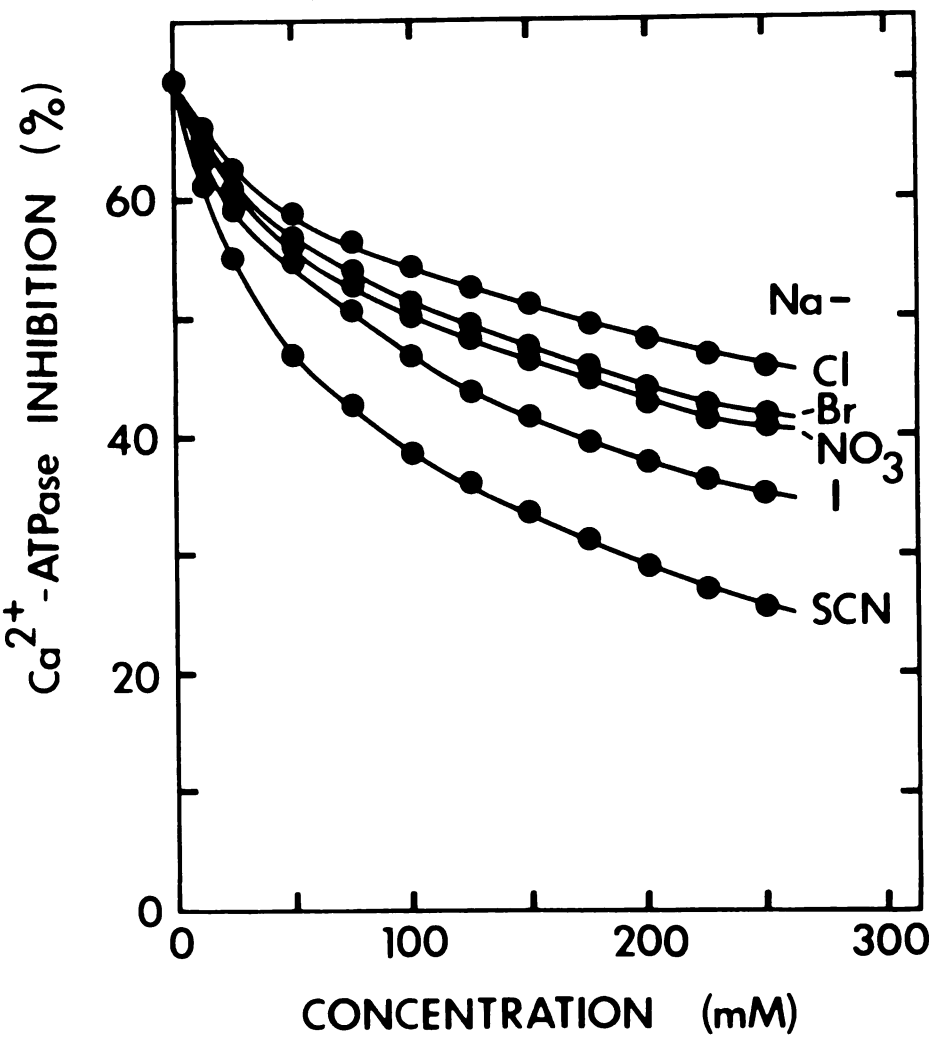

Figure 19. *Effect of different anions on the reversal of Cd^{2+} inhibition of the Ca^{2+}-dependent ATPase activity by Na^{+}.* The effect of Na^{+} with the given counterions on the inhibition of the Ca^{2+}-dependent ATPase by 1 mM $CdCl_2$ was determined as described in Figure 17.

of the Ca^{2+}-dependent ATPase activity were also measured. The following sequence $Cl^- > Br^- > NO_3^- = I^- > SCN^-$ was found (data not shown), demonstrating that Cl^- enhances Na^+ stimulation of the Ca^{2+}-dependent ATPase more than SCN^-. NaF was also tested and found to inhibit the ATPase completely at concentrations above 25 mM (data not shown), a result similar to that obtained with other plant plasma membrane-bound ATPases (Cambraia and Hodges 1980).

DISCUSSION

The plasma membrane-bound ATPase activities of barley roots require divalent cations for optimal activity (Caldwell and Haug 1980, Chapter 2). Kinetic analysis of the Ca^{2+}- and Mg^{2+}-dependent ATPase activities of the barley root plasma membranes strongly suggests that divalent cation-ATP complexes serve as the active substrates for the enzyme (Caldwell and Haug 1980, Chapter 2). However, even those divalent cations which complex with ATP to form active substrates can inhibit the ATPase (Caldwell and Haug 1980, Chapter 2). As previously discussed (Caldwell and Haug 1981, Chapter 3), the observed inhibition of the barley root Ca^{2+}-dependent ATPase activity by high levels of Ca^{2+} may be related to the ability of Ca^{2+} to bind to negatively charged phospholipids, restricting the mobility of the lipid polar head groups. However, the results presented (Caldwell and Haug 1981, Chapter 3) did not preclude alternative mechanisms.

At least four major mechanisms for the inhibition of ATPase activity by multivalent cations are possible. First, the added

cations could compete with Ca^{2+} for ATP^{4-}, forming partially or totally inactive cation-ATP complexes. Second, the cation could directly modify some essential component of the ATPase catalytic site. Third, the added cations could inhibit the ATPase by changing the local concentration of the charged substrate at the membrane surface through alterations in the membrane surface charge by cation accumulation in the electrical double layer above the membrane (Wojtczak and Nalecz 1979). Four, the cations could bind to the membrane lipids, especially boundary lipids, modifying the ATPase activity by altering the characteristics of the lipid-protein interactions.

Under the experimental conditions employed in this study, corrections were made for the formation of inactive substrate at high divalent cation concentrations. Therefore, the first mechanism is not likely to be a factor. As mentioned in the Results, Hg^{2+} inhibited the Ca^{2+}-dependent ATPase at concentrations below those which produced observable effects on the properties of the membrane lipids (Figure 16D). Therefore, it seems likely that Hg^{2+} acts directly upon the ATPase protein, without lipid mediation. It has already been suggested that the inhibition of plant ATPases by Hg^{2+} involves the action of the ion on essential sulfhydryl groups in the enzyme (Hodges 1976).

Alterations in the membrane surface charge may also influence the activities of membrane-bound enzymes which have charged substrates (Wojtczak and Nalecz 1979). Agents which reduce the negativity of the membrane surface would allow an increase in the local concentration of anionic substrates, such $CaATP^{2-}$, and, thereby, stimulate enzyme activity. According to this model, divalent cations should

stimulate the Ca^{2+}-dependent ATPase activity, since they decrease the negativity of the membrane surface (Figure 16). However, Sr^{2+} had little effect on ATPase activity, even though it decreased membrane surface negativity (Figure 16B). Moreover, UO_2^{2+} inhibited the Ca^{2+}-dependent ATPase activity at concentrations below those which modified the membrane surface charge (Figure 16C). Therefore, according to these findings, the third mechanism for the ATPase inhibition by divalent cations does not appear to be a major factor under the experimental conditions employed in this study.

The effects of Sr^{2+} and UO_2^{2+} on the Ca^{2+}-dependent ATPase activities of the barley root plasma membranes support the fourth mechanism for the divalent cation inhibition of the ATPase. The inhibition of the ATPase activity by UO_2^{2+} closely follows the UO_2^{2+}-induced reduction in lipid polar head group mobility (Figure 16C). As previously demonstrated (Caldwell and Haug 1981, Chapter 3), the activities of the barley root membrane-bound ATPase responded quite sensitively to temperature-induced changes in the motion of the surrounding lipids. Consequently, a temperature-induced reduction in ATPase maximal velocities with decreasing temperature (Caldwell and Haug 1981, Chapter 3) may be compared to an isothermal enzyme inhibition by divalent cations which restrict lipid polar head group mobility. Divalent cations such as Sr^{2+} which do not alter the motion of the lipid polar head groups (Figure 16B) would be expected to have little effect on the ATPase activity.

Monovalent cations can also modulate the motion of membrane lipids by changing the electrolyte environment (Träuble and Eibl 1974). Nonspecific screening effects by monovalent cations may markedly influence the surface potential which, in turn, modifies

the ionization of surface-associated sites (Träuble and Eibl 1974). Therefore, upon addition of monovalent cations, the apparent binding constants for the association of divalent cations with the lipid phosphodiester groups are altered by the increased ionic strength, resulting in a release of bound divalent cations from the membrane surface. Such a release may enhance the head group mobility of the membrane lipids, leading to a stimulation of the membrane-bound enzyme.

Reversal of the Cd^{2+}-induced inhibition of the Ca^{2+}-dependent ATPase activity closely followed the monovalent cation-induced increase in lipid polar head group mobility (Figure 17). The greater change in $\Delta\psi_s$ by Na^+ relative to ethanolamine·HCl (Figure 17) may account for the differences in the ability of these cations to reverse the Cd^{2+}-induced ATPase inhibition. Considering the difference in ionic radii between Na^+ and ethanolamine·HCl and the ability of monovalent cations to bind to membrane lipids (Hauser *et al.* 1976), the combined binding and screening effects of Na^+ could essentially neutralize the surface charge of the membrane. Since a certain amount of charged lipid is required for ATPase activity (Fourcans and Jain 1974), the loss of negative charge by Na^+-lipid binding and screening effects could inhibit the Ca^{2+}-dependent ATPase activity. Choline was ineffective in reversing the Cd^{2+} inhibition of the ATPase and changing ETC, while significantly altering the membrane surface charge (Figure 17D). Choline was also ineffective in stimulating the Ca^{2+}-dependent ATPase activity in the absence of Cd^{2+} (data not shown). This result is consistent with the earlier report of Ratner and Jacoby (1973), who found that choline had no effect on the Mg^{2+}-dependent ATPase activity of barley roots, while the ATPase was stimulated by Na^+

and ethanolamine·HCl. The enhancement of membrane lipid motion by monovalent cations appears to be a prerequisite for the stimulation of the ATPase activity by monovalent cations in barley root plasma membranes.

As a results of their ability to reverse the inhibition of the Ca^{2+}-dependent ATPase by Cd^{2+}, Na^{+} and ethanolamine·HCl gave high apparent stimulations of the ATPase activity in the presence of Cd^{2+}. For example, 50 mM NaCl stimulated the Ca^{2+}-dependent ATPase activity by 21% in the absence of Cd^{2+} and by 103% in the presence of 1 mM Cd^{2+}. Similar effects were obtained with low concentrations of Hg^{2+} and Al^{3+} (data not shown). It is possible that inhibitory levels of cations are introduced into the ATPase reaction solution from reaction components, particularly ATP (Tornheim *et al.* 1980). Therefore, a portion of the observed stimulation of the Ca^{2+}-dependent ATPase activity by monovalent cations may actually result from a deinhibition of the ATPase activity by monovalent cations and not from specific ion-protein interactions.

Anions also bind to phospholipids (Hauser *et al.* 1976). The strength of interaction of anions with phospholipid $-N(CH_3)_3^+$ groups has been shown to be as follows $SCN^- > I^- > NO_3^- > Br^- > Cl^- > F^-$ (Hauser *et al.* 1976). Neglecting F^-, which may inhibit the ATPase by direct action on the ATPase protein, this sequence is essentially the same as that found for the effect of anions on the degree of Na^+ reversibility of the Cd^{2+} inhibition of the Ca^{2+}-dependent ATPase activity (Figure 19). Therefore, anions may influence the Cd^{2+} inhibition of the ATPase by direct association with membrane lipid, modulating the cation-binding properties of the lipid phosphodiester groups (Hauser *et al.* 1976). Conversely, the sequence of anion

effects on the Na^+ stimulation of the Ca^{2+}-dependent ATPase activity suggests that anion binding to lipids diminishes the effectiveness of Na^+ in stimulating the ATPase.

In conclusion, it is apparent that divalent cations can inhibit the Ca^{2+}-dependent ATPase activity of barley root plasma membranes by binding to membrane lipids and that this effect can be partially reversed by monovalent cations. In the absence of added inhibitory cations, the monovalent cation stimulation of the barley root ATPase activities does not necessarily indicate ion-protein interaction and is, therefore, not suggestive of the ATPase activity being involved in the transport of these ions. Nonetheless, the results suggest the possibility that other phytotoxic heavy metals or lipophilic agents can modify plant growth and development by alteration of the physical properties of the plasma membrane or the membranes of cytoplasmic organelles which, in turn, change the activities of membrane-associated biochemical processes,

CHAPTER 5

SOLUBILIZATION, PURIFICATION, AND LIPID REQUIREMENTS OF THE DIVALENT CATION-DEPENDENT ATPase OF BARLEY ROOT PLASMA MEMBRANES

INTRODUCTION

As shown in Chapter 2, the divalent cation-dependent ATPase of barley root plasma membrane-rich microsomes displayed complex kinetics, characterized by nonlinear double reciprocal plots. Since it was not possible to confirm unambiguously enzyme negative cooperativity with the membrane preparation used in that study, the results were analyzed and interpreted in terms of multiple catalytic sites. Determination of negative cooperativity requires the knowledge of the number of different ATPases in the barley root plasma membrane preparation. One method for the determining the number of different ATPases in the membrane is to solubilize and purify the ATPase. If a single ATPase is found which possesses the kinetic properties of the ATPase activities in the intact membrane, then negative cooperativity is indicated. Conversely, if multiple ATPases are found, then the use of the multiple catalytic site model of the barley root ATPase activities is justified.

The kinetic behavior of the barley root plasma membrane-bound ATPase (Caldwell and Haug 1980, Chapter 2) resembled that of the Ca^{2+}-ATPase in erythrocyte membranes (Richards *et al.* 1978). In the latter case, the two classes of catalytic sites apparently result from the partial activation of a single enzyme by the Ca^{2+}-dependent cytoplasmic activator protein, calmodulin (CaM)(Rega *et al.* 1979). Furthermore, the Mg^{2+}-dependent ATPase of corn was stimulated by CaM in the presence of Ca^{2+} (Dieter and Marmé 1981). In view of these aspects, a preliminary study was conducted to ascertain the sensitivity of the barley root ATPase towards CaM. Although a Ca^{2+}-dependent stimulation of barley ATPase by CaM was observed, the

CaM-stimulated activity was rapidly lost. Considering the possible high phospholipase activity in barley membrane preparations (Gibrat and Rossignol 1977) and the essential requirement for certain phospholipids in the CaM sensitivity of the erythrocyte Ca^{2+}-ATPase (Gietzen *et al.* 1980, Niggli *et al.* 1981), it seemed possible that the lability of the CaM sensitivity of the barley root ATPase activities might be related to the loss of essential phospholipids by phospholipase action. Since inhibition of phospholipases during membrane isolation is difficult, confirmation of this hypothesis would be facilitated by the use of purified ATPase, allowing the determination of the lipid requirements of the various ATPase activities.

The solubilization and purification of plant membrane-bound ATPases has been the subject of a number of recent publications (Benson and Tipton 1978, DuPont and Leonard 1980, Baydoun and Northcote 1981, Dieter and Marmé 1981, Tognoli and Marrè 1981). However, only DuPont and Leonard (1980) employed partially purified plant plasma membranes as the source of the ATPase. Therefore, the cellular location of the ATPases isolated by the other investigators is not clear. The degree of purity and % recovery of the various ATPases varied considerably, even when the same tissue was employed. For the ATPase isolated from corn roots, the molecular weights of the purified and partially purified ATPases ranged from 30,000 daltons (Benson and Tipton 1978) to 36,000 daltons (Baydoun and Northecote 1981) to greater than 500,000 daltons (DuPont and Leonard 1980). In the latter case, the molecular weight was based on gel filtration of detergent-lipid-protein micelles and, therefore, of little significance.

Since the purification of the barley ATPase might allow the determination of both the mechanism for the complex enzyme kinetics and the involvement of phospholipids in certain types of ATPase activity, an effort was made to solubilize and purify the barley root ATPase.

MATERIALS AND METHODS

Chemicals and syntheses. ε-Amino-n-caproic acid, 1,1'-carbonyldiimidazole, Sepharose 4B-CL, L-α-phosphatidylethanolamine (type IV), L-α-phosphatidylinositol (grade III), L-α-phosphatidyl-L-serine (bovine brain), L-α-phosphatidylcholine (type III-S), and asolectin were purchased from Sigma Chemical Co. (St. Louis, MO, USA). Chromium perchlorate was obtained from Alfa (Danvers, MA, USA). Zwittergent 3-14 was purchased from Calbiochem (La Jolla, CA, USA). All other chemicals were obtained from the sources given in the Materials and Methods of Chapter 2.

CrATP was prepared by the methods of DePamphilis and Cleland (1973), using the ion exchange column with aniline elution method of CrATP purification. The CrATP was stored as an aqueous solution at 4 °C until needed. Sepharose 4B-CL was activated with cyanogen bromide and derivatized with ε-amino-n-caproic acid (March *et al.* 1974). The ε-amino-n-caproic acid-Sepharose was washed on a sintered glass funnel with methanol and then methanol containing increasing levels of anhydrous dioxane. After washing the gel with 100% anahydrous dioxane, the gel was suspended in dioxane and 1,1'-carbonyldiimidazole added to give a final concentration of 50 mM. After shaking at room temperature for 20 min, the gel was washed with

anhydrous dioxane, air dried on a sintered glass funnel for 1 min, and then added to a chilled aqueous solution of CrATP (pH 7). After shaking overnight at 4 °C, the gel was washed with 50 vol of chilled distilled water, saturated NaCl, and again with distilled water. The derivatized gel had a green tint from the immobilized CrATP. It was assumed that the CrATP was immobilized by esterification of its 3' hydroxy group (Jeng and Guillory 1975). The reaction sequence and the probable structures of the reaction intermediates can be found in Scheme 1.

Plant material and membrane isolation. The growth conditions for the barley (*Hordeum vulgare* L. cv. Conquest) seedlings and the procedure for the isolation of a plasma membrane-rich microsome fraction from the barley roots can be found in the Materials and Methods of Chapter 2.

ATPase assay procedures. All ATPase assays were performed at 16 °C in a 1 ml reaction volume, containing 20 mM Tris-MES buffer (pH 6.5) and various concentrations of Tris-ATP, divalent cations, CaM, chlorpromazine (CPZ), EGTA, and phospholipids. The procedures for the determination of proper incubation times and the amount of released P_i are given in Chapter 2. The Ca^{2+}- and Mg^{2+}-dependent ATPase activities are as defined in Chapter 2. Ca^{2+}, Mg^{2+}-dependent ATPase represents the enzyme activity found in the presence of both Ca^{2+} and Mg^{2+}, subtracting the activities produced by the given concentrations of the divalent cations alone. All ATPase activities have the unit μmol P_i released x $(mg\ protein)^{-1}$ x h^{-1} and are the means of at least two determinations. In assays which contained phospholipids, the phospholipids were added from clarified lipid solutions prepared by freeze-thaw-sonication. The stock lipid

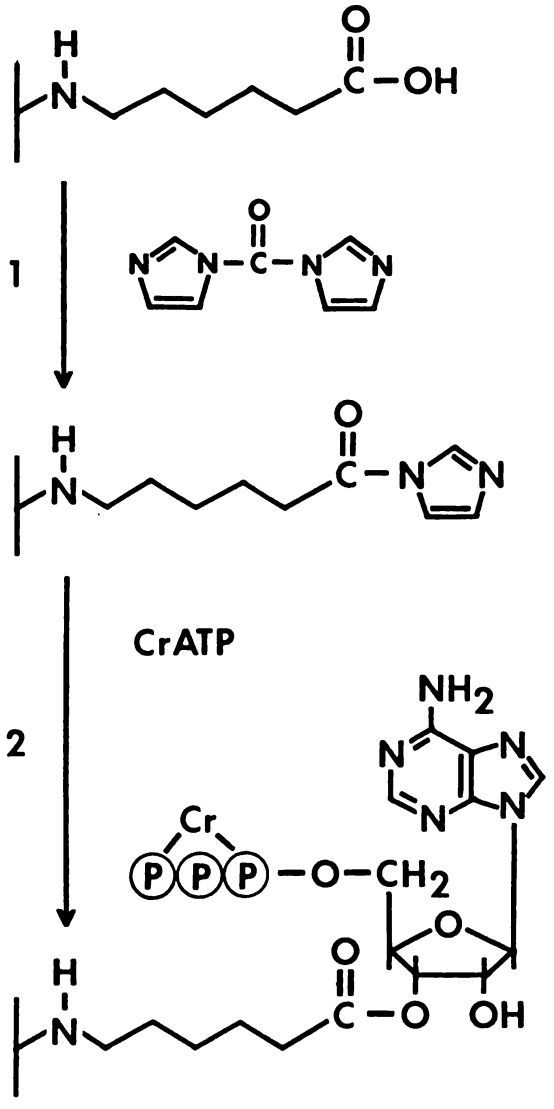

Scheme 1. *Reaction sequence for the preparation of CrATP immobilized to Sepharose 4B-CL.* **Aminohexanoic acid-Sepharose 4B-CL was prepared by the reaction of aminohexanoic acid with cyanogen bromide activated Sepharose 4B-CL and then treated with carbonyldiimidazole under strictly anhydrous conditions (1). The activated Sepharose was then combined with a aqueous solution of CrATP (2) to give the desired product.**

solutions were prepared by drying chloroform solutions of the various lipids in test tubes with N_2, adding the desired buffer, and then briefly sonicating the solution in a bath type sonicator to disperse the lipids. The lipid suspensions were then frozen in a dry ice-acetone bath, thawed at room temperature, and sonicated again.

ATPase solubilization. Zwittergent 3-14 solubilization of the ATPase was performed with a modification of the methods of Malpartida and Serrano (1980). The barley root plasma membrane-rich microsomes were washed in 10 mM Tris-MES buffer (pH 6.5), containing 10 % glycerol, 250 μM PMSF, and 0.5 mM EGTA. The membranes were resuspended in wash buffer at a concentration of 2 mg membrane protein/ml and 1.5 mg/ml Zwittergent 3-14 added to the vortexed membrane suspension. Vortexing was continued for 10 min during which the membrane solution partially clarified. After a 30 sec sonication in a bath type sonicator, the solution was centrifuged at 150,000 *g* for 45 min. The supernatant was collected and is the solubilized ATPase fraction. The solubilized ATPase was used immediately for the affinity chromatography.

Affinity chromatographic purification of barley root ATPase. The immobilized CrATP was packed in a 5 ml column and washed with 5 column volumes of 10 mM Tris-MES buffer (pH 6.5), containing 0.15 mg/ml Zwittergent 3-14, 0.05% Triton X-100, 0.25 mg/ml phosphatidylcholine, 1 mM EGTA (Tris salt), 0.25 mM PMSF, 0.5 mM DTT, and 10 % glycerol (Buffer A). To reduce the amount of ATPase eluted by buffer A at the column void volume, it was essential that this buffer be absolutely clear, indicating the absence of any large phospholipid vesicles. Freeze-thaw-sonication facilitated the preparation of the buffers

containing phosphatidylcholine. The solubilized ATPase was applied to the washed column and the unbound protein eluted with buffer A at a flow rate of 3 ml/h. All the affinity chromatographic procedures were performed at 4 °C. One ml fractions were collected and the absorbance at 280 nm monitored continuously with a spectrophotometer equipped with a flow cell. After elution of the unbound protein, the bound protein was eluted with either a gradient of 0 to 15 mM Tris-ATP in buffer A with 5 mM $CaCl_2$ replacing the EGTA or a single step of 10 mM Tris-ATP in buffer A, replacing the EGTA with 5 mM $CaCl_2$. Since ATP elution of the bound protein prevents the use of 280 nm absorbance for protein estimation, the protein in each fraction was determined by the method of Wang and Smith (1975), having first precipitated the protein to reduce interference by buffer components (Benadoun and Weinstein 1976). ATPase activity was determined at 16 °C in 1 ml of 20 mM Tris-MES buffer (pH 6.5), containing 1 mM Tris-ATP and 11 mM $CaCl_2$. Since only 1 to 2 µl of the bound protein fractions was required for the ATPase assay, the ATP in the column fractions did not appreciably supplement that ATP in the ATPase reaction solutions. Since the purified ATPase was labile in the absence of phospholipids and glycerol, the column fractions containing the ATPase activity were pooled and stored frozen at -60 °C in the elution buffer.

Phosphorylation procedures. The assay mixture contained 20 mM Tris-MES buffer (pH 6.5), 5 mM $CaCl_2$, 1 mM [γ-^{32}P]ATP (100 mCi/mmol), and 30 µg of purified ATPase in a reaction volume of 0.25 ml. Preliminary experiments indicated that to obtain high rates of phosphorylation it was necessary to add 0.5 mg/ml phosphatidylcholine. The reaction was carried out at 16 °C and initiated by the addition

of ATPase protein. The reaction time was 15 s. The stop and wash procedure followed the methods of Amory *et al.* (1980). The phosphorylated samples were analyzed by SDS polyacrylamide gel electrophoresis as described below.

Calmodulin purification. Electrophoretically pure CaM was isolated from bovine brain acetone powder by 2-chloro-10-(3-aminopropyl)-phenothiazine-Affi-Gel 10 affinity chromatography (Appendix 2). Barley root CaM was prepared from the 80,000 *g* supernatant from the plasma membrane-rich microsome isolation procedure (Chapter 2). This supernatant was concentrated to approximately 25% of its original volume by ultrafiltration (Amicon PM-10). The concentrate was then treated with ammonium sulfate as described in Appendix 2. After dialysis of the 55% ammonium sulfate precipitate (pH 4), the sample was frozen and stored at -40 °C until material equivalent to about 500 g fresh weight of barley roots was accumulated. The barley root CaM was then isolated by affinity chromatography (Appendix 2). The purified barley root CaM migrated as a single band in both SDS polyacrylamide gels and polyacrylamide isoelectric focusing gels.

Polyacrylamide gel electrophoresis. Non SDS polyacrylamide gel electrophoresis was performed according to the procedures of Davis (1964) with 6% polyacrylamide tube gels. Proteins were stained with coomassie brilliant blue (Weber and Osborn 1969). Carbohydrates were stained as described by Fairbanks *et al.* (1971). ATPase activity was visualized in the gels by immersing the gels in 20 mM Tris-MES buffer (pH 6.5), containing 3 mM Tris-ATP and 13 mM $CaCl_2$. A white precipitin band appeared in the region of the ATPase protein within 5 min. The position of the ATPase activity in the gels was recorded with a spectrophotometer equipped with gel scanner at 500 nm.

SDS polyacrylamide gel electrophoresis was performed with 10% polyacrylamide slab gels (1.5 mm)(Laemmli 1970). Sample preparation for the SDS polyacrylamide gels was performed as described by Laemmli (1970) except that the samples were heated in boiling water for 2 min. Samples of phosphorylated proteins were incubated in the boiling water bath for various times. Sample preparation was not required for the non SDS polyacrylamide gels, since all the buffers used in the solubilization and purification of the ATPase contained 10% glycerol.

RESULTS

Calmodulin stimulation of the ATPase in intact membranes. As shown in Figure 20, increasing concentrations of either bovine brain or barley CaM stimulated the Ca^{2+}, Mg^{2+}-dependent ATPase activity of the barley root plasma membrane-rich microsomes. The CaM stimulation was inhibited by CPZ, confirming that this was a CaM-dependent process. The 50% maximal response of the Ca^{2+}, Mg^{2+}-dependent ATPase to CaM was obtained at about 500 ng/ml. The Ca^{2+}-dependent and Mg^{2+}-dependent ATPase activities were also apparently stimulated by CaM at much higher concentrations of the activator. However, these stimulations were less sensitive to CPZ than the Ca^{2+}, Mg^{2+}-dependent ATPase activity, suggesting that the apparent stimulations by CaM of the Ca^{2+}- or Mg^{2+}-dependent ATPase activities represent stimulation by some substance tightly bound to the CaM or introduced during CaM purification. However, within 4 h at 2 °C, all the CaM stimulation of the Ca^{2+}, Mg^{2+}-dependent ATPase was lost.

Zwittergent solubilization of the barley membrane-bound ATPase. Solubilization of the barley root membrane-bound ATPase with

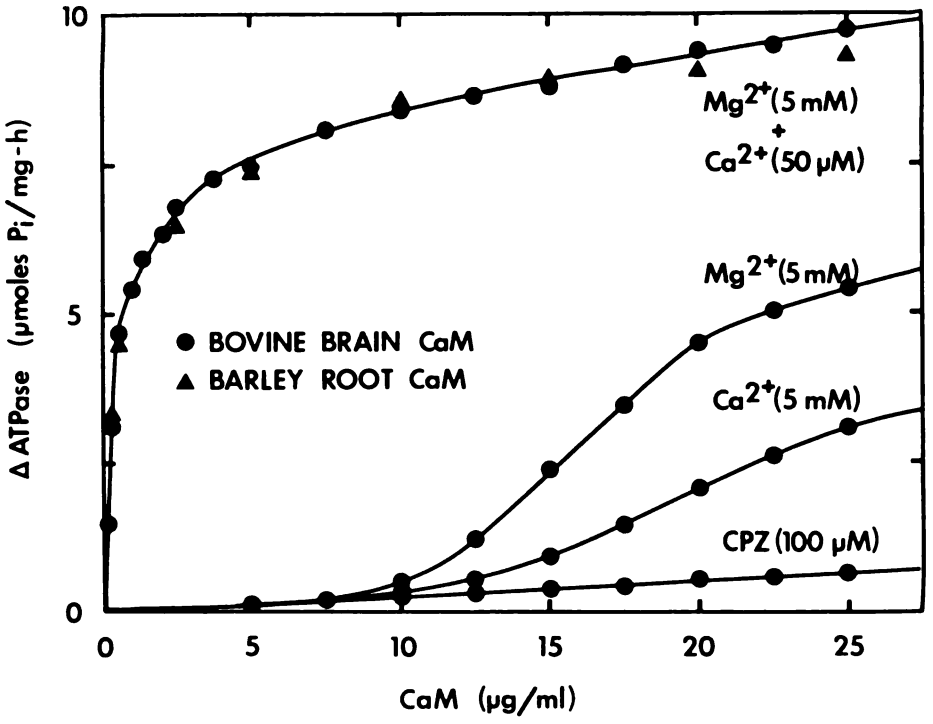

Figure 20. *Effect of calmodulin on the ATPase activities of barley root plasma membranes.* The effect of various concentrations of CaM isolated from either barley roots or bovine brain on the ATPase activities of barley root plasma membrane-rich microsomes was determined at 16 °C as described in the Materials and Methods. The curves are labelled with the concentrations of divalent cations employed with the curve labelled CPZ representing the Ca^{2+}, Mg^{2+}-ATPase activity in the presence of chlorpromazine. The effect of CaM on the ATPase activities is presented as a ΔATPase, representing the increase in ATPase activity by CaM relative to the activity determined in the absence of CaM.

Zwittergent 3-14 by the procedure of Malpartida and Serrano (1980) resulted in the release of about 50% of the membrane protein and 87% of the Ca^{2+}-dependent ATPase activity (Table 4). The ATPase was assayed in the presence of 0.25 mg/ml phosphatidylcholine. In the absence of added phospholipids, the divalent cation-dependent ATPase activity was reduced by about 50% (Table 5). All the phospholipids tested could reactivate the Ca^{2+}-dependent ATPase (Table 5). The highest activity was found with phosphatidylethanolamine and the lowest activity was produced by phosphatidylinositol (Table 5). However, CaM-stimulated Ca^{2+}, Mg^{2+}-dependent ATPase activity was obtained only with phosphatidylcholine and asolectin (Table 5). Since asolectin contains phosphatidylcholine, the Ca^{2+}, Mg^{2+}-dependent ATPase activity probably has a specific requirement for phosphatidylcholine.

The solubilized ATPase was relatively stable when stored in the presence of Tris-ATP in solubilization buffer at -40 °C. Since the presence of ATP would interfere with any subsequent attempts to purify the ATPase by affinity chromatography of the stored samples, EDTA was added to the sample to give a final concentration of 2 mM before application to the affinity column.

Affinity chromatographic purification of the barley membrane-bound ATPase. Greater than 95% of the applied protein was eluted in the absence of ATP from the CrATP affinity column (Figure 21). However, a significant portion of the applied ATPase activity eluted with at the column void volume. The amount of unbound ATPase was reduced in subsequent experiments by the use of more highly clarified phospholipid buffers. This suggests that the unbound ATPase may represent ATPase protein associated with large phospholipid vesicles

Table 4. *Balance sheet for ATPase isolation.* The Ca^{2+}-dependent ATPase activity was determined with 1 mM Tris-ATP and 11 mM $CaCl_2$ and the Ca^{2+},Mg^{2+}-ATPase was determined with 5 mM $MgCl_2$ and 50 μM $CaCl_2$ as described in the Materials and Methods. With the exception of the microsomes, the ATPase activity was also determined in the presence of 250 μg/ml phosphatidylcholine. CaM was added at 25 μg/ml and chlorpromazine (CPZ) was added to give a final concentration of 100 μM. Units are in μmol P_i x h^{-1} and specific activity is μmol Pi x $(mg\ protein)^{-1}$ x h^{-1}.

Sample	Protein (mg)	Ca^{2+}-ATPase			Ca^{2+},Mg^{2+}-ATPase		
		Units	%yield	SA	SA	SA(CaM)	SA(CPZ)
Microsomes	10.2	1070	100	107	0.3	0.6	0.2
Soluble ATPase	4.7	940	87	201	4.4	16.1	4.2
Purified ATPase	0.1	174	16	1738	26.4	101.8	21.2

Table 5. *Phospholipid activation of the solubilized ATPase.* All ATPase activities were determined as described in Table 4 except that the type of lipid used was varied and the activity in the presence of 100 μM EDTA was also determined.

Lipid	ATPase Specific Activity				
	+EDTA	$+Ca^{2+}$	$+Ca^{2+},Mg^{2+}$	+CaM	+CPZ
None	0.4	70.7	0	0	0
phosphatidylcholine	0.7	138.5	4.1	15.2	3.7
phosphatidylserine	0.3	125.3	0	0	0
phosphatidylethanolamine	12.1	177.5	0	0	0
phosphatidylinositol	0.5	99.4	0	0	0
asolectin	0.6	142.3	1.6	5.6	1.4

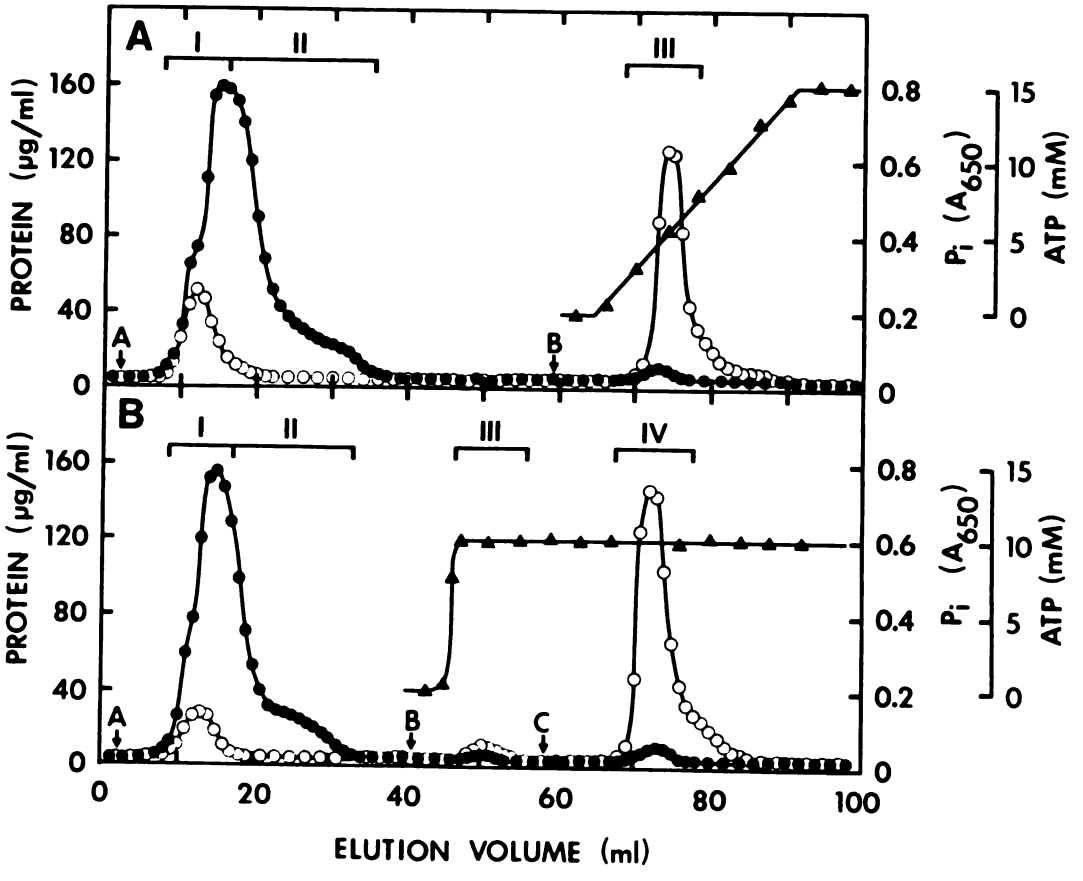

Figure 21. *Affinity chromatographic purification of barley root ATPase.* Zwittergent solubilized barley root plasma membrane-rich microsomal proteins were applied to a 5 ml CrATP-Sepharose 4B-CL column at 4 °C and the unbound protein eluted as described in the Materials and Methods (A). In Part A, the bound protein was released with a gradient of ATP from 0 to 15 mM and 5 mM $CaCl_2$ (B). In Part B, the bound protein was eluted with 10 mM ATP and 5 mM $CaCl_2$ (C), having first attempting elution with 10 mM ATP and 1 mM EDTA (B). The amount of P_i released from 1 mM Tris-ATP in the presence of 10 mM $CaCl_2$ by small aliquots (10-25 μl) of the column fractions was determined as described in the Materials and Methods.

which are mechanically prevented from binding to CrATP.

The bound ATPase was eluted from the CrATP affinity column by ATP in the presence of Ca^{2+} (Figure 21). When the ATP gradient method was employed, the ATPase was eluted at about 6 mM ATP (Figure 21A). The bound ATPase could also be released by 10 mM ATP in the presence of 5 mM $CaCl_2$ (Figure 21B). The bound ATPase was not eluted by ATP in the absence of added divalent cations and with 1 mM EDTA (Figure 21B), indicating an essential requirement for divalent cations in the displacement of the CrATP-bound ATPase by ATP. As shown in Table 4, the affinity chromatography resulted in a considerable increase in the specific activities of both the Ca^{2+}-dependent and the Ca^{2+}, Mg^{2+}-dependent ATPase activities determined in the presence of phosphatidylcholine. The Mg^{2+}-dependent ATPase activity had a similar enrichment (data not shown).

Polyacrylamide gel electrophoresis of the various fractions obtained during the isolation of the barley root ATPase indicated that the purified ATPase fraction consisted of one major protein of 75,000 daltons (Figure 22B). There was also a 63,000 dalton minor protein. The 75,000 dalton protein was enriched during the ATPase purification procedure (Figure 22B). Native gels of the solubilized and purified ATPase fractions inducated a single region of Ca^{2+}-dependent ATPase activity (Figure 22A). The region of ATPase activity corresponded to a single protein visualized with coomassie brilliant blue (Figure 22A). This protein did not contain carbohydrate. However, a major protein solubilized by the Zwittergent from the barley root plasma membranes is a glycoprotein (Figure 22A).

Phosphorylation of the purified ATPase. To determine which of the proteins observed on the SDS polyacrylamide gels had catalytic

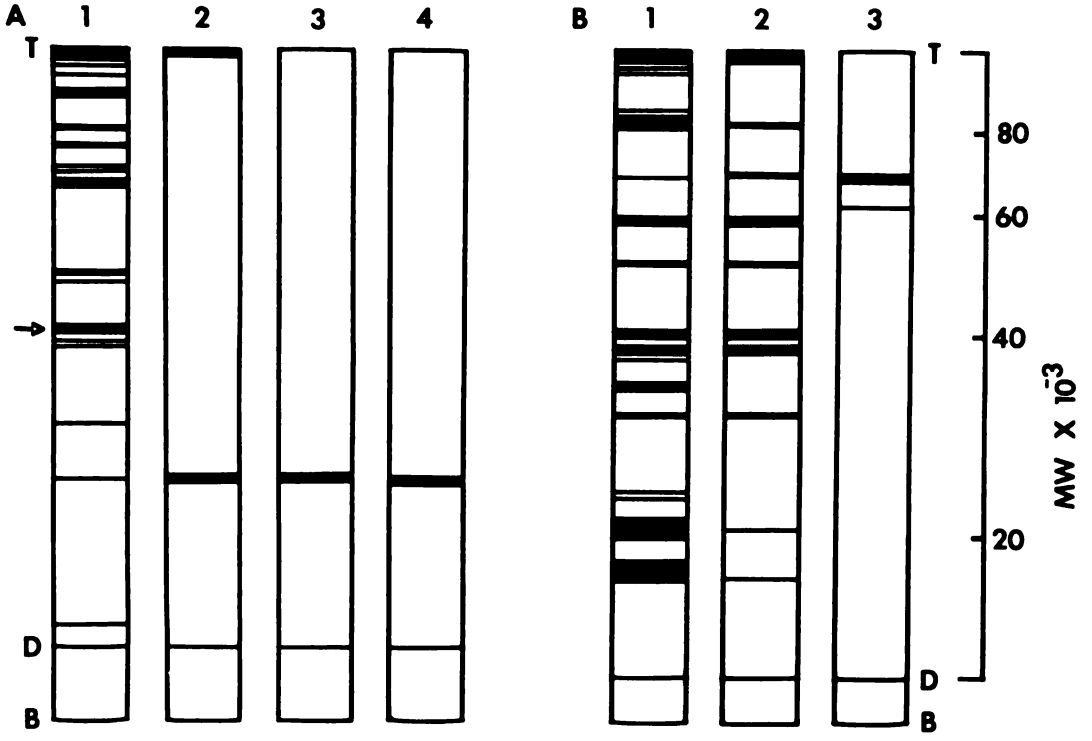

Figure 22. *Polyacrylamide gel elctrophoresis of various fractions obtained during ATPase purification.* The procedures for sample preparation, staining, and gel elctrophoresis can be found in the Materials and Methods. As a result of the different staining methods employed, the results are presented as facimiles of the electrophoretic seoarations of the protein fractions. The top (T), bottom (B), and position of the tracking dye (D) are designated. The protein band of gel A1 marked with an arrow also stained positive for carbohydrate. The molecular weights given for the SDS gels were determined with standard proteins run in the same slab gel. Part A. Non SDS polyacrylamide gels (6%) of the Zwittergent solubilized proteins (1,2) and purified ATPase (3,4) stained for protein (1,3) or ATPase activity (2,4). Part B. SDS polyacrylamide gels (10%) of the plasma membrane-rich microsomes (1), Zwittergent solubilized proteins (2), and purified ATPase (3) stained for protein.

activity, the purified ATPase fraction was phosphorylated with [γ-^{32}P]ATP and then run on SDS polyacrylamide gels (7%). Under the experimental conditions employed, the catalytic site of the ATPase should be phosphorylated if the enzyme catalytic cycle involves the formation of a phosphorylated intermediate. Two phosphoproteins were detected in the SDS gel (Figure 23). The majority of the radioactivity was found in the gel at a molecular weight of 75,000 daltons, corresponding to the major protein observed with protein staining of 10% polyacrylamide gels (Figure 22B). The 63,000 dalton protein was not phosphorylated (Figure 23). However, a significant amount of radioactivity was found to be associated with a 135,000 dalton protein (Figure 23). The 135,000 dalton protein was not observed in the 10% polyacrylamide gels (Figure 22B). However, this large protein would not migrate into the 10% polyacrylamide separating gel and was present in such small amounts that visualization with coomassie brilliant blue would be difficult. The amount of 135,000 dalton protein was dependent upon the length of sample incubation in the boiling water bath (data not shown). This suggests that the large protein may actually be a dimer of the 75,000 dalton protein which is not completely dissociated by SDS.

DISCUSSION

The results of these experiments strongly suggest specific associations of certain phospholipids with barley root plasma membrane-bound ATPase. Furthermore, this may represent the first demonstration of a phosphoprotein intermediate in the catalytic cycle of a plant

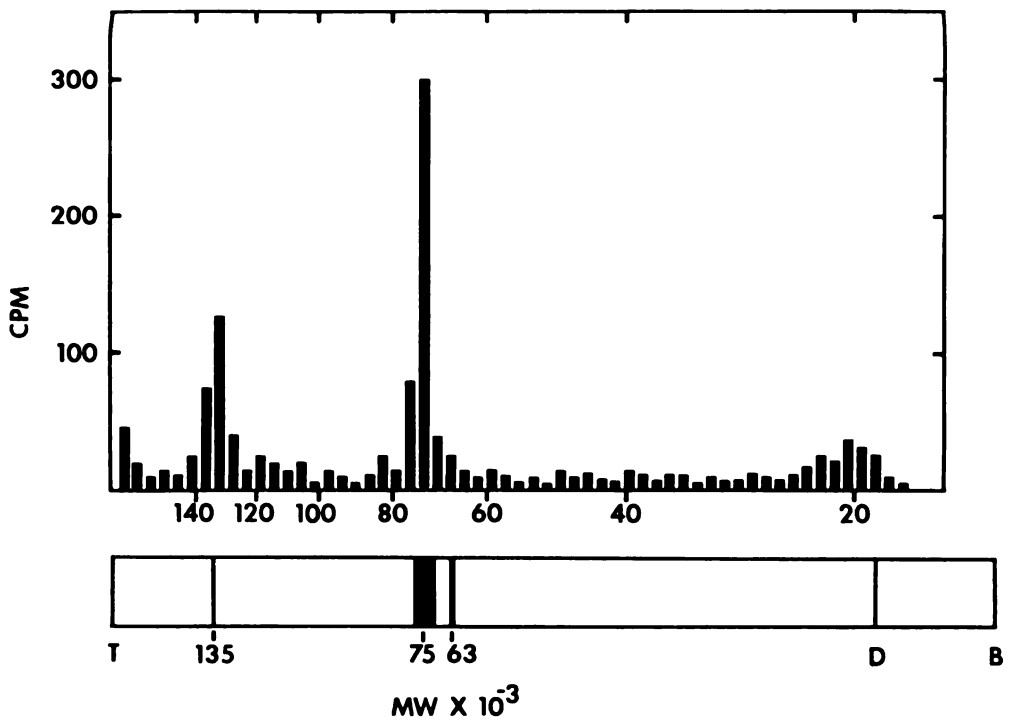

Figure 23. *Polyacrylamide gel electrophoresis of the phosphorylated ATPase.* The purified ATPase fraction prepared by affinity chromatography was phosphorylated with [γ-^{32}P]ATP as described in the Materials and Methods. The phosphorylated sample was then applied to an SDS polyacrylamide slab gel (7%) and the phosphoproteins separated by electrophoresis. After completion of the electrophoresis, the gel was sliced and the radioactivity in the slices determined by liquid scintillation counting. Below the radioactivity profile is a facimile of a gel run under the same conditions and stained for protein. The molecular weights were based on molecular weight standard proteins run in the same slab gel.

ATPase. The obligatory requirement of the CaM-stimulated Ca^{2+}, Mg^{2+}-dependent ATPase of barley root plasma membranes for phosphatidylcholine (Table 5) is consistent with the results obtained with erythrocyte membranes (Gietzen *et al.* 1980, Niggli *et al.* 1981). The erythrocyte Ca^{2+}, Mg^{2+}-dependent ATPase was insensitive to CaM in the absence of phosphatidylcholine. As previously demonstrated for yeast (Dufour and Goffeau 1980) and the erythrocyte (Ronner *et al.* 1977), membrane-bound ATPases require phospholipids for optimal activity. Total delipidation of the purified ATPases from these sources resulted in inactive enzymes which could be partially reactivated by appropriate relipidation. Therefore, it is not surprising that the solubilized ATPase from barley root plasma membranes has increased activity in the presence of phspholipids (Table 5). The low activity of the solubilized ATPase in the absence of added phospholipids probably results from residual lipids still associated with the ATPase or the possible activation of the enzyme by the lipid-like Zwittergent.

Since none of the previously purified ATPases from plant membranes were assayed in the presence of phospholipids (Benson and Tipton 1978, DuPont and Leonard 1980, Baydoun and Northcote 1981, Dieter and Marmé 1981, Tognoli and Marrè 1981), comparison of the results obtained by other workers with those presented here is rather difficult. Furthermore, considering the lipid requirements of membrane-bound ATPases (Fourcans and Jain 1974), the low activity of these purified ATPases is expected. Benson and Tipton (1978) noted that the ATPase purified from corn root microsomes was no longer sensitive to high levels of Ca^{2+} and other inhibitors of the microsomal enzyme. However, the purified ATPase was not examined in the presence of

lipids. Moreover, recently it was demonstrated for the barley ATPase that Ca^{2+} inhibition of the divalent cation-dependent ATPase activity may reflect Ca^{2+}-lipid interaction (Caldwell and Haug 1981). If a similar situation should exist for the corn ATPase, then Ca^{2+} would have little effect on the purified corn ATPase stripped of lipids. Furthermore, the ATPase isolated by Benson and Tipton (1978) was much less substrate specific than the microsomal enzyme. Conceivably, boundary lipids may also be involved in the substrate specificity of the membrane-bound ATPases. The possible high phospholipase activity in barley root membrane preparations (Gibrat and Rossignol 1977) might alter the lipids around the barley ATPase, resulting in the observed poor substrate specificity of the barley enzyme (Caldwell and Haug 1980, Chapter 2).

As mentioned in the Introduction, the molecular weight of corn microsomal ATPase ranges from 30,000 to 36,000 daltons (Benson and Tipton 1978, Baydoun and Northcote 1981). The ATPase isolated from pea stem microsomes had two major proteins of 30,000 and 48,000 daltons (Tignoli and Marrè 1981). These ATPases are quite small when compared to the transport ATPases of animal cells. The erythrocyte Ca^{2+}, Mg^{2+}-ATPase has a molecular weight of about 125,000 daltons (Niggli *et al.* 1979). The catalytic subunit of the Na^{+}, K^{+}-ATPase has a molecular weight around 110,000 daltons (Hastings and Reynolds 1979). The H^{+}, K^{+}-ATPase of gastric mucosa has a molecular weight of 105,000 daltons (Sachs *et al.* 1979). Although the γ subunit of the F1 proton translocating ATPase of bacteria has a molecular weight of 32,000 daltons and, therefore, is of similar size as the plant ATPases, the F1-ATPase requires more than this single subunit for enzymatic activity (Sone *et al.*

1979). Although considerably larger than the other plant ATPases, the barley root plasma membrane-bound ATPase of 75,000 dalton molecular weight is still smaller than the ATPases of animal cells.

It is of interest that the purified ATPase fraction from barley roots contains a single major catalytic unit and this fraction has Ca^{2+}-dependent, Mg^{2+}-dependent, and CaM-stimulated Ca^{2+}, Mg^{2+}-dependent ATPase activities. Although the minor proteins found in this fraction might have catalytic activity not observed under the experimental conditions employed in this study, this suggests that all these ATPase activities are properties of a single enzyme. Possibly, many of the activities attributed to different ATPases in plant plasma membranes actually represent different functional states of a single enzyme.

CHAPTER 6

GENERAL DISCUSSION

Based on the results presented in Chapters 2 and 3, the kinetics of the barley root plasma membrane-bound ATPase activities are rather complex. The complexity of the barley root ATPase kinetics is of interest not only because of the differences between the barley ATPase kinetics and those of other plants, but also because of the similarities between the kinetic properties of the barley enzyme and the ATPase kinetics of animal systems. As discussed in Chapter 2, the differences between the barley kinetics reported here and the kinetics of other plant plasma membrane-bound ATPases can be partially explained in terms of methodological considerations. If the improved procedures for the kinetic analysis of plant ATPases described in Chapters 2 and 3 are employed with plasma membrane preparations from other plants, then more detailed information concerning the functional characteristics of plant ATPases could be obtained.

The kinetics of the barley root plasma membrane-bound ATPase was qualitatively similar to that of animal membrane-bound ATPases. The involvement of membrane lipids in the regulation of the constituent ATPase activities has been studied extensively in animal membranes. As in plant membranes, Arrhenius plot discontinuities generated from experiments on animal and microbial ATPases were automatically attributed to phase transitions of the membrane bulk lipids. Although these transitions can cause major changes in the activities of membrane-bound enzymes, temperature-dependent alterations in the

electrostatic properties of the lipid-ATPase interaction may be the basis for some of the Arrhenius plot discontinuities observed in experiments on membrane-bound ATPases (Rice *et al.* 1979). The results obtained with the barley ATPase are consistent with this concept.

If the activity of the barley root membrane-bound ATPase depends upon the ionic properties of the surrounding membrane lipids, then a number of phenomena previously attributed to properties of the ATPase protein may, in fact, represent lipid properties. The Na^+, K^+-ATPase from bovine brain is at least partially controlled by electrostatic alterations of the charged lipids surrounding the ATPase (Ahrens 1981). Previously considered to be evidence for multiple cation binding sites, the action of monovalent and divalent cations on the Na^+, K^+-ATPase was ascribed to ion-induced changes in the electrostatic conditions of the annular ATPase lipids.

A multitude of different cation- and anion-sensitive ATPases are reported in the plant literature. However, these different ATPases possibly represent different functional states of a few membrane-bound enzymes. On the other hand, some ion stimulations of plant ATPases seem to indicate the specific interaction of the ion with the ATPase protein. Notably, the K^+-stimulated Mg^{2+}-dependent ATPase of corn roots has a specific requirement for K^+ (Hodges 1976). Similarly, the synergistic response of the sugar beet Na^+, K^+-ATPase to Na^+ and K^+ (Hansson and Kylin 1969) strongly supports the concept that this ATPase has specific sites for monovalent cations. It is also noteworthy that the sugar beet Na^+, K^+-ATPase may have a specific lipid requirement (Kylin *et al.* 1972). Other ion-stimulated ATPase activities of plant membranes

may also reflect the direct association of the ion with the ATPase protein. Nevertheless, considering the spectrum of ionic affinities for lipids (Hauser *et al.* 1976), a simple demonstration of ion stimulation of ATPase activity does not constitute sufficient evidence for a direct interaction of the ion with the enzyme protein.

Assuming that the barley ATPase senses the ionic properties of the membrane lipids, the different degree of ATPase activation by phospholipids (Chapter 5) may result from the different ionic properties of the various phospholipids tested. Even though the lipid composition of plant membranes is heterogeneous, the lipids directly associated with the membrane-bound ATPase may have a different lipid composition than the membrane as a whole. Furthermore, as was suggested for the mitochondrial membrane (Cunningham and Sinthusek 1979), rather homogeneous microenvironments may exist within the barley root plasma membrane which consist of a specific class of phospholipids. If, for example, some of the barley root ATPase is localized in a phosphatidylcholine-rich microenvironment, then the ATPase might display CaM-stimulated Ca^{2+}, Mg^{2+}-dependent ATPase activity. The same ATPase protein in a different lipid domain would not necessarily exhibit the CaM-stimulated ATPase activity. Therefore, it is possible for a multitude of different ATPase activities to appear to be present, when only one enzymatic protein exists.

A variety of plant physiological responses may be influenced by the characteristics of membrane lipids and the membrane-bound ATPase activities. The ability of certain plants to withstand saline growth conditions may be correlated to modifications in the membrane lipid composition which maintains the constituent ATPase

activity (Kylin and Quatrano 1975). Unfortunately, many of the studies of the changes in lipid composition of plant membranes in response to environmental stresses involve to isolation of whole cell lipids. If a particular stress causes a major modification in the lipid composition of the plant plasma membrane, then the isolation of the whole cell lipids would dilute the observed lipid changes. As isolation methods for plant plasma membranes and the membranes of cytoplasmic organelles are improved, it would be worthwhile to repeat some of the earlier experiments on stress-induced lipid changes.

The hormonal regulation of K^+ transport and ATPase activity in rice shoots requires the presence of phosphatidylcholine (Erdei *et al.* 1979). Growth of wheat seedlings in the presence of choline chloride resulted in an increase in the amount of phosphatidylcholine in the wheat seedling's membranes (Horváth *et al.* 1981). The choline treated seedlings were as frost resistant as hardened seedlings, suggesting that the amount of phosphatidyl-choline in the plant membranes may be related to the frost tolerance of wheat.

In conclusion, the activity of the barley root plasma membrane-bound ATPase is apparently sensitive to modifications in the physico-biochemical properties of the membrane lipids. Assuming that other membrane-bound ATPases are also modulated by changes in the membrane lipid structure, further investigations of the properties of membrane-bound ATPases should consider the role of the membrane lipids in modulating the membrane-associated processes. Furthermore, considering the dependence of the membrane lipid physical structure on changes in temperature, the continued

use of nonphysiological ATPase assay conditions results in data which cannot be directly related to *in vivo* physiological processes.

APPENDICES

APPENDIX 1

COMPUTER PROGRAMS FOR THE CALCULATION OF SUBSTRATE CONCENTRATIONS AND FOR THE ANALYSIS OF ATPase REACTION KINETICS

INTRODUCTION

In order to perform the experiments described in the preceding chapters, it was necessary to use a variety of computer methods to facilitate the proper analysis of the ATPase reaction kinetics. Program 1 provides the means to calculate the concentrations of the various metal cation-ATP complexes and the levels of free ATP and other reaction components. Program 2 allows the evaluation of the kinetic constants of the two catalytic components of the ATPase activities observed in the double reciprocal plots. Program 3 is a simple search program which gives the value of the nonlinearity parameter, n, by determining the value of n which produces the most linear plot of the data as $1/v$ vs. $1/S^n$.

All three programs are presented with a short description of the method, followed by a listing of the major variable designations, and then a detailed flowchart of the program. The standard flowchart nomenclature has been employed with the following exceptions. The punched card symbol indicates any data input from a peripheral source, such as magnetic tape or keyboard entry. A symbolic presentation of a loop has been employed throughout. This consists of a rectangle divided into three sections. In the standard format, the upper left section contains the variable and its starting position, for example I = 1. The right section contains the upper limit of the loop and the lower left section contains the step size, generally 1.

A fourth program was frequently used. This is the nonlinear least squares program described in the Materials and Methods of Chapter 2. Since this is a rather standard method, the program has

not been presented here.

All the programs used were written in Basic for use with a Tektronix 4051 microcomputer. Data output consisted of copying the data from the computer screen, hard copy output by data transfer to a Tektronix X-Y plotter, or storage on the integral magnetic tape unit of the 4051 computer.

PROGRAM 1

CALCULATION OF THE CONCENTRATION OF $MeATP^{2-}$ AND OTHER IONS IN SOLUTION

Although information is available that the ATPases from plant cell membranes utilize the $MeATP^{2-}$ complex as the true substrate, many researchers studying the plant ATPases are seemingly unaware that they employ methods which provide incorrect estimates of substrate concentrations. Therefore, to analyze the ATPase activities, good estimates of substrate concentrations and the levels of potentially inhibitory components in the ATPase reaction solutions are required. In the present program, a simplified method is presented for the computation of the necessary values (Storer and Cornish-Bowden 1976).

Although a detailed description of the computations may be found elsewhere (Storer and Cornish-Bowden 1976), the principle of this method is briefly outlined. In a reaction solution containing m different complexes formed from a combination of n different components, the total concentration, A_i, of the ith component is the sum of its free concentration, a_i, and the concentrations x_j of all the m complexes, each of the latter being given a weight α_{ij} equal to the number of molecules of the ith component in one molecule of complex:

$$A_i = a_i + \sum_{j=1}^{m} \alpha_{ij} x_j$$

The concentration x_j of the jth complex can be expressed in terms of the free component concentrations and the association constant K_j:

$$x_j = K_j \prod_{k=1}^{n} a_k^{\alpha_{kj}}$$

By substitution and rearrangement in terms of total concentrations

and free concentrations of the components (Storer and Cornish-Bowden 1976), a general equation is obtained:

$$a_i = A_i a_i / [a_i + \sum_{j=1}^{m} (\alpha_{ij} K_j \prod_{k=1}^{n} a_k^{\alpha_{kj}})]$$

Initially, it is assumed that $a_i = A_i$. However, with each successive application of the equation, the improved estimates of a_i are inserted into the right-hand side of the equation. The program then performs the necessary number of iterations to obtain the desired degree of convergence.

Much of the program consists of data input, initiation of required parameters, correction of the association constants for changes in pH, temperature, and ionic strength, and data output in the desired format. To shorten computation time, the proton concentration is considered to be constant in a buffered system and free protons are not considered to be components. Instead, prior to the first iteration and after each iteration, the relative amounts of the various ionic forms of ATP (ATP^{4-}, $HATP^{3-}$, H_2ATP^{2-}) which are relevant at physiological pH values are calculated and used as components in subsequent calculations. This reduces the number of variables to be considered. After the program determines the free concentrations of the various components, these values are used for the calculation of complex concentrations before data output.

Table A1. *Designations for the prinicple variables employed in Program 1.*

Variable	Designation
number of components	N
number of complexes	M
initial component concentration	N(I)
current component concentration	F(I)
value of constant component	X(I)
pH	V1
ionic strength (calculated)	U2
association constants	K(J)
final complex concentrations	X(J)
number of iterations	Z
α_{ij} matrix	T(I,J)

For the given flowchart:

Component	Designation
ATP (Total)	G5
$MgCl_2$ (Total)	F(4)
KCl (Total)	Z5, F(5)
NaCl (Total)	Z8, F(8)
$CaCl_2$ (Total)	Z7, F(7)
Cl^- (Total)	F(6)
H^+ (Total)	F(9)
ATP^{4-} (Total)	F(1)
$HATP^{3-}$ (Total)	F(2)
H_2ATP^{2-} (Total)	F(3)

Figure A1. *Flowchart of program 1.* **The flowchart was prepared as described in the Introduction of Appendix 1 with the variable designations given in Table A1.**

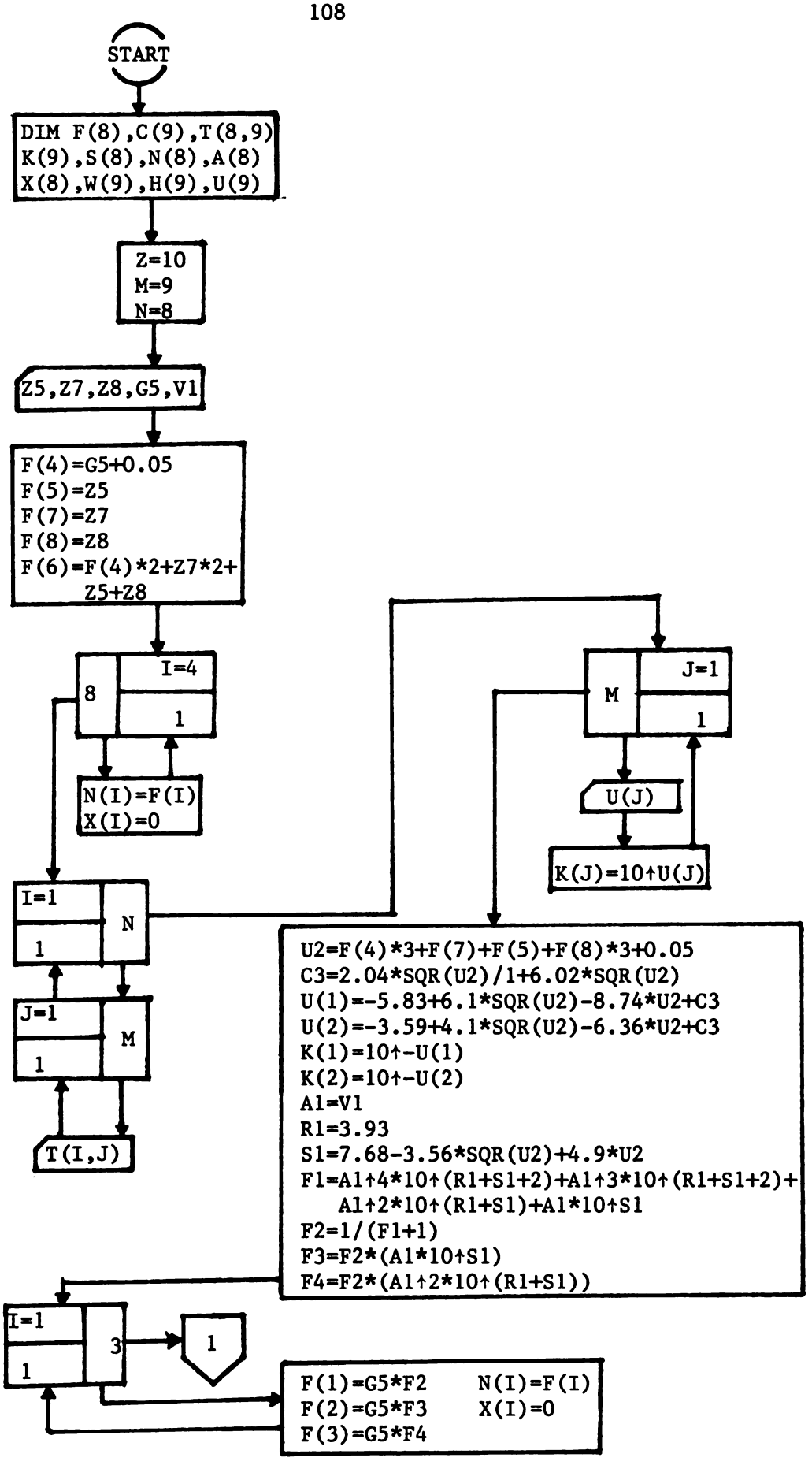
START
DIM F(8),C(9),T(8,9)
K(9),S(8),N(8),A(8)
X(8),W(9),H(9),U(9)
Z=10
M=9
N=8
Z5,Z7,Z8,G5,V1
F(4)=G5+0.05
F(5)=Z5
F(7)=Z7
F(8)=Z8
F(6)=F(4)*2+Z7*2+
Z5+Z8
I=4
8
1
N(I)=F(I)
X(I)=0
J=1
M
1
U(J)
K(J)=10↑U(J)
I=1
N
1
J=1
M
1
T(I,J)
U2=F(4)*3+F(7)+F(5)+F(8)*3+0.05
C3=2.04*SQR(U2)/1+6.02*SQR(U2)
U(1)=-5.83+6.1*SQR(U2)-8.74*U2+C3
U(2)=-3.59+4.1*SQR(U2)-6.36*U2+C3
K(1)=10↑-U(1)
K(2)=10↑-U(2)
A1=V1
R1=3.93
S1=7.68-3.56*SQR(U2)+4.9*U2
F1=A1↑4*10↑(R1+S1+2)+A1↑3*10↑(R1+S1+2)+
A1↑2*10↑(R1+S1)+A1*10↑S1
F2=1/(F1+1)
F3=F2*(A1*10↑S1)
F4=F2*(A1↑2*10↑(R1+S1))
I=1
3
1
1
F(1)=G5*F2
F(2)=G5*F3
F(3)=G5*F4
N(I)=F(I)
X(I)=0

Figure A1.

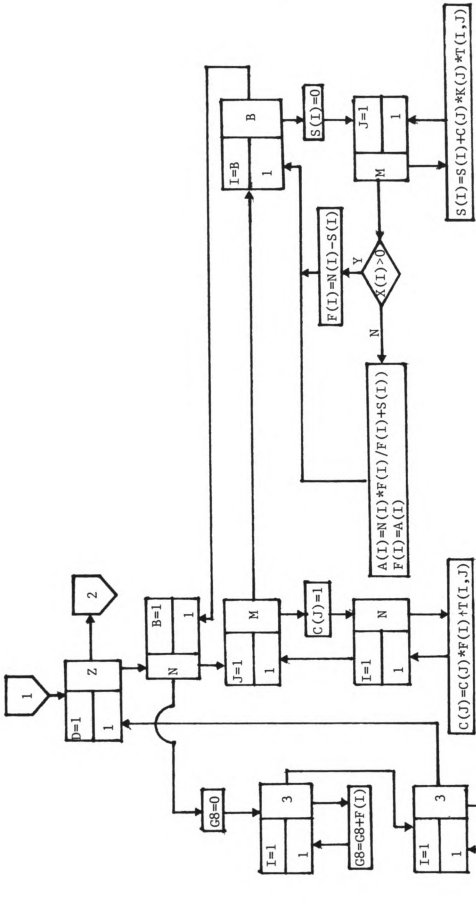

Figure A1. (cont'd)

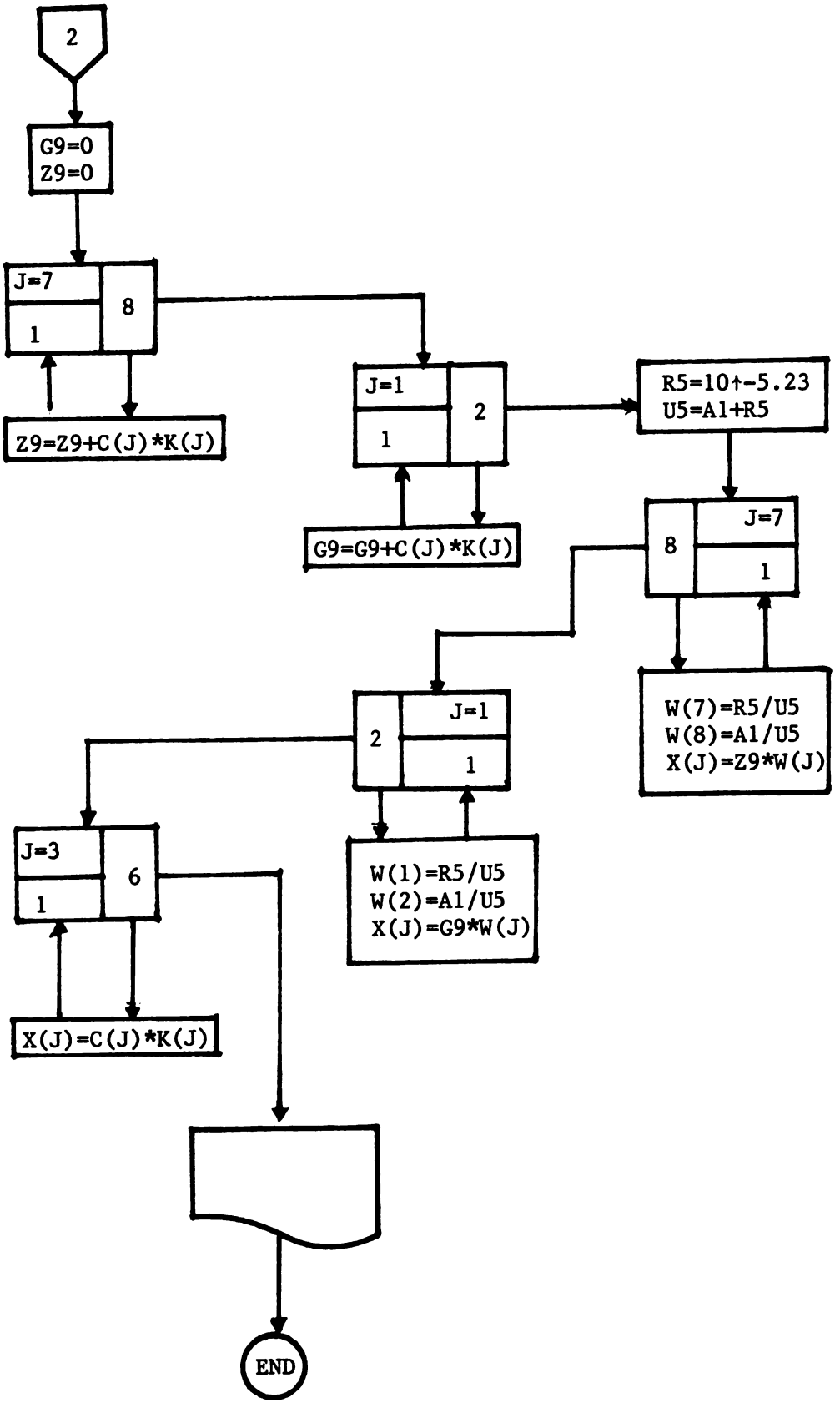

Figure A1. (cont'd)

PROGRAM 2

CALCULATION OF THE KINETIC CONSTANTS OF ATPase ACTIVITIES CHARACTERIZED BY NONLINEAR DOUBLE RECIPROCAL PLOTS

This program utilizes the method of Cornish-Bowden and Eisenthal (1978) to calculate the kinetic constants of the ATPase activities characterized by nonlinear double reciprocal plots. This method is known as the direct linear plot. Essentially, lines are drawn from the substrate concentration, S, on the negative x-axis through the respective velocity, V, on the y-axis. Subsequently for all sets (S_i, V_i), the x_0-y_0 coodinates for all unique intercepts are recorded. The median value for all the x_0 values gives the K_m and the median value for all y_0 values gives the V_{max}. This procedure does not necessitate prior knowledge of the error distribution of the enzyme data. Therefore, the weighting factors needed for kinetic analysis via double reciprocal plots are not required.

In the current program, the substrate (S_i) and velocity (V_i) are read into the program along with the number of S_i, V_i pairs. Then the S_i, V_i pair closest to the inflexion point of the double reciprocal plot is noted. In cases where substrate inhibition is apparent and the entire data set is initially read into the program, the numbers of the S_i, V_i pairs not to be included in the calculations is also entered. The program then takes one of the two partitioned data sets and calculates the coordinates of all unique intercepts with a direct linear plot. The subroutine then computes the medians of the x_0 and y_0 coordinate sets to give a K_m and V_{max} value for the partial data set. These values are used in a Michaelis-Menten

equation to compute the V values for the first catalytic component at the substrate concentrations used in the second data set. The calculated V values are then subtracted from the experimental V values and the process repeated for the second data set. The successive removal of the activity of one component in the data set for the other component allow the calculation of the kinetic constants for each component independently. A second subroutine is used for the statistical analysis of the computed constants.

Table A2. *Designations for the principle variables employed in Program 2.*

Variable	Designation
Number of iterations	IO
Number of data pairs	M
Substrate concentration	S(I)
Velocity	V(I)
Partition S(I)	P1
Exclusion range around P1	P3
Median value from subroutine 1	C3
Intercept x coordinate	X(I),D(T)
Intercept y coordinate	Y(I),G(T)
Slope of S(I)-V(I) line	M(I)
Y-intercept of S(I)-V(I) line	B(I) (=V(I))
Number of unique intercepts	T,N
Corrected K_m	K1,K2
Corrected V_{max}	V1,V2

Figure A2. *Flowchart for program 2.* **The flowchart was prepared as described in the Introduction of Appendix 1 with the variable designations given in Table A2. Subroutine 1 determines the median of sorted intercepts and subroutine 2 computes the standard error of the calculated kinetic contsants.**

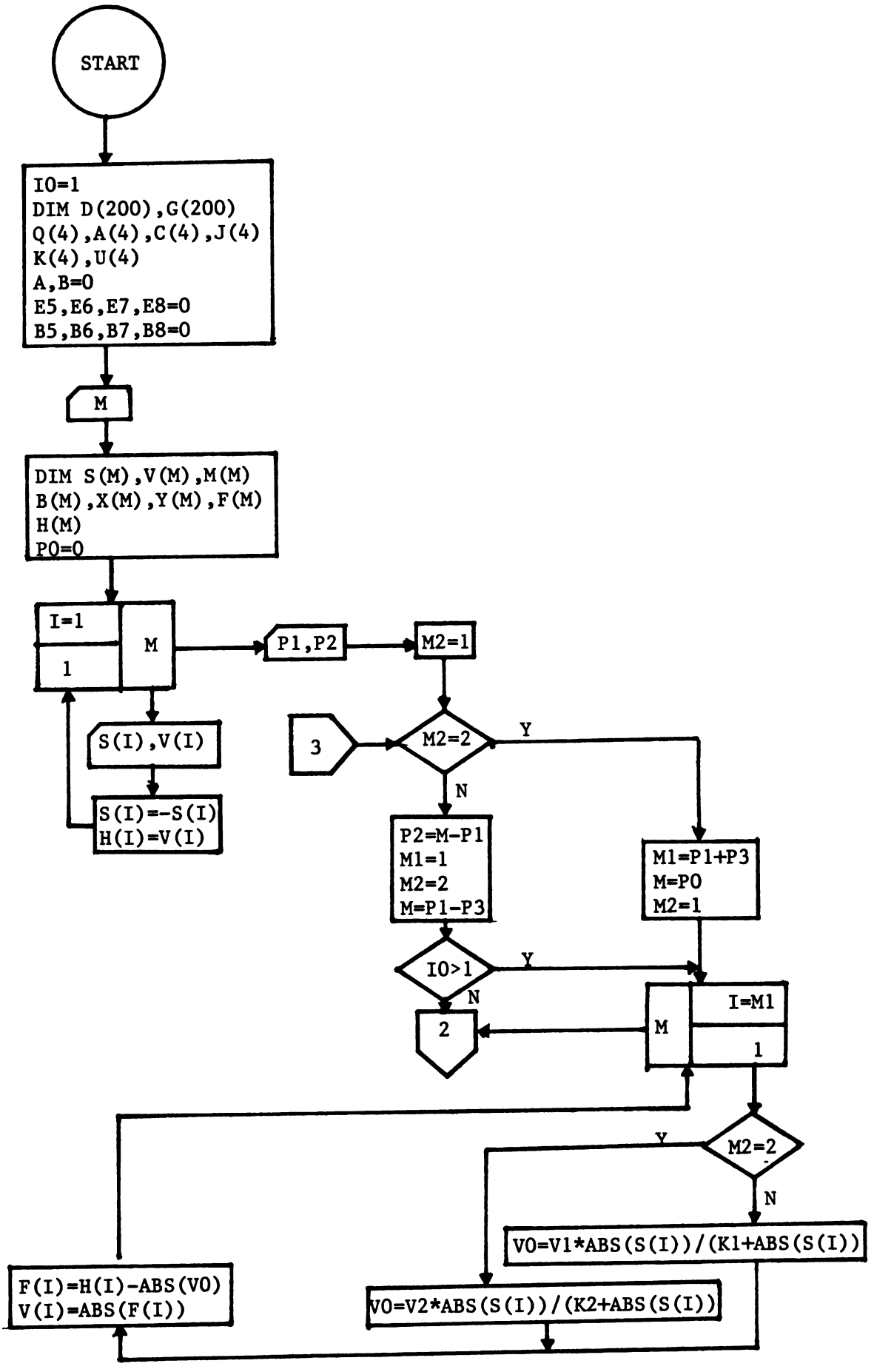
START
I0=1
DIM D(200),G(200)
Q(4),A(4),C(4),J(4)
K(4),U(4)
A,B=0
E5,E6,E7,E8=0
B5,B6,B7,B8=0
M
DIM S(M),V(M),M(M)
B(M),X(M),Y(M),F(M)
H(M)
P0=0
I=1
1
M
P1,P2
M2=1
3
M2=2
Y
N
S(I),V(I)
S(I)=-S(I)
H(I)=V(I)
P2=M-P1
M1=1
M2=2
M=P1-P3
M1=P1+P3
M=P0
M2=1
I0>1
Y
N
2
M
I=M1
1
M2=2
Y
N
V0=V1*ABS(S(I))/(K1+ABS(S(I))
V0=V2*ABS(S(I))/(K2+ABS(S(I))
F(I)=H(I)-ABS(V0)
V(I)=ABS(F(I))

Figure A2.

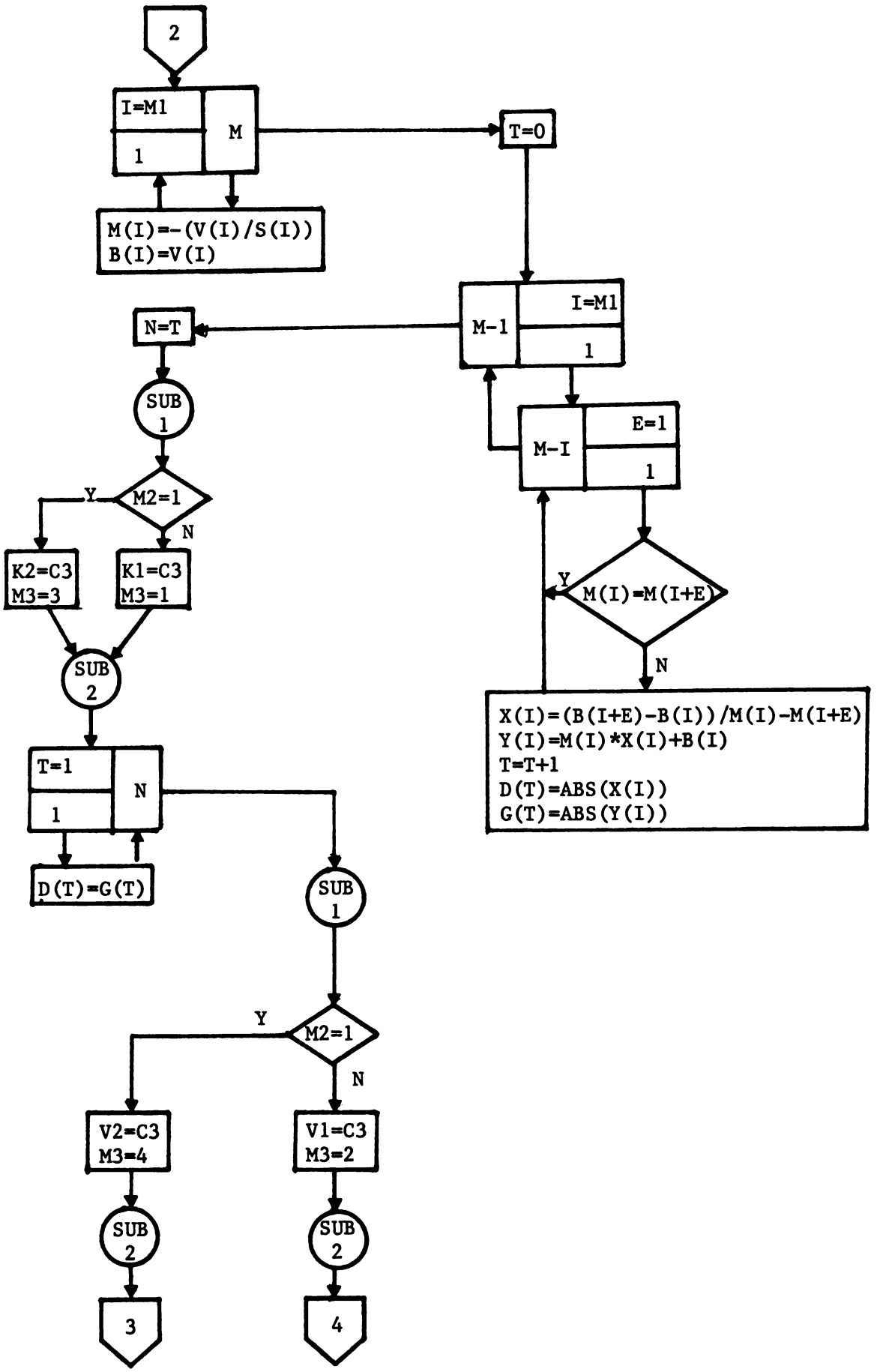

Figure A2 (cont'd)

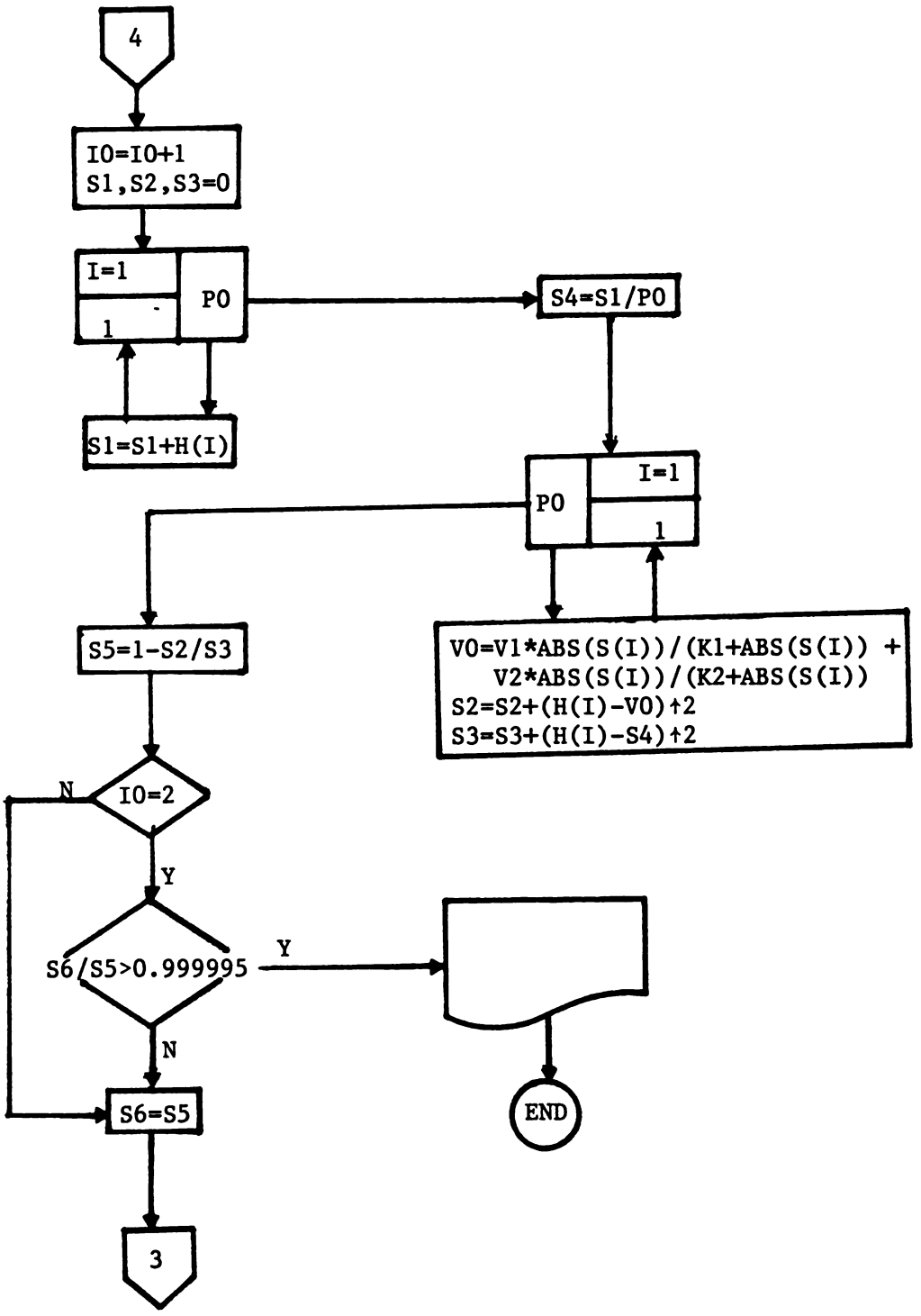

Figure A2. (cont'd)

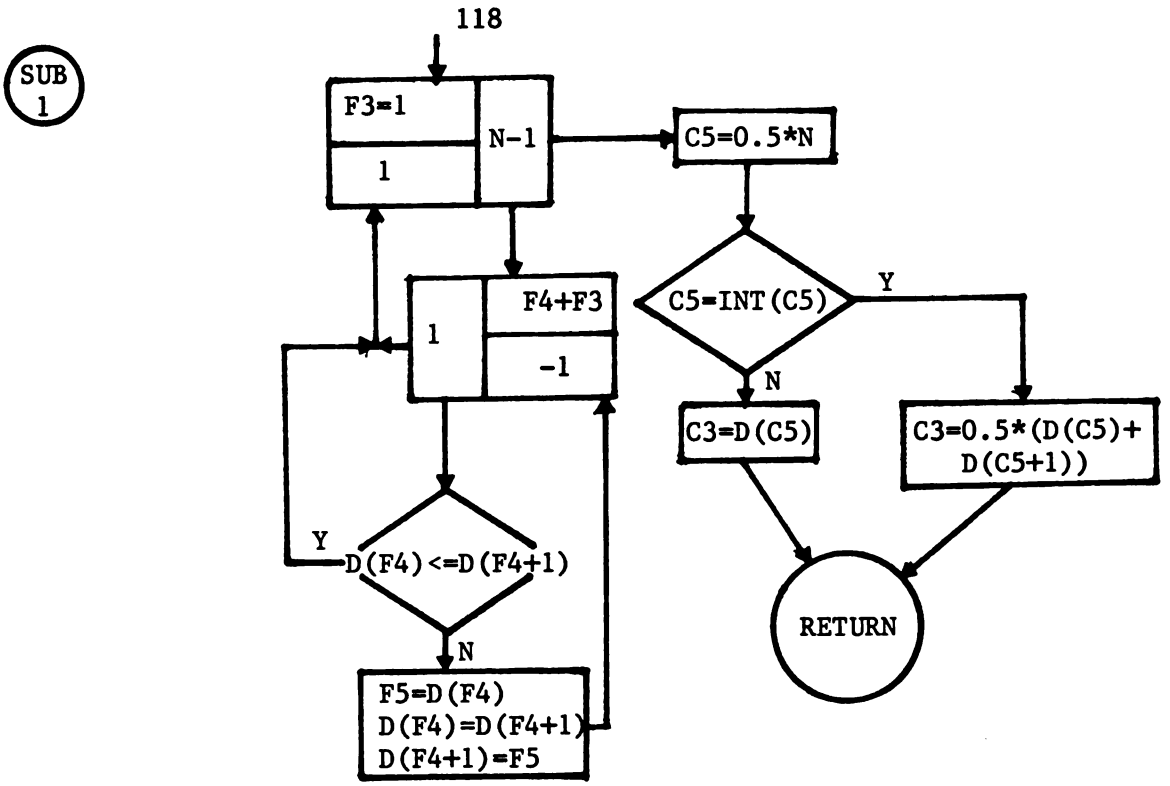

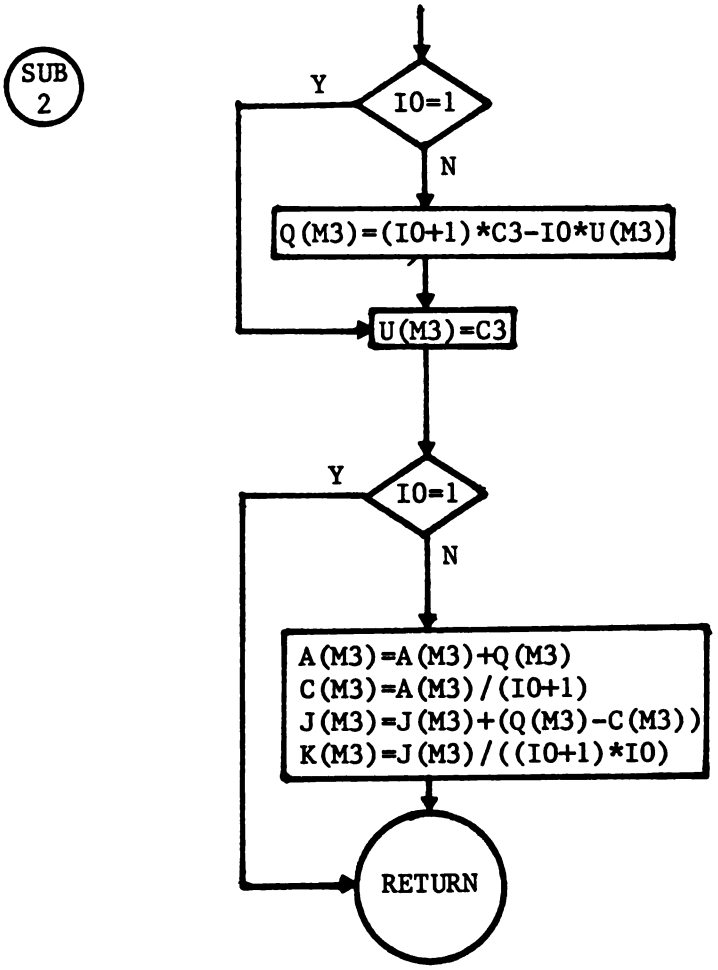

Figure A2. (cont'd)

PROGRAM 3

COMPUTATION OF THE NONLINEARITY FACTOR OF DOUBLE RECIPROCAL PLOTS

This program calculates the nonlinearity factor, n, which was used in Chapter 2 as an index of the degree of nonlinearity of the double reciprocal plots of ATPase activity. The factor, n, is computed which gives the best linear double reciprocal plot of 1/velocity vs. $1/\text{substrate}^{n}$. The program is a simple search program which considers the data in the double reciprocal form and determines the best value of n to give the linear correlation coefficient closest to 1. Initially, the program searches from 0 to 1 in 0.1 unit increments until the value of R is lower than the preceding value. Then the search is narrowed with a decrease in step size. Since the n value will be less than unity by examination of the double reciprocal plots, 1 was the upper limit of the search. To confirm the computed value, the program can then be run in the opposite direction from 1 to 0 and the values of n compared.

Table A3. *Designations for the principle variables employed in Program 3.*

Variable	Designation
Number of data pairs	N
Substrate concentration	S(I)
Velocity	V(I)
Upper limit of search	B
Lower limit of search	A
Search step size	C
Nonlinearity parameter	H
Linear correlation coefficient	H2
Reciprocal of substrate concentration to Hth power	X(J)
Reciprocal of velocity	Y(J)
Number of iterations	T

Figure A3. *Flowchart of program 3.* **The flowchart was prepared as described in the Introduction of Appendix 1 with the variable designations given in Table A3. The subroutine given on page 123 computes the linear correlation coefficient.**

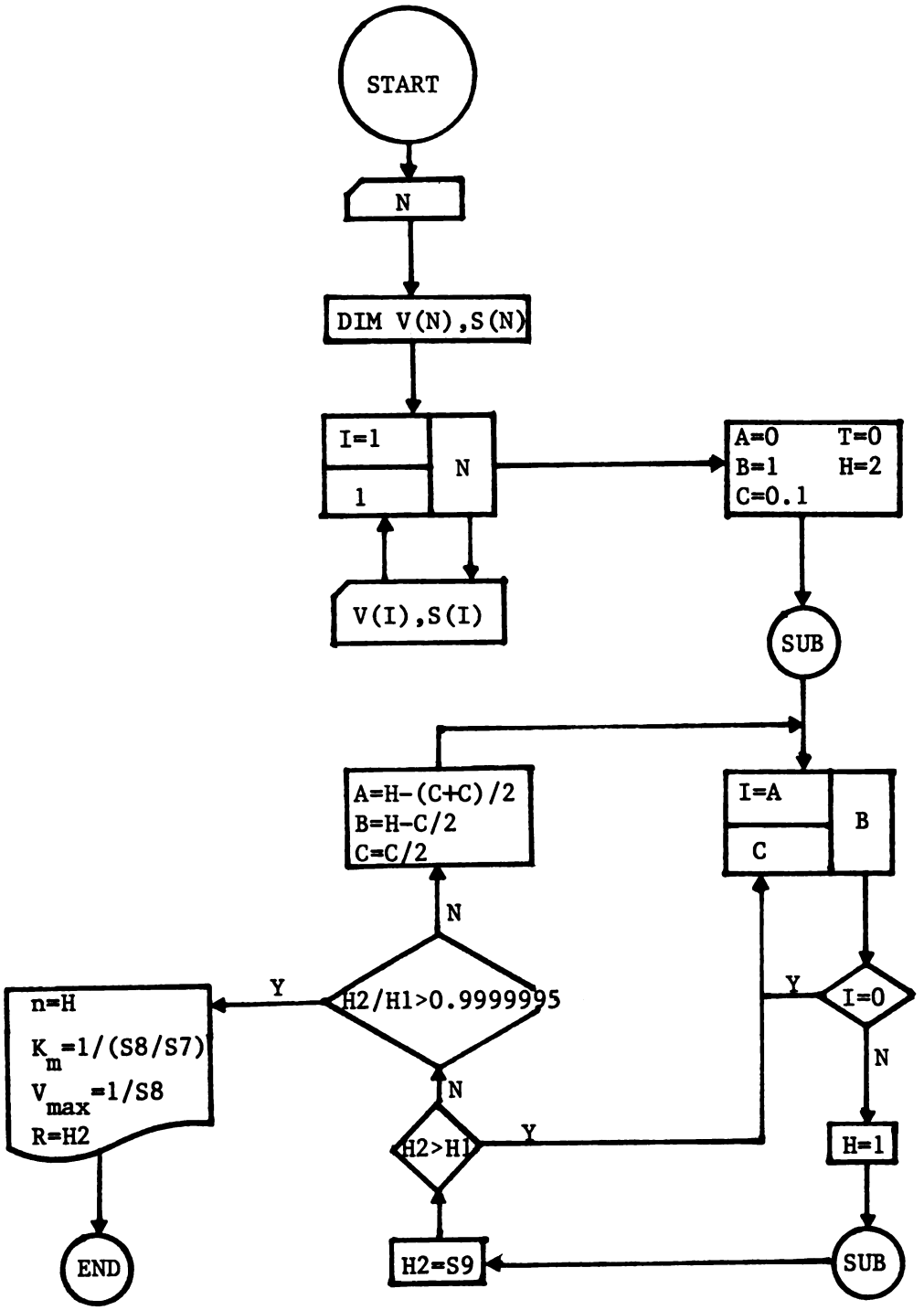
START
N
DIM V(N),S(N)
I=1
1
N
V(I),S(I)
A=0 T=0
B=1 H=2
C=0.1
SUB
A=H-(C+C)/2
B=H-C/2
C=C/2
I=A
C
B
N
Y
H2/H1>0.9999995
Y
I=0
N
n=H
K_m=1/(S8/S7)
V_max=1/S8
R=H2
N
H2>H1
Y
H=1
END
H2=S9
SUB

Figure A3.

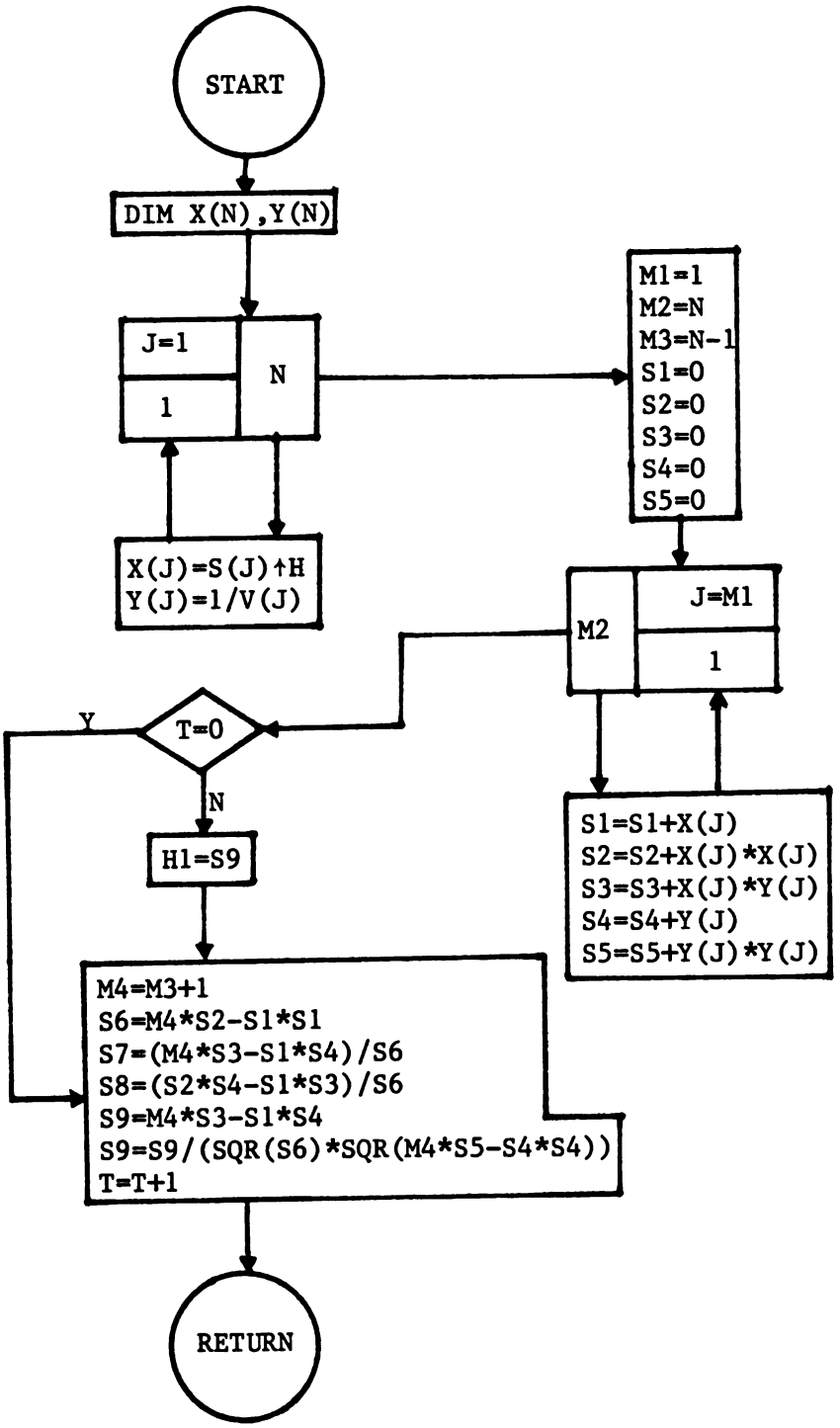

Figure A3 (cont'd)

APPENDIX 2

AFFINITY CHROMATOGRAPHIC ISOLATION OF CALMODULIN FROM BOVINE BRAIN ACETONE POWDER

The following manuscript has been accepted for publication in Analytical Biochemistry.

INTRODUCTION

The calcium modulator protein, camodulin, has been implicated in a number of biochemical and physiological processes (Wang and Waisman 1979, Klee *et al.* 1980). As a result of the considerable experimental interest in calmodulin, a variety of isolation procedures has been developed (Klee *et al.* 1980). In particular, the recent application of immobilized phenothiazine affinity chromatography has greatly reduced the time required for the isolation of highly purified calmodulin from a variety of sources (Charbonneau and Cormier 1979, Jamieson and Vanaman 1979). To further simplify the isolation of calmodulin, methods have been developed to facilitate the preparation of an immobilized phenothiazine affinity column and the isolation of calmodulin in high yield from a commercially available bovine brain acetone powder.

MATERIALS AND METHODS

Chemicals. 2-Chlorophenothiazine, acrylonitrile, benzyltrimethylammonium hydroxide, sodium borohydride, lithium aluminium hydride, trifluoroacetic acid, and ethanolamine·HCl were purchased from Aldrich Chemical Co. (Milwaukee, WI, USA). PMSF, cAMP, 5'-nucleotidase (grade IV), DEAE-Sephacel, and bovine brain acetone powder were obtained from Sigma Chemical Co. (St. Louis, MO, USA). Affi-Gel 10, Bio-Lyte 3/10 ampholytes, and dye binding protein assay reagent are products of Bio-Rad Laboratories (Richmond, CA, USA). Fresh bovine brain was obtained locally and stored frozen at -40 °C until needed. All other chemicals were purchased from various commercial

sources and were of the highest purity available.

Synthesis of 2-chloro-10-(3-aminopropyl)phenothiazine·HCl. All reactions involving the phenothiazine compounds were performed under reduced light and the chemical structures confirmed with IR spectroscopy. 2-Chloro-10-(2-cyanoethyl)phenothiazine (CCEP) was prepared by the reaction of 2-chlorophenothiazine (CP) with acrylonitrile and catalytic quantities of a 50% methanolic colution of benzyltrimethylammonium hydroxide (Smith 1951). The crude CCEP was dissolved in a minimum of hot ethyl acetate, treated with Norit A, and filtered hot on a sintered glass funnel containing a Celite pad. After cooling, the crystalline CCEP (89% yield) was collected by filtration and used without further purification.

A solution of $NaBH_3(OCOCF_3)$ in THF was prepared by the slow addition of 6.4 ml of CF_3COOH (75 mmol) in 7,5 ml THF to a stirred suspension of 2.84 g of finely powdered $NaBH_4$ (75 mmol) in 50 ml of THF at 20 °C (Umino *et al.* 1976). The solution of $NaBH_3(OCOCF_3)$ was then added to a stirred suspension of CCEP (14.3 g, 50 mmol) in 250 ml THF and the stirring continued for 8 hr at room temperature, during which the solution clarified. Water was carefully added dropwise to decompose the excess reagent and the THF removed *in vacuo*. To the solid residue was then added 500 ml of anhydrous ether and the solution stirred until a fine white suspension was formed. The ether solution was extracted (X3) with 250 ml of 1 N NaOH and dried over anhydrous sodium sulfate. The clarified ether solution was chilled and chilled ether saturated with HCl gas was added dropwise. The precipitated 2-chloro-10-(3-aminopropyl)-phenothiazine·HCl (CAPP·HCl) was collected by filtration and

recrystallized (X3) from ethanol, affording 8.1 g of white needles (56% yield).

Preparation of CAPP-Affi-Gel 10. Affi-Gel 10 (N-hydroxysuccinimide ester of crosslinked succinylated aminoalkyl Bio-Gel A-5m) was supplied as a suspension of 25 ml gel in anhydrous isopropanol in a serum vial. CAPP·HCl (100 mg) was dissolved in warm absolute ethanol and injected into the serum vial containing the Affi-Gel 10. The vial was gently rocked overnight in the dark at 4 °C. Ethanolamine·HCl was then injected into the vial to give a final concentration of 0.1 M and the rocking continued for 2 h at 4 °C. The gel suspension was removed from the vial and successively washed with 40 vol of chilled absolute ethanol, distilled water, saturated NaCl, and 20 mM MES-NaOH (pH 7), containing 300 mM NaCl and 1 mM mercaptoethanol (Buffer A). After packing the column with the CAPP-Affi-Gel 10 suspended in Buffer A, the column was washed with 500 ml of Buffer A and then 250 ml of Buffer A, containing 1 mM $CaCl_2$. To protect the CAPP-Affi-Gel 10 from the light, the column was wrapped with electrical tape. Coupling was estimated to be between 80 and 93% by direct UV spectroscopy of the derivatized gel, using ethanolamine-Affi-Gel 10 as the reference.

Calmodulin isolation from bovine brain acetone powder and intact bovine brain. Bovine brain acetone powder (BBAP) was homogenized in 20 vol of chilled 50 mM Tris-HCl (pH 7), containing 2 mM EDTA, 1 mM mercaptoethanol, and 250 μM PMSF, with a Waring blender for 2 min at high speed. Frozen bovine brain (BB) was broken into small pieces and while still frozen homogenized in 5 vol of homogenization buffer as described above for 3 min at low speed and 2 min at high

speed. The BB homogenate was then filtered through two layers of cheesecloth. All subsequent procedures were carried out at 4 °C and all buffers were adjusted to the specified pH at 4 °C. The homogenate from either BBAP or BB was stirred for 1 h and then centrifuged for 30 min at 7500 *g*. The supernatant was filtered through glass wool and solid ammonium sulfate added in small portions to give 55% of saturation. After readjusting the pH to pH 7, the solution was stirred for 1 h and then centrifuged at 12,500 *g* for 30 min. The pellet was saved for PDE preparation as described below. The supernatant was collected and the pH adjusted to pH 4 with 2 N H_2SO_4, containing ammonium sulfate at 55% of saturation. The solution was stirred for a minimum of 2 h and then centrifuged at 12,500 *g* for 30 min. The pellet was dissolved in and dialyzed against Buffer A, containing 5 mM $CaCl_2$. The dialyzed solution was clarified by centrifugation at 100,000 *g* for 1 h.

The solution prepared from 25 g of BBAP or 500 g of BB was applied to a 50 ml CAPP-Affi-Gel 10 column, prepared as described above, and the column washed with Buffer A, containing 1 mM $CaCl_2$, at a flow rate of 50 ml/h. The absorbance at 235 nm was continuously monitored and the wash continued until all the unbound material was eluted. The column was then washed with Buffer A, containing 10 mM EGTA, and the eluted calmodulin collected. $CaCl_2$ was immediately added to give a final concentration of 15 mM. After dialysis against 10 mM ammonium bicarbonate and then exhaustive dialysis against distilled water, the calmodulin fraction was lyophilized. The purity of the lyophilized calmodulin was determined by SDS gel electrophoresis on 12.5% polyacrylamide slab gels, containing 0.1 mM EGTA (Jamieson and Vanaman 1979), and by

acrylamide gel isoelectric focussing (Jarrett and Penniston 1978).

After completion of the affinity chromatography, the column was washed with 250 ml of 6 M deionized urea and then 500 ml of Buffer A, containing 1 mM $CaCl_2$. If the column was not to be used within 5 days, the final wash also contained 1 mM sodium azide. The urea wash was found to be essential in maintaining the column's ability to bind calmodulin.

Phosphodiesterase preparation and assay. Activator-deficient PDE was prepared from the 55% ammonium sulfate precipitate (pH 7) from BBAP essentially by the methods of Klee and Krinks (1978). The precipitate was resuspended in 20 mM Tris-HCl (pH 7.5), containing 50 mM ammonium sulfate and 250 μM PMSF, and dialyzed against the same buffer overnight. The solution was clarified by centrifugation at 100,000 *g* for 1 h. The solution was applied to a DEAE-Sephacel column (4x40 cm) equilibrated with dialysis buffer. The column was washed with dialysis buffer until the 280 nm absorbance of the column effluent returned to baseline. The column was then washed with 20 mM Tris-HCl buffer (pH 7.5), containing 80 mM ammonium sulfate and 250 μM PMSF, as above. The partially purified, activator-deficient PDE was eluted with the same buffer, containing 150 mM ammonium sulfate. The PDE fraction was dialyzed against 20 mM Tris-HCl buffer (pH 8), containing 3 mM $MgCl_2$ and 250 μM PMSF, and the dialyzed solution frozen and stored at -40 °C until needed. This PDE preparation was stimulated eight- to tenfold by calmodulin and had a specific activity in the presence of calmodulin of 75 nmole cAMP hydrolyzed/ mg protein-min at 30 °C. The total yield of protein was 890 mg.

PDE was assayed in a 0.5 ml reaction volume consisting of 20 mM Tris-HCl buffer (pH 8), containing 3 mM $MgCl_2$, 1 mM cAMP, 0.1 mM dithioerythritol, and 100 µg of PDE fraction protein. The basal activity was determined in the presence of 50 µM EGTA and the activator-dependent activity determined in the presence of 50 µg $CaCl_2$ and 250 ng calmodulin. After incubation of the reaction solution for 10 min at 30 °C, the reaction was stopped by heating in boiling water and 1 unit of 5'-nucleotidase added. After incubation at 30 °C for 30 min, the reaction was stopped and the amount of released phosphate determined (Rathbun and Betlach 1969). Protein was measured by dye binding assay (Bio-Rad reagent) (Bradford 1976).

RESULTS AND DISCUSSION

The application if immobilized phenothiazine affinity chromatography has become the preferred method for the isolation of calmodulin from a variety of tissues (Charbonneau and Cormier 1979, Jamieson and Vanaman 1979, Anderson *et al.* 1980, Van Eldik *et al.* 1980). In the previous reports describing the preparation of immobilized phenothiazine for calmodulin isolation (Charbonneau and Cormier 1979, Jamieson and Vanaman 1979), the phenothiazine compounds were obtained courtesy of pharmaceutical companies. Since these compounds are apparently not available commercially and may not always be available from other sources, it was desirable to be able to synthesize them in the laboratory. Furthermore, since the published procedure (Craig *et al.* 1978) for the reduction of CCEP to CAPP with $LiAlH_4$ was not successful (Scheme A1), a detailed description of a method for the synthesis of CAPP·HCl in relatively high yield has

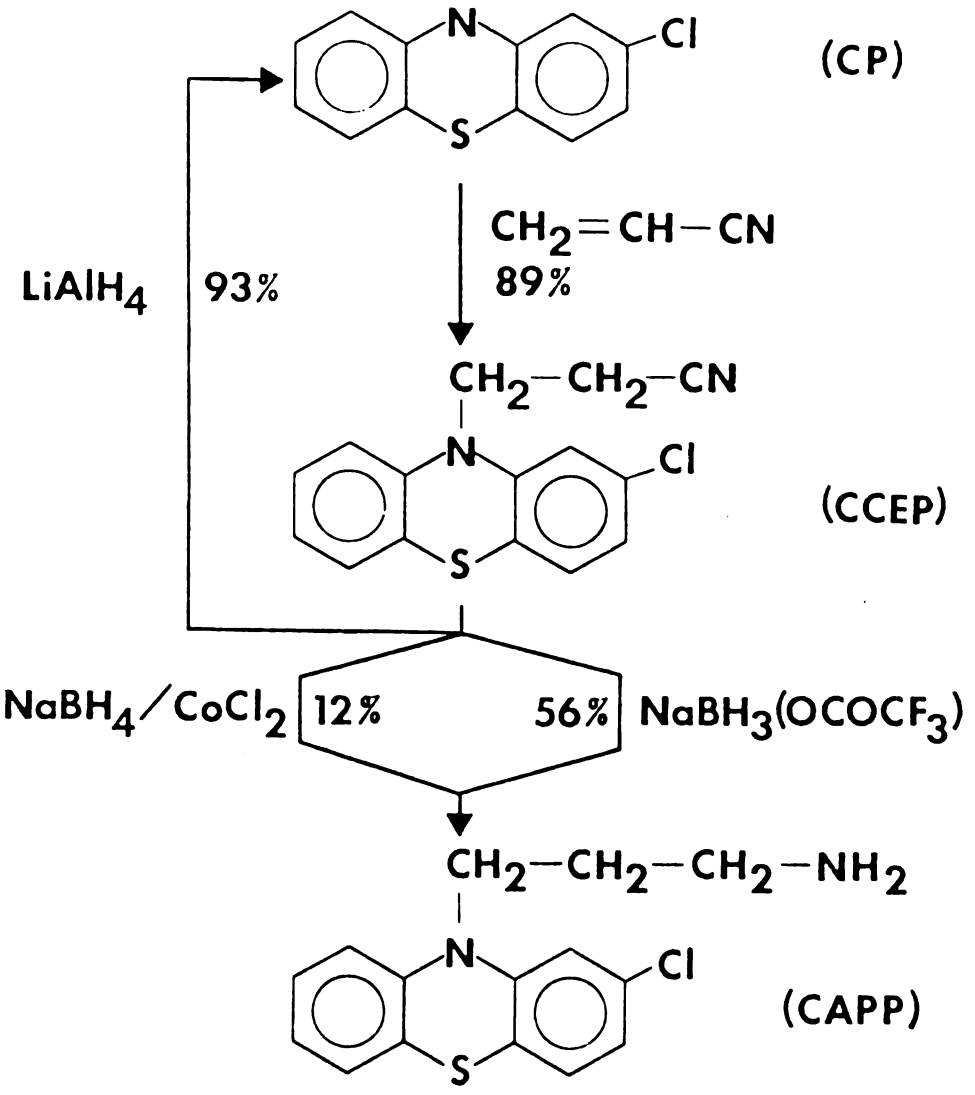

Scheme A1. *Synthesis of 2-chloro-10-(3-aminopropyl)phenothiazine (CAPP).* 2-Chloro-10-(2-cyanoethyl)phenothiazine (CCEP) was prepared by the reaction of 2-chlorophenothiazine (CP) with acrylonitrile and reduced to CAPP with either $NaBH_3(OCOCF_3)$ or $NaBH_4/CoCl_2$. $LiAlH_4$ reduction resulted only in CP formation. Molar yields are the reaction steps are given in parenthesis with the yield of CAPP being given in terms of its HCl form.

been included in this report and summarized in Scheme A1. An alternative method for CCEP reduction with somewhat less toxic materials (Satoh *et al.* 1969) is also presented (Scheme A1).

It has already been demonstrated that the bovine brain calmodulin prepared from intact brain by affinity chromatography with CAPP-Sepharose 4B is chemically and functionally identical to the bovine brain calmodulin prepared by more standard procedures (Jamieson and Vanaman 1979). The application of CAPP-Affi-Gel 10 for the isolation of calmodulin has several advantages over the previously used CAPP-Sepharose 4B columns. Being already activated and ligand coupling being efficient in alcohol, Affi-Gel 10 eliminates the activation with highly toxic cyanogen bromide and the problem of CAPP·HCl solubility in coupling buffer (Jamieson and Vanaman 1979). It is only necessary to inject an ethanolic solution of CAPP·HCl into the vials containing the Affi-Gel 10 to initiate coupling.

The isolation method for calmodulin described in this report is essentially the combination of portions of three previously published procedures (Jamieson and Vanaman 1979, Klee 1977, Wang and Desai 1977). By reduction of the sample volume for application to the affinity column with ammonium sulfate precipitation of the crude calmodulin, it was possible to rapidly isolate a relatively large amount of electrophoretically pure calmodulin in a single affinity chromatographic run. As shown in Figure A4, CAPP-Affi-Gel 10 affinity chromatography has the same capabilities as CAPP-Sepharose 4B (Jamieson and Vanaman 1979) in the preparation of bovine brain calmodulin. Essentially all the calmodulin in the sample applied to the affinity column was retained by the column in the presence of $CaCl_2$ (Figure A4). The bound calmodulin was easily eluted with

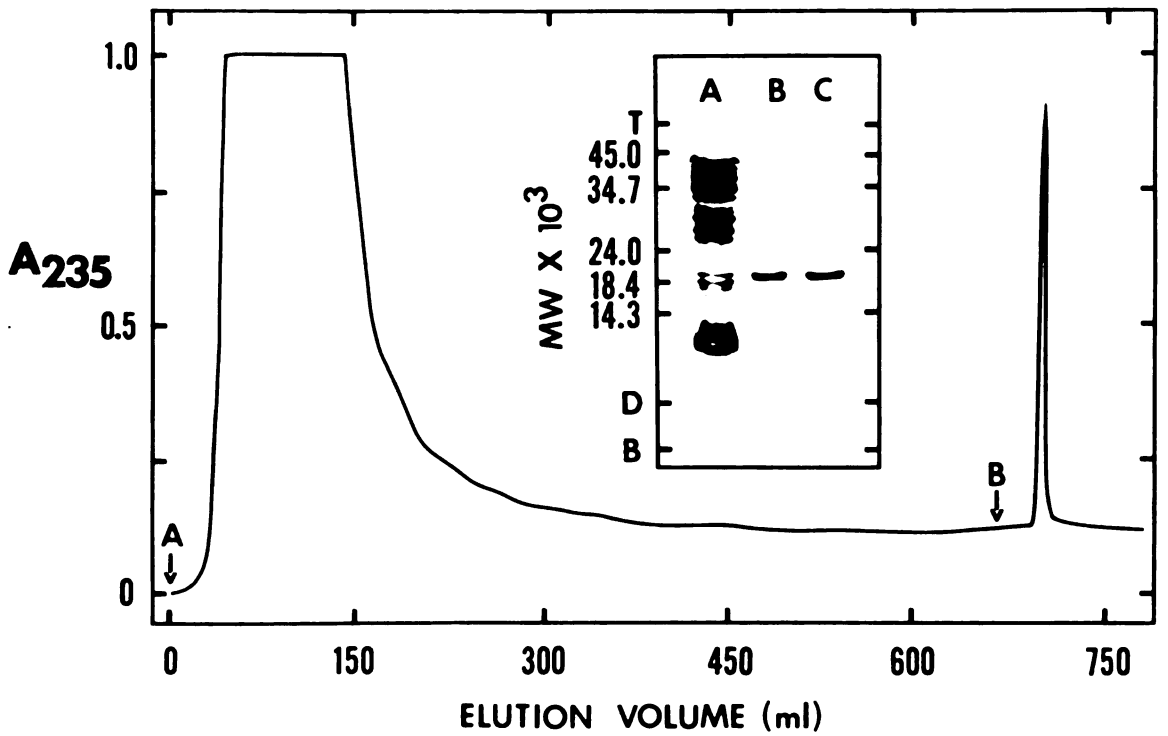

Figure A4. *Isolation of calmodulin (CaM) from bovine brain acetone powder by CAPP-Affi-Gel 10 affinity chromatography.* As described in the text, a sample prepared from 25 g of bovine brain acetone powder (BBAP) was applied to a 50 mL CAPP-Affi-Gel 10 affinity column (A) and the unbound protein eluted. After the 235 nm absorbance reached its new baseline, the CaM was eluted by replacing the $CaCl_2$ in the wash buffer with EDTA (B). The flow rate was 50 ml/hr. The inset shows the results of SDS gel electrophoresis on 12.5% polyacrylamide slab gels. Gel slot A is 100 µl of the unbound protein fraction. Slot B is CaM isolated from BBAP (10 µg). Slot C is CaM isolated from intact bovine brains by the same procedure (10 µg). The ordinate of the inset is marked with the positions of the top (T), bottom (B), and tracking dye (D). The molecular weights were obtained with molecular weight standard proteins run in the same gel.

EGTA and contained no observable contaminating proteins (Figure A4). Bovine brain calmodulin preparations isolated from either BBAP or BB were indistinguishable by SDS gel electrophoresis (Figure A4) and had almost identical abilities to activate PDE (Table A1). An estimated molecular weight of 19,250 for calmodulin from BBAP in the absence of Ca^{2+} (Figure A4) is within the range of values for bovine brain calmodulin isolated by other methods (Klee *et al.* 1980, Wang and Waisman 1979).

The bovine brain calmodulin purified by CAPP-Affi-Gel 10 affinity chromatography had the same properties of bovine brain calmodulin prepared by other methods. The protein migrated as a single band in an isoelectric focusing gel and gave an isoelectric pH of 4.1 (Jarrett nad Penniston 1978). The purified calmodulin also had the typical UV spectra of calmodulin, giving peaks at 253, 259, 265, 269, and 277 nm (data not shown)(Wang and Waisman 1979).

Application of this procedure for calmodulin isolation with 25 g of BBAP afforded 30.6 g of purified calmodulin. Assuming that about 180 g of bovine brain acetone powder is produced from 1 kg of intact brain (Morris 1973), the calmodulin yield from 25 g of BBAP is equivalent to a yield of 220.3 mg/kg intact bovine brain or about 2.5 times that of the highest reported yield from intact brain (Jamieson and Vanaman 1979). The yield of calmodulin from BB by this procedure was 74.6 mg/kg which is slightly less than the 87.5 mg/kg obtained with CAPP-Sepharose 4B (Jamieson and Vanaman 1979). These results indicate that the use of the acetone powder of bovine brain produces a considerable increase in calmodulin yield compared to the use of intact brain. A similar conclusion was reached by Klee 1977), who used a more lengthy isolation procedure.

Table A1. *Activation of phosphodiesterase by bovine brain calmodulin prepared by CAPP-Affi-Gel 10 Affinity chromatography.*

Reaction solution	PDE Activity (nmol cAMP/mg-min)
+ EGTA (50 μM)	8.9 ± 0.13
+ BBAP calmodulin (250 ng) + $CaCl_2$ (50 μM)	74.6 ± 1.47
+ BB calmodulin (250 ng) + $CaCl_2$ (50 μM)	71.4 ± 1.89
+ BBAP calmodulin (250 ng) + EGTA (50 μM)	5.2 ± 0.32

REFERENCES

Ackermann, W.W. and Potter, V.R. (1949) Proc. Soc. Exp. Biol. Med. 72:1-9.

Ahrens, M-L. (1981) Biochim. Biophys. Acta 642:252-266.

Amory, A., Foury, F., and Goffeau, A. (1980) J. Biol. Chem. 255: 9353-9357.

Anderson, J.M., Charbonneau, H., Jones, H.P., McCann, R.O., and Cormier, M.J. (1980) Biochemistry 19:3113-3120.

Balke, N.E. and Hodges, T.K. (1975) Plant Physiol. 55:83-86.

Balke, N.E. and Hodges, T.K. (1979) Plant Physiol. 63:58-61.

Barron, J.T. and Disalvo, J. (1979) Proc. Soc. Exp. Biol. Med. 160:258-262.

Baydoun, E.A-H. and Northcote, D.H. (1981) Biochem. J. 193:781-792.

Bensadoun, A. and Weinstein, D. (1976) Anal. Biochem. 70:241-250.

Benson, M.J. and Tipton, C.L. (1978) Plant Physiol. 62:165-172.

Bishop, D.G., Kenrick, J.R., Bayston, J.H., MacPherson, A.S, Johns, S.R. and Willing, R.I. (1979) In Low Temperature Stress in Crop Plants: The Role of the Membrane (J.M. Lyons, D. Graham, and J.K. Raison eds), pp. 375-389. Academic Press, New York.

Boss, W.F. and Mott, R.L. (1980) Plant Physiol. 66:835-837.

Bradford, M.M. (1976) Anal. Biochem. 72:248-254.

Briggs, D.E. (1978) Barley. pp. 264-265. Chapman and Hall, London.

Brunette, D.M. and Till, J.E. (1971) J. Membr. Biol. 5:215-224.

Burns, D.J.W. and Tucker, S.A. (1977) Eur. J. Biochem. 81:45-52.

Caldwell, C.R. and Haug, A. (1980) Physiol. Plant. 50:183-193.

Caldwell, C.R. and Haug, A. (1981) Physiol. Plant. *in press.*

Cambraia, J. and Hodges, T.K. (1980) In Plant Membrane Transport: Current Conceptual Issues (R.M. Spanswick, W.J. Lucas, and J. Dainty eds.), pp. 211-222. Elsevier/North-Holland Biomedical Press, New York.

Cantley, L.C., Jr. and Josephson, L. (1976) Biochemistry 15: 5280-5287.

Charbonneau, H. and Cormier, M.J. (1979) Biochem. Biophys. Res. Comm. 90:1039-1047.

Christiansen, J.L. and Lindberg, S. (1976) Physiol. Plant. 36:110-112.

Cleland, W.W. (1970) In The Enzymes: Kinetics and Mechanisms. (P.D. Boyer ed.), III:60. Academic Press, New York.

Cornish-Bowden, A. (1974) Biochem. J. 137:143-144.

Cornish-Bowden, A. and Eisenthal, R. (1978) Biochim. Biophys. Acta 532:268-272.

Craig, J.C., Gruenke, L.D., and Lee, S-Y.C. (1978) J. Labelled Compd. Radiopharm. 15:31-40.

Cunningham, C.C. and Sinthusek, G. (1979) Biochim. Biophys. Acta 550:150-153.

Dammkoehler, R.A. (1966) J. Biol. Chem. 241:1955-1957.

Davis, B.J. (1964) Ann. N.Y. Acad. Sci. 121:404.

Davis, D.G., Inesi, G. and Gulik-Krzywicki, T. (1976) Biochemistry 15:1271-1276.

DePamphilis, M.L. and Cleland, W.W. (1973) Biochemistry 12:3714-3724.

Dieter, P. and Marmé, D. (1981) FEBS Lett. 125:245-248.

Dixon, M. (1953a) Biochem.J. 55:170-171.

Dixon, M. (1953b) Biochem. J. 55:161-170.

Dufour, J-P. and Goggeau, A. (1980) J. Biol. Chem. 255:10591-10598.

DuPont, F.M. and Leonard, R.T. (1980) Plant Physiol. 65:931-938.

DuPont, Y. (1977) Eur. J. Biochem. 72:185-190.

Erdei, L., Tóth, I., and Zsoldos, F. (1979) Physiol. Plant. 45:448-452.

Fairbanks, G., Steck, T.L., and Wallach, D.F.H. (1971) Biochemistry 10:2606-2617.

Fourcans, B. and Jain, M.K. (1974) In Advances in Lipid Research, Vol. 12 (R. Paoletti and D. Kritchevsky eds.), pp. 148-226. Academic Press, New York.

Frieden, C. (1970) J. Biol. Chem. 245:5788-5799.

Froelich, J.P. and Taylor, E.W. (1975) J. Biol. Chem. 250:2013-2021.

Gibrat, R. and Rossignol, M. (1977) C.R. Acad. Sci. Ser. D:1171-1179.

Gietzen, K, Tejcka, M., and Wolf, H.U. (1980) Biochem. J. 189: 81-88.

Glynn, I.M. and Karlish, S.J.D. (1976) J. Physiol. 256:465-496.

Gomez-Lepe, B. and Hodges, T.K. (1978) Plant Physiol. 61:865-870.

Gordon, L.M., Sauerheber, R.D., and Esgate, J.A. (1978) J. Supramol. Struc. 9:299-326.

Griffith, O.H. and Jost, P.C. In Spin Labeling:Theory and Applications (L.J. Berliner ed.), pp. 453-523. Academic Press, New York.

Hansson, G. and Kylin, A. (1969) Z. Pflanzenphysiol. 60:270-275.

Hastings, D.F. and Reynolds, J.A. (1979) In Na, K-ATPase: Structure and Kinetics (J.C. Skou and J.G. Norby eds.), pp. 15-20. Academic Press, New York.

Hauser, H., Levine, B.A., and Williams, R.J.P. (1976) TIBS 1:278-281.

Hendrix, D.L. and Kennedy, R.M. (1977) Plant Physiol. 59:264-267.

Hirata, F., Viveros, O.H., Diliberto, E.J., Jr., and Axelrod, J. (1978) Proc. Natl. Acad. Sci. USA 75:1718-1721.

Hodges, T.K. (1976) In Encyclopedia of Plant Physiology, New Series, Vol. 2, Part A. (M.G. Pitman and U. Lüttge eds.), pp. 260-283. Springer-Verlag, New York.

Hodges, T.K. and Leonard, R.T. (1974) In Methods in Enzymology, Vol. 32B. (S. Fleischer and L. Packer eds.), pp. 392-406. Academic Press, New York.

Hoffman, W., Sarzala, M.G., and Eletr, S. (1979) Proc. Natl. Acad. Sci. USA 76:3860-3864.

Horváth, I., Vigh, L, and Farkas, T. (1981) Planta 151:103-108.

Inesi, G., Millman, M., and Eletr, S. (1973) J. Mol. Biol. 81: 483-504.

Jamieson, G.A., Jr. and Vanaman, T.C. (1979) Biochem. Biophys. Res. Comm. 90:1048-1056.

Jarrett, H.W. and Penniston, J.T. (1978) J. Biol. Chem. 253: 4676-4682.

Jeng, S.J. and Guillory, R.J. (1975) J. Supramol. Struc. 3:448-468.

Jost, P.C., Griffith, O.H., Capaldi, R.A., and Vanderkooi, G. (1973) Proc. Natl. Acad. Sci. USA 70:480-484.

Kawasaki, T., Kähr, M., and Kylin, A. (1979) Physiol. Plant. 45:437-439.

Klee, C.B. (1977) Biochemistry 16:1017-1024.

Klee, C.B. and Krinks, M.H. (1978) Biochemistry 17:120-126.

Klee, C.B., Crouch, T.H., and Richman, P.G. (1980) Ann. Rev. Biochem. 49:489-515.

Kylin, A. and Kähr, M. (1973) Physiol. Plant. 28:452-457.

Kylin, A. and Quatrano, R.S. (1975) In Plants in Saline Enviroments (A. Poljakoff-Mayber and J. Gale eds.), pp. 147-176. Springer-Verlag, New York.

Kylin, A., Kuiper, P.J.C., and Hansson, G. (1972) Physiol. Plant. 26:271-278.

Laemmli, U.K.(1970) Nature 227:680-682.

Laidler, K.J. and Bunting, P.S. (1973) The Chemical Kinetics of Enzyme Action. Clarendon Press, Oxford.

Leonard, R.T. and Hotchkiss, C.W. (1978) Plant Physiol. 61:175-179.

Leonard, R.T., Hansen, D., and Hodges, T.K. (1973) Plant Physiol. 51:749-754.

Leonards, K.S. and Haug, A. (1980) Biochim. Biophys. Acta 600: 817-830.

Lin, T-I. and Morales, M.F. (1977) Anal. Biochem. 77:10-17.

Lindberg, S., Hansson, G., and Kylin, A. (1974) Physiol. Plant. 32:103-107.

Lyons, J.M., Graham, D., and Raison, J.K. (1979) In Low Temperature Stress in Crop Plants:The Role of the Membrane. (J.M. Lyons, D. Graham, and J.K. Raison eds.) pp. 549-555. Academic Press, New York.

Malpartida, F. and Serrano, R. (1980) FEBS Lett. 111:69-72.

March, S.C., Parikh, I., and Cuatrecasas, P. (1974) Anal. Biochem. 60:149-152.

Marmé, D. and Gross, J. (1979) In Recent Advances in the Biochemistry of Cereals (D.L. Laidman and R.G. Wyn-Jones eds.), pp. 27-36. Academic Press, New York.

Marquardt, D.W. (1973) J. Soc. Ind. Appl. Math. 2:431-441.

McLaughlin, S.G.A., Szabo, G., and Eisenman, G. (1971) J. Gen. Physiol. 58:667-687.

McMurchie, E.J. (1979) In Low Temperature Stress in Crop Plants: The Role of the Membrane (J.M. Lyons, D. Graham, and J.K. Raison eds.), pp. 163-176. Academic Press, New York.

Mehlhorn, R.J. and Packer, L. (1976) Biochim. Biophys. Acta 423: 382-397.

Nagahashi, G. (1975) Dissertation, University of California, Riverside. Xerox University Microfilms, Ann Arbor.

Nagahashi, G., Leonard, R.T., and Thompson, W.W. (1978) Plant Physiol. 61:993-999.

Nash, J.C. (1979) Compact Numerical Methods for Computers: Linear Algebra and Function Minimization. pp. 175-177. John Wiley and Sons, New York.

Neet, K.E. and Green, N.M. (1977) Arch. Biochem. Biophys. 178: 588-597.

Nelder, J.A. and Mead, R. (1965) Comput. J. 7:308-313.

Niggli, V., Penniston, J.T., and Carafoli, E. (1979) J. Biol. Chem. 254:9955-9958.

Niggli, V., Adunyah, E.S., Penniston, J.T., and Carafoli, E. (1981) J. Biol. Chem. 256:395-401.

Nissen, P. (1977) Physiol. Plant. 40:205-214.

Pike, C.S., Berry, J.A., and Raison, J.K. (1979) In Low Temperature Stress in Crop Plants: The Role of the Membrane (J.M. Lyons, D, Graham, and J.K. Raison eds.), pp. 305-318. Academic Press, New York.

Quinn, P.J. and Williams, W.P. (1978) Prog. Biophys. Molec. Biol. 34:109-173.

Quintanilha, A.T. and Packer, L. (1977) FEBS Lett. 78:161-165.

Raison, J.K. (1973) In Membrane Structure and Mechanisms of Biological Energy Transduction (J. Avery ed.) pp. 559-583. Plenum Press, New York.

Raison, J.K. and Chapman, E.A. (1976) Aust. J. Plant Physiol 3: 291-299.

Rathbun, W.B. and Betlach, M.V. (1969) Anal. Biochem. 28: 436-445,

Ratner, A. and Jacoby, B. (1973) J. Expt. Bot. 24:231-238.

Rega, A.F., Garrahan, P.J., Barrabin, H., Horenstein, A., and Rossi, J. (1979) In Cation Flux Across Biomembranes (Y. Mukohaya and L. Packer eds.), pp.67-76. Academic Press, New York.

Rice, D.M., Meadows, M.D., Scheinman, A.O., Göni, F.M., Gómez-Fernández, J.C., Moscarello, M.A., Chapman, D., and Oldfield, E. (1979) Biochemistry 18:5893-5903.

Richards, D.E., Rega, A.F., and Garrahan, P.J. (1978) Biochim. Biophys. Acta 511:194-201.

Ronner, P., Gazzotti, P., and Carafoli, E. (1977) Arch. Biochem. Biophys. 179:578-583.

Sachs, G., Rabon, E., and Saccomani, G. (1979) In Cation Flux Across Biomembranes (Y.Mukohata and L. Packer eds.), pp. 53-66. Academic Press, New York.

Satoh, T., Suzuki, S., Suzuli, Y., Miyaji, Y., and Imai, Z. (1969) Tetrahedron Lett. 52:4555-4558.

Segel, I.H. (1975) Enzyme Kinetics: Behaviour and Analysis of Rapid Equilibrium and Steady-state Enzyme Systems. John Wiley and Sons, New York.

Semenza, G. and von Balthazar, A-K. (1974) Eur. J. Biochem. 41: 149-162.

Silvius, J.R. and McElhaney, R.N. (1980) Proc. Natl. Acad. Sci. USA 77:1255-1259.

Silvius, J.R. and McElhaney, R.N. (1981) J. Theor. Biol. 88:135-152.

Silvius, J.R., Read, B.D., and McElhaney, R.N. (1978) Science 199:902-904.

Sinensky, M., Pinkerton, F., Sutherland, E., and Simon, F.R. (1979) Proc. Natl. Acad. Sci. USA 76:4893-4897.

Smith, N.L. (1951) J. Org. Chem. 16:415-418.

Somero, G.N. and Hochachka, P.W. (1976) In Adaptation to Enviroment: Essays on the Physiology of Marine Animals (R.C. Newell ed.), pp. 125-190. Butterworths, London.

Sone, N., Yoshida, M., Hirata, H., and Kagawa, Y. (1979) In Cation Flux Across Biomembranes (Y. Mukohata and L. Packer eds.), pp. 279-290. Academic Press, New York.

Sprague, E.D., Larrabee, C.E., Jr., and Halsall, H.B. (1980) Anal. Biochem. 101:175-181.

Storer, A.C. and Cornish-Bowden, A. (1976) Biochem. J. 159:1-5.

Strittmatter, W.J., Hirata, F., and Axelrod, J. (1979) Biochem. Biophys. Res. Comm. 88:147-153.

Taylor, J.S. and Hattan, D. (1979) J. Biol. Chem. 254:4402-4407.

Thilo, L., Träuble, J., and Overath, P. (1977) Biochemistry 16: 1283-1290.

Tikhaya, N.E., Mishustina, N.E., Kurkova, E.B., Vakhmistriv, D.B., and Samiolova, S.A. (1976) Fiziol. Rast. 23:1197-1206.

Ting-Beall, H.P., Clark, D.A., Suelter, C.H., and Wells, W.W. (1973) Biochim. Biophys. Acta 291:229-236.

Tognoli, L. and Marrè, E. (1981) Biochim. Biophys. Acta 642:1-14.

Tornheim, K., Gilbert, T.R., and Lowenstein, J.M. (1980) Anal. Biochem. 103:87-93.

Träuble, H. and Eibl , H. (1974) Proc. Natl. Acad. Sci. USA 71: 214-219.

Travis, R.L. and Booz, M.L. (1979) Plant Physiol. 63:573-577.

Umino, N., Iwakumi, T., and Itoh, N. (1976) Tetrahedron Lett. 33: 2875-2976.

Van Eldik, L.J., Grossman, A.R., Iverson, D.B., and Watterson, D.M. (1980) Proc. Natl. Acad. Sci. USA 77:1912-1916.

Vianna, A.L. (1975) Biochim. Biophys. Acta 410:389-406.

Wang, C-S. and Smith, R.L. (1975) Anal. Biochem. 63:414-417.

Wang, J.H. and Desai, R. (1977) J. Biol. Chem. 252:4175-4184.

Wang, J.H., and Waisman, D.M. (1979) In Current Topics of Cellular Regulation (B.L. Horecker and E.R. Stadtman eds.), Vol. 15, 47-107. Academic Press, New York.

Weber, K. and Osborn, M. (1969) J. Biol. Chem. 244:4406-4415.

Williams, J.P. and Merrilees, P.A. (1970) Lipids 5:367-370.

Wojtczak, L. and Nalecz, M.J. (1979) Eur. J. Biochem. 94:99-107.

Wolfe, J, and Bagnall, D.J.(1980). Ann. Bot. 45:485-488.